Non-invasive Estimation of Blood Pressure using Harmonic Components of Oscillometric Pulses

By

David Ayo Abolarin

A Thesis Presented to Faculty of Graduate Studies and Research in partial fulfillment of the
Requirements for the degree of

Masters of Applied Science (MASc.)

Electrical and Computer Engineering
University of Ottawa

I hereby declare that I am the sole author of this thesis. This is a true copy of the thesis, including any required final version, as accepted by examiners. Also, I authorize the University of Ottawa to lend this document to other institutions for the purpose of scholarly research.

David Ayo Abolarin

I further authorize the University of Ottawa to reproduce this document by photocopying or by any other means, in total or in part, at the request of other institution or individuals for the purpose of research

David Ayo Abolarin

Abstract

This research presents a pulse-by-pulse analysis of Oscillometric blood pressure waveform at systolic, diastolic and mean arterial pressure points.

Using a mathematical optimization technique, pulses are characterized into component harmonic by minimizing the least square error. The results at the important pressure points are analyzed and compared for different subject using different waveform extraction techniques.

Blood pressure is estimated using the harmonic parameters. The approach studies changes in the parameters as oscillometric blood pressure recording is done. 8 harmonic parameters are obtained from the pulse characterization and are used to estimate Systolic arterial Blood Pressure, Mean arterial Blood Pressure, and Diastolic arterial Blood Pressure. The estimates are compared with our reference value to determine which has the best agreement. The proposed method is further compared with Maximum Amplitude Algorithm and Pulse Morphology Algorithm.

The effect of oscillometric waveform extraction methods on the proposed method is observed. The experiment established the fact that the extraction technique can alter the shape of oscillometric pulses. The methods were compared and it was observed that the used extraction methods did not make any significant difference on the accuracy, using this technique.

Acknowledgement

First of all, I thank you Jesus for the great courage, grace, help and wisdom you bestowed on me to undertake this project and to see to completion. It could never have been possible without you.

Special thanks to my astute professor and supervisor Dr. Voicu Groza, whose expertise, support and patience, added greatly to my graduate experience. I appreciate his vast knowledge and skill in this field of study and his guidance in writing this thesis.

I must also acknowledge the help of my research committee members and collaborators Dr. Hilmi Dajani, Dr. Miodrag Bolic, Dr. Izmail Batkin, Dr. Saif Ahmad and Dr. Sreeraman Rajan for their insightful comments and contributions which incented me to broaden my research perspective.

I thank my lab mate and research fellow Dr. Mohamad Forouzanfar, Koohi Iraj, Xinyang Zhang and Junjie Yin for the efforts and work we did together. I am particularly grateful to Erfan Niazi (PhD) who served as my graduate mentor for enlightening me through the process of this research.

Last but not the least I am heartily thankful to my family most especially my parents Mr. and Dr. (Mrs.) Abolarin for their endless spiritual, financial and moral support, for the period of my graduate studies. I also acknowledge the immeasurable support of Dr. and Mrs. Alice Kazah; Dr. and Dr. (Mrs.) Medu, as well as my brothers Abolarin Opeyemi, Ajayi Tunde and Awobusiyi Tolulope, not forgetting my godparents and guardians Colin & Mary McKenzie, for the quality care advice and support they rendered as well as my fiancé and best friend Nyaguthii Muraguri I thank you for the love, care and patience you exhibited during the time of this thesis.

I celebrate and acknowledge every one mentioned above; this thesis could not have been possible without you.

Table of Contents

List of Figures

List of Tables

List of Acronyms

A0 – Fundamental Frequency Amplitude

A1 – First Harmonic Amplitude

A2 – Second Harmonic Amplitude

A3 – Third Harmonic Amplitude

AI – Augmentation Index- A pressure ratio in mmHg and is defined as the difference of the systolic peak (F) and diastolic peak (P) over systolic peak of pulse waveform.

ANIBP Monitor – Automatic Non-Invasive Blood Pressure Monitor

BP – Blood Pressure- Measure of the pressure exerted by the blood in the arteries.

DBP – Diastolic Blood Pressure- Minimum pressure produced in the arteries that happens at the end of each cardiac cycle.

DC – DC Component is the mean value of the waveform. If the mean amplitude is zero, there is no DC offset.

DIA – Diastole – refers to the refilling of the heart with blood. The heart muscles are relaxed at diastole.

ECG – Electrocardiogram - Non-invasive recording of the electrical activity of the heart.

FW – forward-going pressure wave- Wave produced by flow of the blood into the arteries from left ventricle to the periphery side during systole phase of the heart.

MAA – Maximum Amplitude Algorithm- Height based algorithm to estimate blood pressure in oscillometry that is based on characteristic ratios.

MAP – Mean Arterial Pressure- Average arterial blood pressure of a person during a cardiac cycle.

mmHg – millimeter mercury- Commonly used unit adopted in blood pressure to measure pressure.

OMW – Oscillometric Waveform

OPI – Oscillometric Pulse Index –

P_c (t) – Function representing Cuff Pressure/ Deflation Waveform

P_p (t) – Function representing Pulse pressure

P_v (t) – Function representing Baseline

Phi1 – Phase parameter of the first harmonic

Phi2 – Phase parameter of the second harmonic

Phi3 – Phase parameter of the third harmonic

PMA – Pulse Morphology Algorithm: Pulse characteristic parameters used to estimate blood pressure in oscillometry. The method is none algorithmic.

PPG – Photoplethysmogram- Non-invasive recording of blood pressure pulse waveform obtained from the tissue pads attached to the ears, fingers, or toes where there is a high degree of superficial vasculature.

RW – Reflected Pressure Wave- Wave which is reflected from periphery side back to the heart in the arteries during the diastole phase of the heart.

RI – Reflection Index- An index to show the pressure reflected from the periphery side back to the arteries around the heart during diastole phase of the heart.

SBP – Systolic Blood Pressure- Maximum pressure produced in the arteries that happens at the beginning of each cardiac cycle.

SYS – Systole – period of contraction of the heart that leads to the gathering of blood. It occurs between the first and first heart sound of the cardiac cycle.

SI – Stiffness Index- An index characterizing features of the contour of pulse that are determined by PWV in the aorta and large arteries and by the stiffness of the arteries

Chapter 1: Introduction

1.1 What is Blood Pressure?

Blood Pressure (BP) is the measure of the pressure exerted by blood flow action against the blood vessel walls during cardiac cycle [4]. The heart is the body pump, pushing blood into the artery, and throughout the body [4] [59]. Arterial BP can be represented as a pulsatory quasi-periodical function of time ($p_b(t)$ - Fig. 1.1). The maximum of an arterial BP pulse is called Systolic BP (SBP), the minimum is Diastolic BP (DBP) and the average is called Mean Arterial BP (MAP).

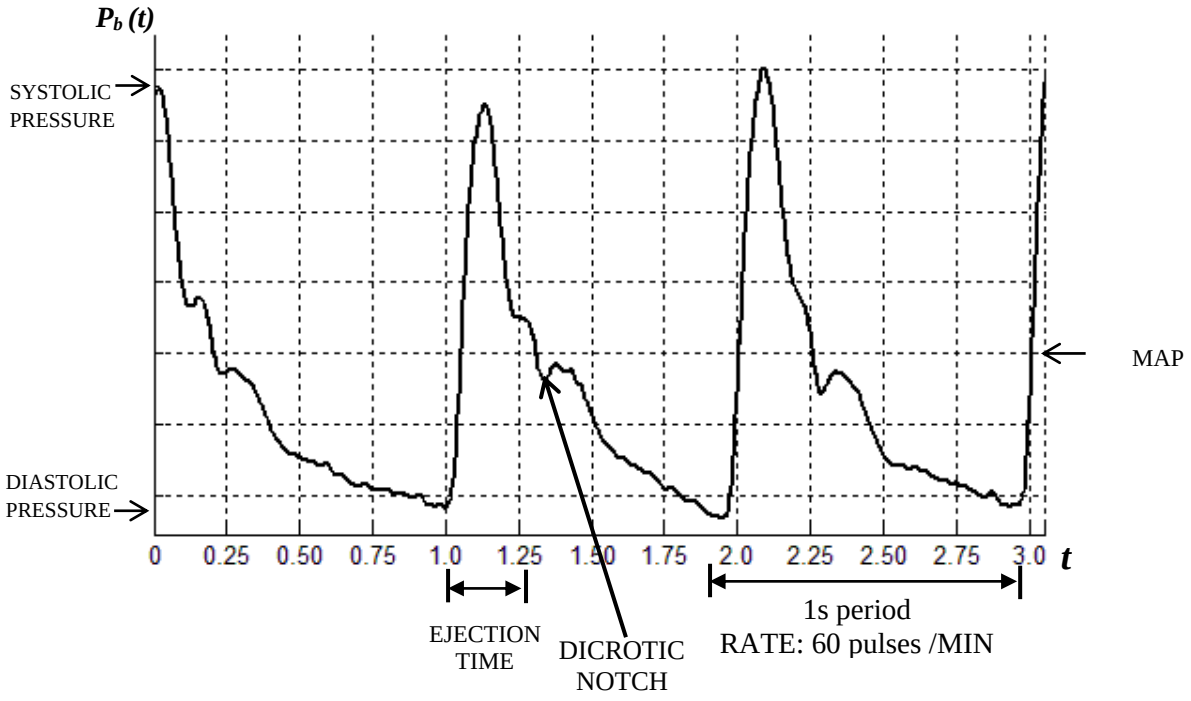

Figure 1-1: Illustration of blood pressure pulses in relation to time.
(Adapted from: http://www.creaghbrown.co.uk/anae/hdmon.htm)

The measurement of BP is currently understood in the medical terminology as to finding SBP and DBP, and/or MAP. BP is an important indicator of the health of an individual. By monitoring blood pressure, one can get important diagnostic information about the decline or ascent in the health of the individual [26]. A low arterial BP reading would

mean the patient is in crisis, and a higher reading could be a sign of some sort of ongoing disease [11]. Blood pressure problems can lead to a severe heart disease, stroke, hypertension (High Blood Pressure), heart failure, heart attack, kidney failure, vision problems and other health problems if left untreated [51]. It can also be the cause of inherent symptoms of eminent hypertensive condition including severe headache, frequent fatigue, disorientation, chest pain, difficulty in breathing, irregular heartbeats and blood in the urine.

In 2008 the National Health and Nutrition Examination Survey reported that approximately 65 million Americans have high blood pressure [8]. Other studies have shown that one of the leading causes of deaths in the world are cardiovascular and heart related diseases [3]. In addition, blood pressure is affected by several factors that are environmental, physiological, emotional, and pathological [36]. Thus, it suffices to say "a blood pressure measurement is only relevant to the circumstances under which it is obtained" [10]. Many works have studied these prevalent factors, emphasizing the need for research into more accurate method of determining blood pressure and other related measures.

Blood pressure has been measured directly (invasively) and indirectly (non-invasively) [1] [32]. The first ever documented measure of blood pressure was in the eighteenth century by Hales and it was done invasively. Invasive measurements are highly clinical, more accurate and more reliable than the non-invasive methods [2] - [4], [26]. It is however inconvenient, requires close monitoring and cannot be done without adequate training [4]. The dangers that cardiovascular diseases pose require consistent blood pressure monitoring and the need for devices that are accurate and easy to handle [4]. Automatic non-invasive blood pressure (ANIBP) monitor provides advantages such as: ease of use and low purchasing cost, and so they are readily found in homes with lesser possibility of

white coat effect [5] [10] [15]. The chief method used in ANIBP monitors in determining BP is oscillometry [3] [16] [17] [18] [20] [28] – [30].

In oscillometry, blood pressure is determined by analysing pressure oscillations. An Oscillometric Pulse Index (OPI) is obtained from the oscillometric pulses and an empirical algorithm is applied [5] [11] [22] [30] [31]. The accuracy of the algorithms used by these devices has often come under scrutiny [11] [15] [22]. Reports have shown that the algorithms amongst other factors cumulatively affect the accuracy of oscillometric BP [11] [30]. Recent ground breaking researches have focused on characterization of pulse wave morphologies [20] [37 – 39] [51]. These works show that pulse contour analyses contain and carry more details about the health status of the patient.

The employment of oscillometric blood pressure device encompasses several processes, which are important to the determination of blood pressure using ANIBP devices [44]. The process starts with the cuff setup, then the inflation/deflation process, Oscillometric Pulse Indexes (OPI) extraction, algorithm implementation and the result display. The focus of this work is the determination of blood pressure by characterizing of oscillometric pulses using mathematical methods. While attention is paid to ensure pulse integrity, the different extraction methods are compared across subject groups.

The most basic information in the analysis of a blood pressure measurement is the systolic and diastolic blood pressure values, which occur at the beginning and at the end of the cardiac cycle respectively [18] [19]. Systolic Blood Pressure occurs at contraction of the ventricles while Diastolic Blood Pressure occurs when the heart is relaxed [1] [5].

1.2 Pulse Characterization

Pulse characterization is the representation of pressure pulses using numerical values. The heart produces beats repeatedly, which causes pulsatile waves with consistent peaks in the

arteries. Pulse waveforms can be obtained non-invasively using Oscillometry [45] [46]. It is known that arterial propagation properties alter frequencies and amplitude characteristic of pulses [35 - 37]. As blood travels away from the heart, the complex artery-cuff interaction produces multiple oscillating harmonics and amplitude modulations [52] – [55]. This behaviour can be represented mathematically using Fourier analysis. The first introduction of this method was in 1950 to quantify flow [54]. The advantage of Fourier analysis of oscillometric waveform is that it enables representation of the frequency components at different pressure points, making it easier to analyze. [53] [54] [58]. Further signal processing makes it possible to easily compare the pulse-to-pulse frequency, amplitude and phases components.

The Fourier analysis is a method of analyzing a signal using weighted sum of cosine and sine with frequencies; such that when added together can best reproduce the original signal [58]. Conditions of periodicity and linearity must be met for Fourier series representation to be possible [54]. Several authors have expressed that blood circulation is not linear, neither is it periodic but the contribution of non-linearity to the steady state operation of the system is negligible [51] – [59]. Research shows the heart comes to a steady state in approximately 0.5 seconds from the time the impulse subsides [51] [59]. In addition, the continuous nature of heartbeats if recorded over a long period can be considered as periodic within an acceptable approximation [59]. Oscilometric pulse waveforms are acquired in various ways. From literature, it is understood that the most common method of extracting oscillometric pulses is by using a high-pass or band-pass filter [15] [29]. The first step after the acquisition of data is the extraction of oscillometric waveform. In this work, individual pulses were extracted from the oscillometric using various methods. Various pulse detection algorithms exist in literature. The proposed method identifies pulses using the Pulse Transit Time (PTT) method [70]. The effect of the extraction techniques on the pulse morphology will be compared.

A data fitting approach is taken to represent oscillometric pulses. The data is fit to a sine model by minimizing the least square error and calculating acquiring an optimal value. The model parameters are analyzed with varying cuff pressure on a pulse-to-pulse basis.

In addition to the above contributions, this work contributes to the list of existing oscillometric BP determination algorithms.

1.3 Motivation

This research is focused on the process of acquisition of pressure pulses from cuff pressure for accurate determination of Mean Arterial Pressure (MAP), Systolic Blood Pressure (SBP) and Diastolic Blood Pressure (DBP) using mathematical methods to characterize oscillometric waveform on a pulse-to-pulse basis. A research like this helps to effectively utilize local variations in the pulse characteristics for blood pressure estimations. Most works have studied these variations from time-domain perspective, and the waveform in a wholesome perspective neglecting the wealth of information in individual pulses. In this thesis work, the harmonic characteristics of individual pulses at specific pressure points are analyzed and compared for different subjects. Also we propose that this approach could provide a good estimate for other cardiovascular measures. Changes in the characteristics of the pulse waveform with different extraction procedures are studied at different cuff pressure points as well as their accuracy using the sine model. The method allows us to determine what extraction method would give the most preferred results using the estimation parameters.

1.4 Contributions

The main contributions of this thesis are as follows:

- Development of a novel approach to characterize oscillometric pulse waveforms using Fourier analysis.

- Developing a new method of estimating blood pressure using the slope of the harmonic characteristics of pulses.
- Development and investigation of a method of extracting oscillometric waveform using numerical integral approach.
- Development and Investigation of outlier pulse identification and correction methods.
- Analyzing the phasor behavior of pulse waveforms at important pressure points.
- Analyzing various methods of extracting oscillometric waveforms and the accuracy of each.

The proposed method uses the slope of the amplitudes and phases of the frequency components of the oscillometric waveform, as well as the slope of the direct current (dc) component to determine BP. The results are compared and reported in subsections of chapters 4 and 5.

1.5 Thesis Overview

In this thesis the characteristics of oscillometric pulse waveforms at different pressure points are obtained for different subject groups. In addition, a new method of estimating blood pressure is proposed using the frequency parameters of the pressure waveforms.

Chapter 2 presents background and review of past and most recent works. The progressive development of blood pressure measurement techniques is also presented. In addition, criticisms of current oscillometric algorithms and research works on their improvement are highlighted. Pulse is defined physiologically and mathematically. An introduction into the representation of pulses is presented and prior works in this art are highlighted. Sections relating to the proposed method are discussed and defined.

Chapter 3 presents the systematic and technical approach taken to achieve the proposed method.

In chapter 4, the reports of the proposed algorithm for the dataset used are presented. Plots of the changes in behavior of the parameters with changing cuff pressure are shown. The algorithm is used to estimate blood pressure. Comparisons between subject groups is presented.

Chapter 5 discusses the results of the proposed methods as presented in chapter 4. The chapter highlights: observations from the results, comparison of different oscillometric waveform extraction methods, and outlier detection and correction mechanisms.

Conclusions are made in chapter 6. The chapter ends with a summary of the work, proposed future work on the topic and the contributions of this work.

Chapter 2: Literature Review

Blood pressure (BP) is the pressure of blood as it flows through the vessels. It is caused by the force of the blood rapidly pumped from the heart, exerted on the wall of the artery. Two values are important when referring to blood pressure: they are systolic and diastolic blood pressure [19]. Systolic blood pressure (SBP) is the maximum pressure achieved at the beginning of the cardiac cycle [19] (figure 2.1). Systole refers to the period of contraction of the ventricular muscle, causing blood to be pumped into the pulmonary artery and the aorta [5]. Diastolic Blood Pressure (DBP) is the minimum pressure at the end of the cardiac cycle [5] [19] (figure 2.1). Diastole is the period of dilation of the heart cavities as they are filled with blood getting ready for the systole. The mean arterial pressure (MAP) is the average pressure value during a cardiac cycle.

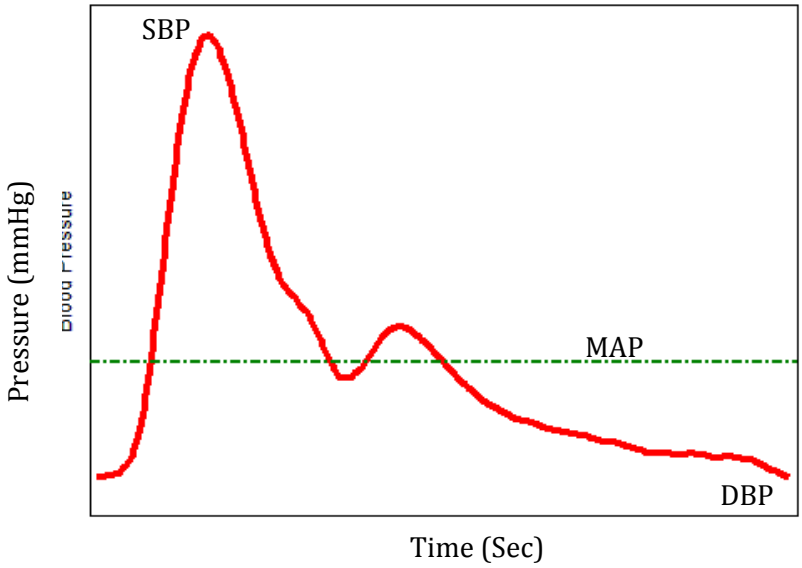

Figure 2-1: Intra-arterial blood pressure pulse showing SBP, DBP and MAP

2.1 Methods of Measuring Blood Pressure

Blood pressure measurement is one important practice in clinical medicine [51]. Methods of determining BP values have advanced with better technology. However, it is worthy of note that despite the advancement in technology, medical experts still find it difficult to determine

a perfect and accurate estimate of BP [11]. This is because, it is affected by various factors, which can be physical, physiological or pathological in nature [36 - 37].

BP measurement techniques can be categorized as direct (invasive) and indirect (non-invasive) methods [32]. Direct measurement uses catheterization. This method is the earliest known and the most accurate of the BP measurement methods. It is not commonly used except in intensive care unit (ICU) for patients with rapidly varying arterial pressure. Direct method is able to monitor the beat-by-beat fluctuations in blood pressure [4] [10].

Indirect method of measuring blood pressure is more frequently used in modern medicine. It is not as accurate as the direct method of measurement [10] [51]. The operation of indirect BP measurement devices is such that it adjusts and correlates known external physical phenomenon and measures it either empirically or clinically [4] [9]. Auscultation and Oscillometry are the two main popular methods in this category [5] [11] [14] [32]. Other indirect measurement methods include: palpation, vascular offloading, tonometry, pulse wave velocity. Table 2.1 gives a brief summary of the advantages and disadvantages of different indirect blood pressure monitoring methods.

A sphygmomanometer is a blood pressure measuring instrument, consisting of an inflatable rubber cuff with a pump and a column of mercury (figure 2.1). The cuff is connected to the mercury column which has a pressure scale. To determine blood pressure, the cuff is wrapped around the arm and gradually inflated by pushing the pump repeatedly until the artery is occluded [5]. The cuff is then gradually deflated by opening the valve connected to the pump. The operator determines the blood pressure by listening to the heart sound (Korotkoff sound) with the aid of a stethoscope, or by palpation. Reference is made to the mercury scale to determine the corresponding pressure.

Both auscultation and oscillometric methods operate with the concept of a sphygmomanometer; requiring an occluding cuff and the detection of pulse. Oscillometry would be further discussed in details.

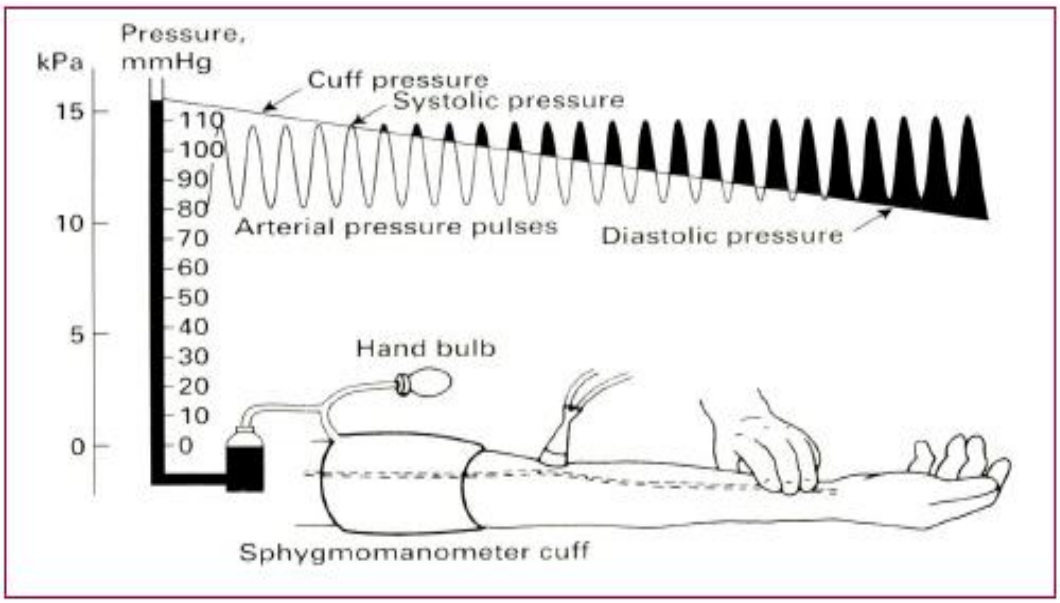

Figure 2-2: Indirect Method of Determining Blood Pressure showing a sphygmomanometer, palpation and a stethoscope.
(SOURCE: John G. Webster. 4th Edition Medical Instrumentation, Application and Design [54] page 325)

When using the sphygmomanometer methods, it is important to first choose the right cuff size [11] and evenly spread it over the arm so that the pressure from it is evenly passed via the interpose tissue to the underlying artery. In addition, care should be taken to place the cuff at the level of the heart so as to have the same hydrostatic component [2] [3] [29]. Standards for choosing cuff sizes and setup procedure are discussed in [2] [29].

2.1.1 Auscultatory Method

Auscultatory method determines BP with the use of the auditory sense by detecting Korotkoff sound (Heart sounds) [2] [9] [11] [13] [29]. To perform auscultation, the cuff of the sphygmomanometer (figure 2.1) is used to occlude the artery. Korotkoff sounds are heard during cuff deflation: as the artery lumen closes and opens, blood is allowed to flow again

[5]. Korotkoff sound occur in 5 phases [5] [29]. SBP is the pressure at which the first phase of Korotkoff sound occurs while, DBP is the pressure at which Korotkoff sounds fades off (Korotkoff phase V) [5] [9].

As heart sound travels through the body, the sound waves are not reflected but are rather attenuated [29]. The attenuation varies with changing width of the blood vessel. Detection of this sound is done with the help of a stethoscope.

This method is the most used (gold standard) in medical practices and can be used quite accurately for infants and hypotensive patients [3] [9] [10] [11] [13] [16] [17] [55]. However, the accuracy of the analysis is largely dependent of the good hearing acuity of the operator [17].

2.1.2 Automated Sphygmomanometer

Automated blood pressure measurement methods became possible with the use of microprocessor [51]. Three successful automation techniques worth mentioning involve the use of an automatically occluding cuff, the incorporation of a microphone to detect the Korotkoff sound [5] [9], motion detection as in ultrasound; and the incorporation of a pressure transducer with a computerized algorithm as in oscillometry.

Table 2-1: Brief details of the various methods of measuring BP

Method	Definition/ advantages and disadvantages
Palpation	Use of tactile sense [7]. Can be used in emergency. Used for determining SBP [9] [32] [51]. MAP cannot be determined [2]
Ultrasound	Use of a transcutaneous Doppler motion detection sensor. Detects motion in various occlusion states. It can be used for infants and hypotensive individuals and can be used in noisy places. It is susceptible to moving artefact. [3][9] [32]
Vascular unloading	It is based on the unloading of artery. The principle is that the artery is unloaded when transmural pressure is zero. Thus, constant and equal pressure is kept at all times on the artery. If external pressure applied to an artery is equal to the arterial pressure at all times the artery will be unloaded and will not change size. [9]

Tonometry	Based on the principle that the external force exerted on the surface of a partially flattened or applanated artery is nearly proportional to the pressure in the artery an arterial waveform [9]
Auscultation	Based on the detection of Korotkoff sound. It requires training to be correctly used. Less accurate in patients with heart failure, pregnancy, obesity and cardiac arrhythmias [3]
Oscillometry	Based on the analysis of oscillometric pulses. It is easy to use. Less accurate in children and elderly people with cardiac arrhythmias [3]
Volume-Oscillometric	The method is similar to the operation oscillometry, but based on arterial volume oscillation [9].

2.2 Oscillometry

Oscillometry is the analysis of the amplitude of oscillations that appear in a deflating cuff [5] [11] [36] [51]. The oscillations are created by the expansion of the arterial wall each time blood is forced through the artery in a deflating cuff [19]. The first introduction of this method was in 1876 by French scientist Etienne-Jules Marey [15] [17] [22] [24] [7]. Marey placed his arm into an airtight chamber and pumped air into it [35]. He noticed that the pressure in the chamber fluctuated as the air was displaced due to his pulses [22] [7]. The magnitude of the fluctuations indicated that the external pressure was equal to the arterial pressure [7]. The oscillation increases from the start of the measurement until it reaches a maximum value; it then begins to decrease [5] [9] [19] [22]. Research has shown the pressure at the point of maximum oscillation is the MAP [5] [15] [22] [23] [24].

2.3 Oscillometric Monitor

The most commonly used Automatic Non-invasive Blood Pressure monitor is the oscillometric device [13]. Oscillometric monitors are easy to use and readily found in homes therefore they have become popular electronic BP monitors [5] [9] [16] [17] [19] [55]. The devices make use of an automatically occluding cuff, which is placed around the arm or wrist. The cuff rapidly inflates to about 20-30 mmHg above the expected systolic pressure (supra-systolic), then it is slowly deflated from this value, to a pressure lower than the diastolic value at a rate of 2 to 3 mmHg per second [13] [15] [16] [17] [20] [23].

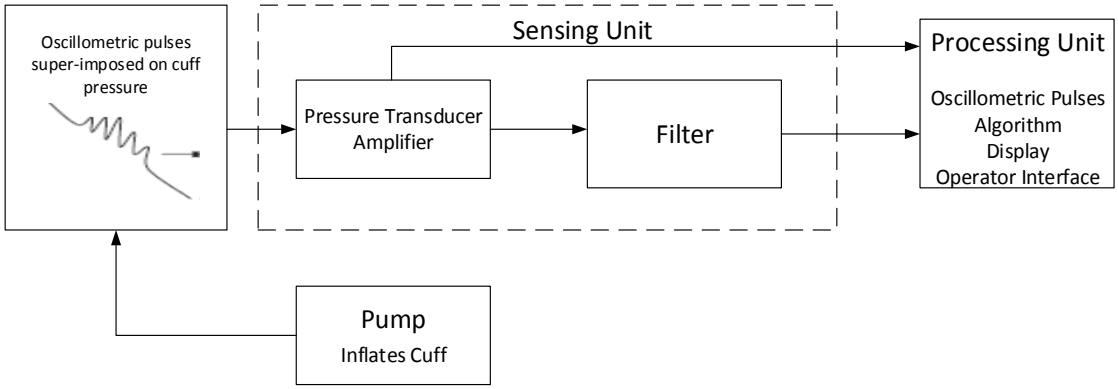

Figure 2-3: Block Diagram Illustrating the Functional Components of an Oscillometric Blood Pressure Monitor.
(Adapted from: [44] J. N. Amoore, "Extracting oscillometric pulses from the cuff pressure: does it affect the pressures determined by oscillometric blood pressure monitors?" and [11] J. N. Amoore, "Oscillometric sphygmomanometers: a critical appraisal of current technology.")

A pressure transducer and an amplifier help to sense the pressure introduced into the cuff [11] [20] [44]. The oscillometric device analyzes the oscillations and derives a waveform with the aid of an amplifier and filter [11]. The systolic and diastolic value is calculated using a programmed algorithm and the oscillometric waveform features [5] [6] [11] [22]. The computed result is then relayed to the display of the device. In comparison with auscultation, this method is able to determine the MAP and it is easier to use. The principal method by which the data for this research was gathered is the oscillometric method. Thus, the focus of this review would be on oscillometry.

2.4 **Definition of Terms in Oscillometry**

Oscillometry involves several processes. They include: inflation and deflation of the cuff to generate the cuff pressure, extraction of the oscillometric waveform (OMW), analysis of pulse characteristics (pulse-by-pulse), construction of the Oscillometric Pulse Index (OPI) and the application of the algorithm [11] [44].

The cuff pressure $P_c(t)$ contains two components: the pressure induced by the pump ($P_v(t)$) and the pulse pressure $P_p(t)$ exerted by the intra-arterial blood pressure $P_b(t)$ onto the cuff

through the arterial wall, flesh, skin and other tissues (Fig. 2.4): $P_c(t) = P_v(t) + P_p(t)$; where $P_b(t) = P_p(t)$.

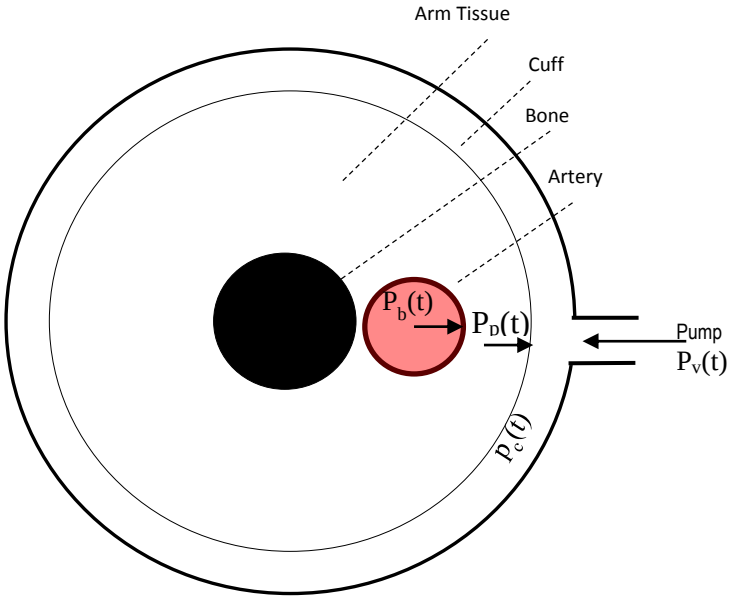

Figure 2-4: Cross-section of the cuff-arm artery system

The pump increases $P_v(t)$ fast from a minimum that is equal to the atmospheric pressure(P_A), till a value higher than the expected SBP, in order to block the blood circulation under the cuff; then, the pump stops. A valve is open to allow the $P_c(t)$ to decrease at a slower pace. As cuff deflates, the cuff pressure gets smaller than the maximum blood pressure, then blood starts to flow through the freed artery and small pressure pulses are induced in the cuff by the blood pulsatory flowing through the artery as shown by $P_c(t)$ – (the blue graph of Fig. 2.5). $P_v(t)$ – referred to as the baseline of the pulse pressure or the induced pressure – is represented by the red graph in Fig. 2.5.

Three important functions are obtainable from an oscillometric BP measurement: the Cuff Pressure (Pc(t)), Pulse Pressure ($P_p(t)$) and derive pressure called the Baseline $P_v(t)$. Methods of determining the baseline is later discussed in this work.

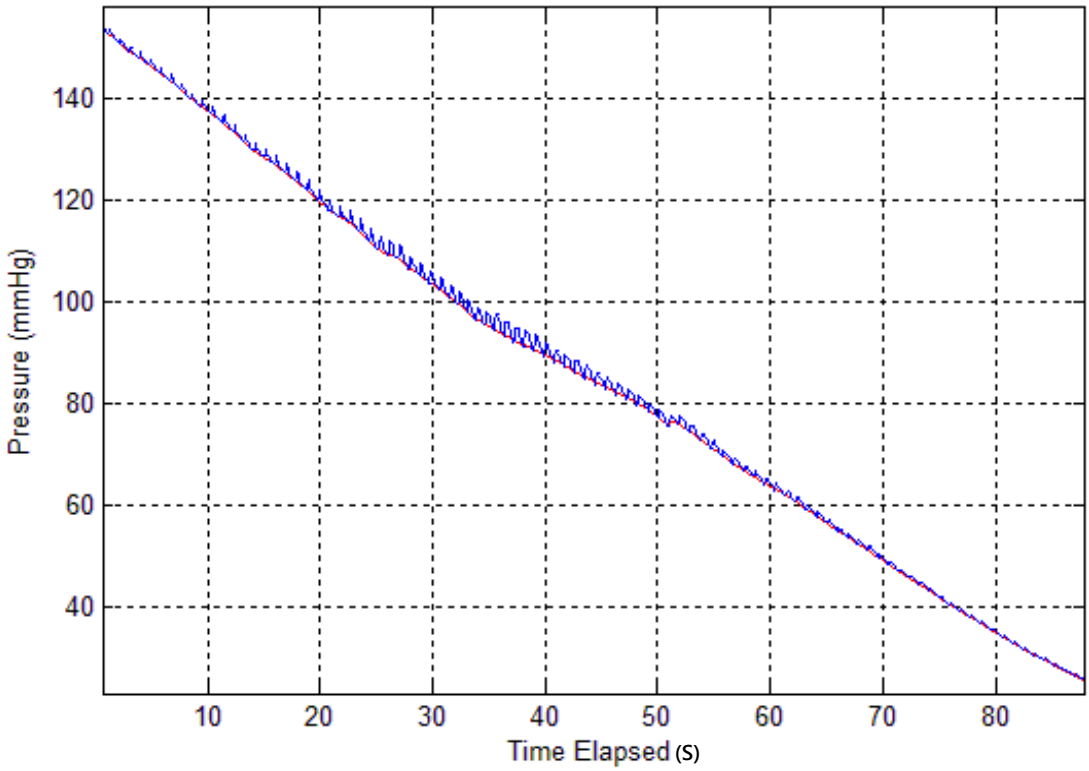

Figure 2-5: Plot of Cuff Pressure Deflation Waveform *(P_c (t))* (Blue) showing the Baseline *(P_v (t)* *(Red)*

$$P_p(t) = P_c(t) - Pv(t)$$

In an oscillometric recording, oscillometric pulses appear as a series of low amplitude pulses that are superimposed on a slow decreasing trend [11]. The baseline is the pressure induced by the device as it is attached to the individual's arm (Fig. 2.5 (red)). This combined with the pulse pressure gives the cuff pressure deflation waveform (Fig. 2.5 (blue)). "A cuff deflation waveform is a graphical representation of the change in pressure within an inflated cuff as the cuff deflates. It shows the complex interactions between the cuff and the surface of the individual's arm as blood flows through the arteries".

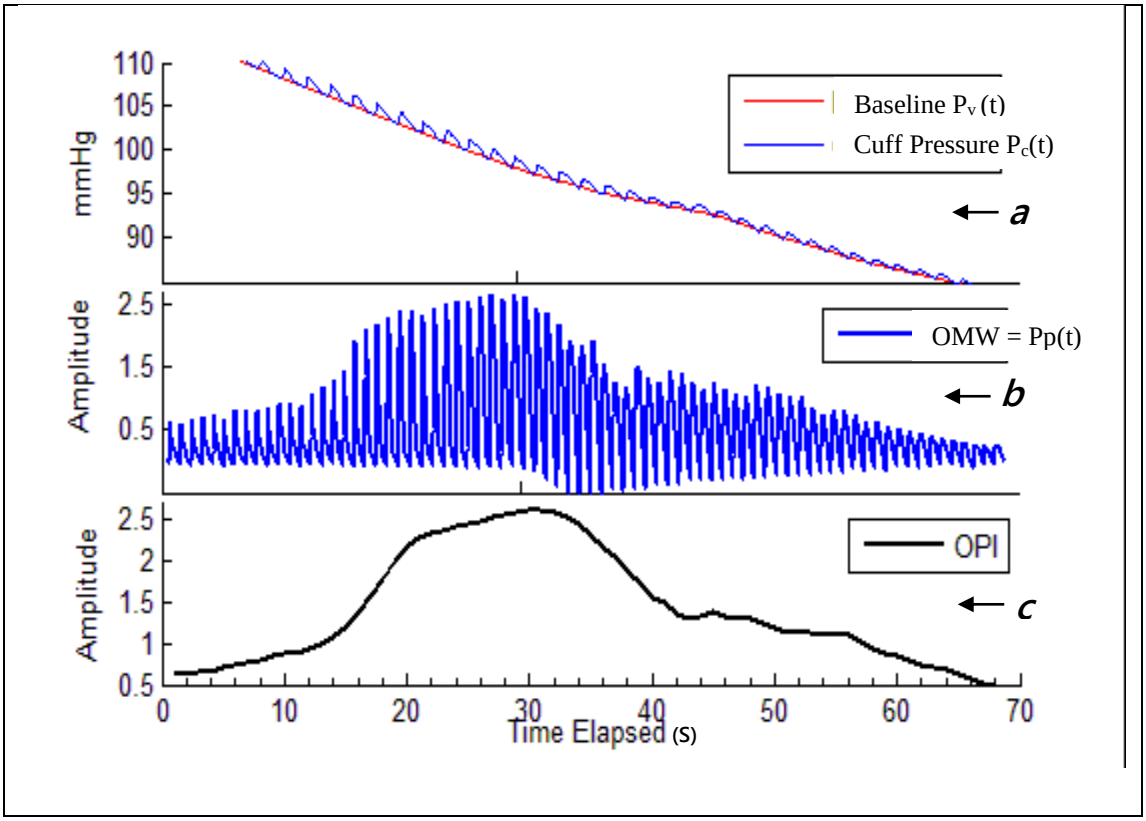

Figure 2-6: (a) Plot of the cuff deflation waveform,
(b) Plot of the extracted oscillometric pulse pressure *(OMW = Pc(t) - Pv(t))*
(c) Plot of the oscillometric pulse index (OPI)

An OMW (Fig 2.6a) is a graphical presentation of the variations and interactions between the oscillometric pulses with the cuff pressure [11] [28] [31]. The OMW (Fig 2.6b) is formed from oscillometric pulses and it is extracted from the cuff deflation waveform [11] [26]. The most typical method of extracting the OMW is by filtering the cuff pressure Pc(t) using a high-pass filter (HPF) or band-pass filter (BPF) [13] [15] [30] [32] [44]. Then a Low-pass filter (LPF) is also used to smoothen the pulses, reduce the noise by removing the low frequency component (dc component) of the deflating cuff [15] [44]. Subtraction of the trend by constructing a baseline has often been used in literature [11].

The oscillometric waveform (OMW) and its accurate extraction is key to the accuracy of the oscillometric BP [28]. Oscillometric BP is determined from the oscillometric pulse index

(OPI) of the oscillometric waveform. The OPI (Fig 2.6c) is determined in various ways. It can be defined as the width of the peak-to-peak OMW pulse amplitude, or the successive baseline amplitudes of the pulse pressure or the partial, or total integration of the oscillometry pulse [9] [19].

By observing, the OPI (fig 2.6c) one can easily identify a maximum. The peak point of the OPI mapped to cuff deflation pressure waveform to find the corresponding pressures value representing the MAP empirical ratios are used to determine SBP and DBP [9] [21] [22] [31].

2.4.1 Algorithms for Blood Pressure Determination

Oscillometric devices make use of vendor specific algorithms to determine SBP and DBP [5] [15] [16] [17] [19] [30]. These algorithms are proprietary and as such, they are not disclosed in the device manual [6] [11] [15 – 17] [20] [31]. Non-disclosure makes it impossible for researchers to test the validity of these algorithms thus, raising controversies as to their accuracy [6] [15] [20] [31]. A few researchers have investigated some of these devices, mainly their algorithms and their variations will be further highlighted.

Oscillometric BP algorithms are categorized based on either height or slope/feature point of the oscillometric envelope [9] [16] [17] [19] [28] [55]. Height based criteria algorithm also known as characteristic ratio algorithm determines SBP and DBP as tested fractions of the oscillometric envelope [16] [19] [22] [23] [35]. The question of the accuracy of ratio algorithm has been the subject of many researches [15] [22] [28]. Amongst other factors, the accuracy of the algorithm is dependent on the accurate construction of the OPI [2].

Using these algorithms, systolic BP (SBP) is found as “the baseline cuff pressure that is greater than the MAP, and the pressure at which the ratio of the oscillometric pulse amplitude over the maximum pulse amplitude is equal to a certain predetermined value” [9]. SBP value is located on the left-hand side of the MAP [19] [56]. On the right-hand side of the MAP

using the same criteria, “the diastolic pressure is determined as the baseline cuff pressure that is lower than the MAP, and the pressure at which the same ratio is equal to another predetermined value” [9] [19] [56].

2.4.2 Maximum Amplitude Algorithm (MAA)

The most common algorithm to finding SBP and DBP is the Maximum Amplitude Algorithm (MAA) [26]. The MAA uses the maximum amplitude of the OPI and the characteristic ratios are applied to determine SBP and DBP. This is done by multiplying the OPI of the MAP with the respective characteristic ratios. Their resultant OPIs are found on the left side for SBP and on the right side for DBP and the pressure value is read from the deflating cuff [13].

Various researchers have reported different values for systolic and diastolic ratios [13] [14] [15] [16] [19] [28] [31]. Research has shown that most devices use values that are within the ranges of 45% - 70% and up to 60% - 80% of maximum amplitude for systolic and diastolic respectively [15 - 16] [19]. This is because different manufacturers use unique algorithms which are different from instrument to instrument.

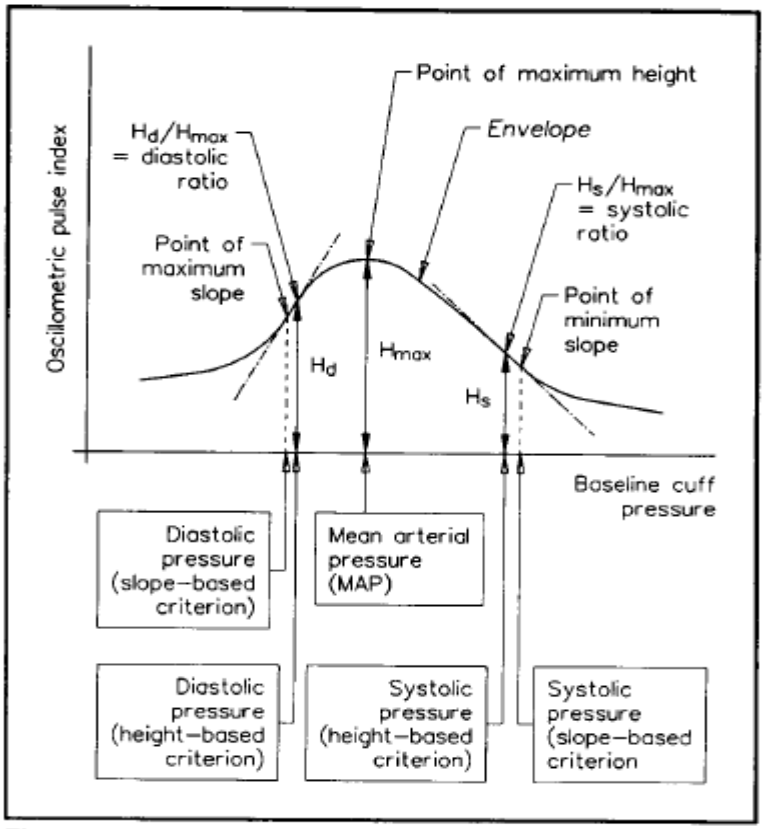

Figure 2-7: Slope and Height criteria for estimation of Oscillometric Blood Pressure (SOURCE: Survey of automated non-invasive blood pressure monitors 2011, [9])

2.4.3 Slope-Based Criteria

Using the slope-based criteria algorithms, the systolic value is determined as the static pressure of rising inflexion of the OPI envelope, while the point of dropping inflexion of the OPI envelope refers to the diastole [17] [52] [57]. That is, the baseline cuff pressure at which the oscillometric pulse amplitude increases rapidly and becomes fairly uniform is taken as the systolic pressure [19]. While that at which the amplitude decreases rapidly is taken as the diastolic pressure [19]. The points on the slope are mapped to the cuff pressure curve and taken as the corresponding systolic and diastolic pressures [19].

Other algorithms have been proposed for the determination of oscillometric BP but most of them were not clinically validated. SBP, MAP, and DBP are determined in this thesis by a harmonic characterization of pulse morphological studies using a mathematical modelling optimization approach. This is presented based on the study of morphological characteristic

of oscillometric pulses to occur with minimal non-linearity as such they can be modeled using Fourier series. The results are compared to the BP values derived from an Omron BP device.

2.5 Challenges and Prior Arts

The strongest arguments against the accuracy of oscillometric blood pressure measurement method have been: the determination of systolic and diastolic blood pressures [15] [22], mode of determination and non-uniformity of characteristic algorithms [5] [11] [15], and the lack of theoretical basis for uniqueness of oscillometric waveform and the fact that it is largely affected by various factors [11] [22] [28]. Some critics of the characteristic ratio algorithmic method have also stated that the oscillometric BP method is more empirical than physiological (i.e. quasi-empirical) and lacking theoretical explanations [5] [11] [15] [28 – 30]. Other reports say that algorithmic approach neglects important arterial mechanics [11] [26] and it is selectively accurate [11] [15] [28] [30] [33] [56].

Because of these challenges, researchers have worked at investigating factors affecting oscillometric algorithms [11]. *J. Moraes* [14] found characteristic ratio and the size of the arm and cuff amongst others, as the biggest influencers of the measurement accuracy of SBP and DBP. *G. Drzewiecki et al* [13] took a mathematical modelling approach, and considered various biomechanical dynamics that affect the choice of empirical ratios. *Rein Raamat et al* [22] determined a more accurate MAP by simulation, using pulse volume and shape relationship stating that accurate MAP would imply be more accurate SBP and DBP using the characteristic ratios. By simulating oscillometric pulses *J. Amoore et al* in [31] found that the shapes of oscillometric pulses was a major determinant in the accuracy ratio algorithms and thus affects the choice of proprietary characteristic ratio. *S. Chen et al.* [19] implemented the Linear Amplitude Algorithm (LAA). LAA considers situations in which it is difficult to ascertain what the exact peak of the envelope corresponding to the MAP is. The amplitude is approximated by two lines of best fits on both sides of the slope. SBP and DBP values are

determined as in MAA. It has been reported that algorithms based on the slope criteria are more robust to artefacts and extraneous noise [9] [19] [20] [22]. Other initiatives have suggested a combination of algorithms to gain better advantage of them [19].

Groza et al. in [20] initiated a better appreciation of the OMW by introducing a method of determining blood pressure using pulse morphologies. Various other attempts have also been made to analyze the shape of oscillometric BP pulses [20] [18] [21] [28] [31 - 36]. These works inspired the need for more in-depth look at the shape of oscillometric waveforms. They suggested that changes in pulse morphologies of the deflation waveform contained important information about the blood pressure and cardiovascular health of an individual [20] [31] [34].

Mathematical modelling of oscillometry has been the subject of most recent research because of the need to understand arterial mechanics and to numerically represent its behaviour [13] [18] [23] [29 – 33]. The influence of respiration on the frequency and amplitudes of pulsatile physiological signals was investigated using a mathematical modelling approach [23 – 25]. *G. Drzewiecki et al* [13] and *Raamat et al.* [30] reported the nonlinear effect of biomechanical factors on oscillometry. *M. Ursino and C. Cristalli* [24] and *Gye-rok Jeon et al* [32] specifically characterized the complex cuff-artery interaction of an occlusive cuff and the pressure-volume dynamics on the brachial artery as relates arterial compliance and nonlinear cuff behaviour. A modelling method of determining blood pressure by identifying the most significant pulse without the use of the OPI was proposed by *K. Barbe et al* in [29]. *Mohamad et al* in [18] and [50] implemented a ratio-independent method and later an algorithm using Neural Networks to determine BP from extracted features of oscillometric pulses [26]. These researchers claim to implement ratio free methods of estimating BP by modeling oscillometry. The proposed method in this thesis takes a mathematical modeling approach, considering a frequency analysis of pulses; we assume a non-linear sinusoidal model to

optimize oscillometric waveform on a pulse-to-pulse basis. The Least Square (LSQ) optimization algorithm is used to determine the best fit to the data by minimizing the least square error.

2.6 Pulse Morphology, Characterization and Modeling

2.6.1 What are Pulses?

This is the characterization of the oscillatory component of the circulatory and respiratory systems. “A blood pressure pulse consists of a sharp upstroke, straight rise to the first systolic peak, a definite sharp incisura and a near exponential pressure decay in late diastole” [36] [51].

Physiologically a pulse is formed from the complex interaction between the left ventricle of the heart and blood circulation system [27]. Figure 2.8 shows two wave strokes that occur in a blood circulation process. The first is a forward-going pressure wave (Fw) called the systole, formed at the contraction of the ventricle [27] [37].

A second stroke originates at the end of the systole as a reflected wave (Rw) caused by the closure of the aorta [27] [37].

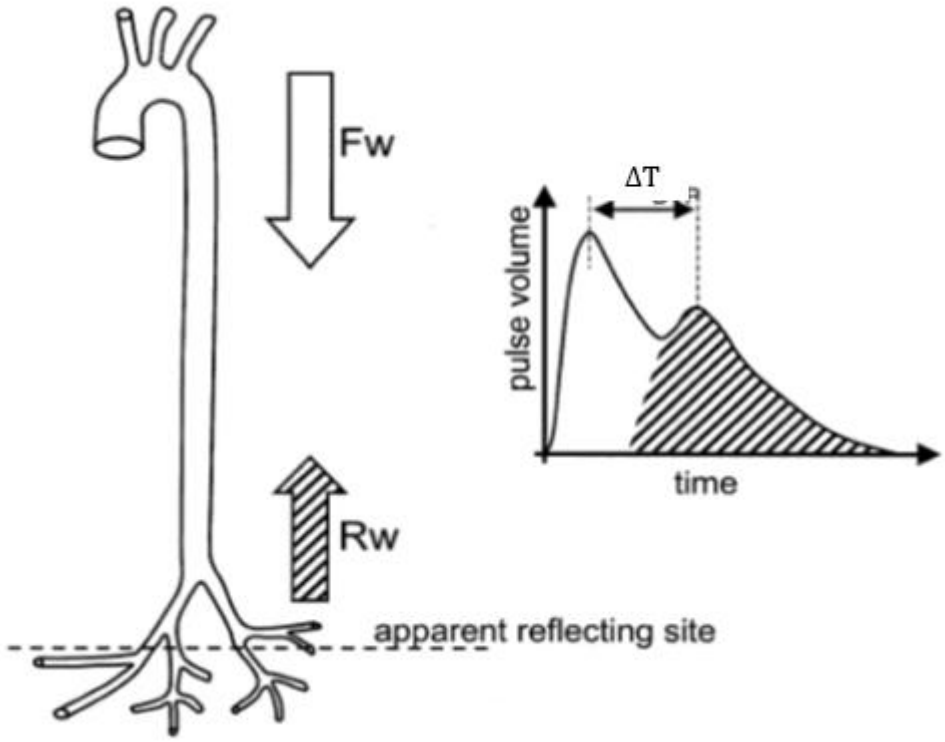

Figure 2-8: Illustration of the Formation of Pulse showing Forward and Reflective wave
(SOURCE: S. C. MILLASSEAU, R. P. KELLY, J. M. RITTER and P. J. CHOWIENCZYK
Determination of age-related increases in large artery stiffness by digital pulse contour analysis [38])

These strokes form the two peaks that are seen on a blood pressure pulse. The notch is a point of superposition of the waves marked by a deepening (figure 2.8). It is usually about three-quarters way into the pulse and it is caused by the closure of the aortic valve. Pulses can be observed while recording an individual's blood pressure. Thus, a pulse waveform can be defined as a combination of blood pressure pulses over a measurement cycle [27] [31]. Parameters describing oscillometric pulse wave are discussed in literature [20] [37 – 39] [41].

2.6.2 Pulse Contour Analysis

Pulse morphology refers to the shape of pulses over a cardiac cycle. Pulse contour parameters have been found to provide significant diagnostic information about the cardiovascular system and the heart functions [4] [13] [20] [27].

It is known that pulses undergo local variations or changes at various pressure points during a recording [4] [13] [17] [20] [27] [34] [36]. Pulse wave analysis studies in [13] [20] [27] [28] [36] [37] showed factors that determine, and affect shape of pulses which can be physiological, pathological and psychological. Some of the factors included are growth, aging, physical fitness, foods, heart rate, exercise, body height, gender and diseases. The dynamics of these factors account for the uniqueness of individual pulse morphology and can be investigated by pulse contour analysis [36]. These factors also affect the ability of the artery to expand and contract as blood flow through [27] [36] [38]. This ability of the artery is referred to as arterial compliance. Arterial compliance affect the flow of the reflected wave ((Rw) fig. 2.8) and the path of the forward wave ((Fw) fig. 2.8)) which determined the pulse shape [27] [36] [38] [44]. Thus, wave propagation properties of cardiovascular systems are what determine the shape of pressure pulse by altering their frequency characteristics [35 - 37] [44] [51].

An obvious change is the amplification and change in shape of arterial pulses in an OMW as they travel away from the heart [4] [11] [22] [31] (fig. 2.9). A closer look makes it clear that there are local variations in the form of multiple ripples in a pulse. This information reflects the state of the vessel over the span of a single cardiac cycle [13]. Pulse morphology studies are thus inevitable if the wealth of information in a pulse is to be tapped [4] [31 - 34].

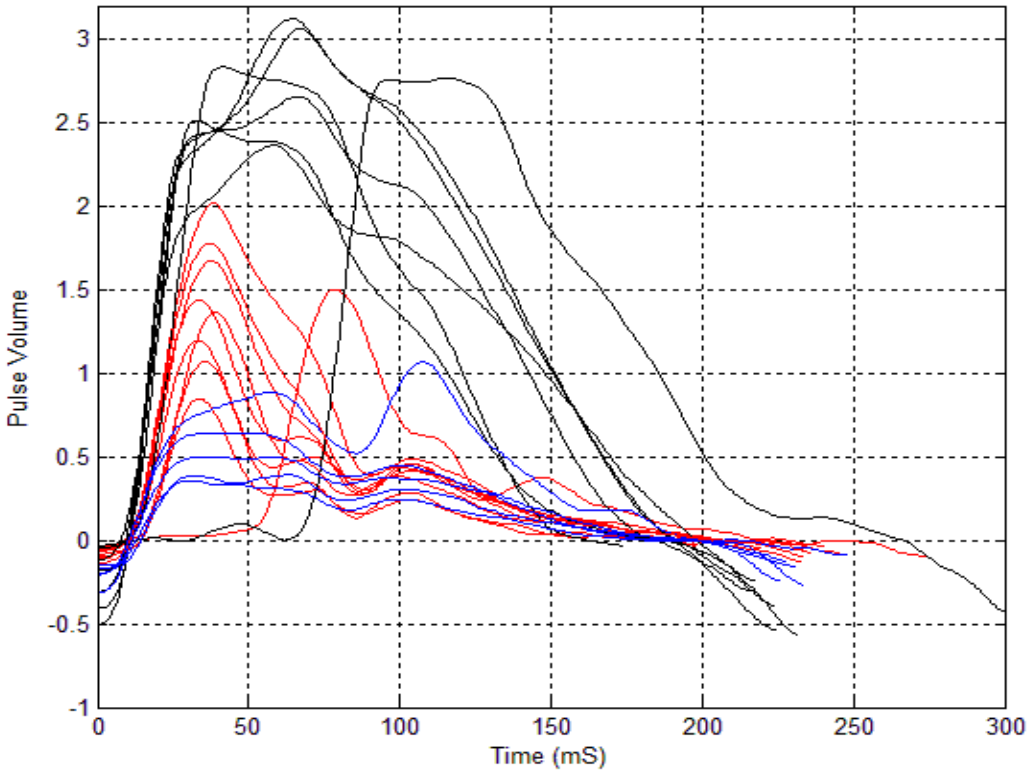

Figure 2-9: Changes in pulse wave contour at different pressure point during a recording. (Red line represents samples of pulses recorded close to SBP (RED), black line represents samples of pulses recorded close to MAP (Black) and blue line represents samples of pulses recorded close to DBP (Blue)[1])

Various researchers have highlighted the preservation of pulse shape as crucial for the correct identification of the information it carries about the heart condition [28]. Shape preservation and extraction procedures would be further discussed in this review.

2.6.3 Oscillometric Pulse Extraction

Pulse waveform can be obtained invasively or non-invasively. Some of the non-invasive methods of acquiring blood pressure pulse waveform are tonometry, photoplethysmography (PPG) and oscillometry [45] [46] [51]. Most commercial NIBP monitors measure SBP and

[1] "Pulse wave contour varies in different parts of the circulation. It depends on physiological or pathophysiological conditions of the organism. The heart rate, the body height and the age, as well as BMI or body fat belong to important physiological phenomena" [37].

DBP only. *Saif et al*. [72] presented a prototype device to record blood pressure pulse waveform as well as the ECG.

Various methods have been used to eliminate pulse artifacts in oscillometric recordings. Most of the methods have been on the analysis of pulse characteristics and the use of pulse transit time (PTT) to track pulse occurrence [9] [45] [46].

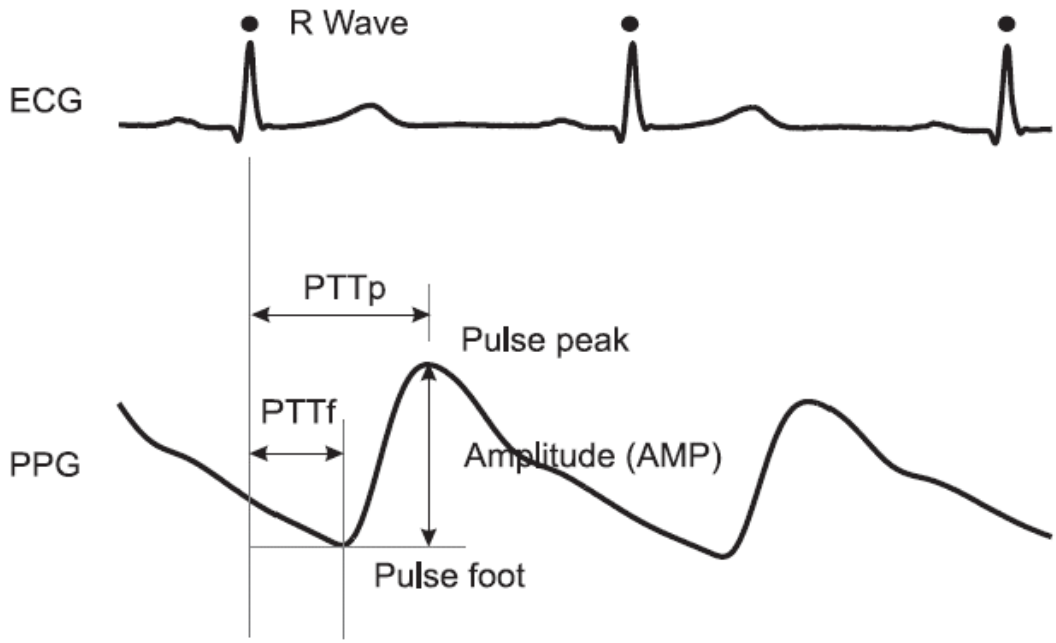

Figure 2-10: Plot of ECG showing how it relates to blood pressure [45]
(Source: J.Allen, "Photoplethysmography and its application in clinical physiological measurement" Clinical Science, Vol. 103, pp. 371-377, 2002 [45])

PTT is the elapsed time between the blood being ejected from the heart and the arrival of the pulse at an extremity, typically a finger. PTT makes it possible to trace beat-to-beat pulse using the QRS complex of the ECG [9] [45] [46] [70]. Two physiological signals are used to determine that PTT: ECG and the Photoplethysmography (PGG) (fig 2.10) [45] [46].

ECG trace can be used to infer the point at which the heart beats in oscillometry [72]. The peak of the R-peak of the QRS complex is a good indicator for the origin of a blood pressure pulse (fig 2.10) [45] [46] [72] [70]. Thus, a combination of an ECG signal and Oscillometric

waveform can help indicate the origin of individual pulse making it easier to extract [45] [46] [72]. Beat and pulse detection algorithms are available in literature [40 – 43].

Because physiological pulse signals (such as OMW or PGG) are weak and occur at low frequency, they can be easily contaminated by artifacts [40]. Artifacts such as deep breathing, tremors and arrhythmias can affect the process of extracting pulses [13] [15] [35]. Thus, much research has been done on the need for careful extraction of pulses and various methods have been used for pulse extraction [19]. *Amoroe et al*. in [44] and [11] based their research on the accuracy of pulse waveforms extraction. They argued that the way to generally improve oscillometric blood pressure measurement is to focus on the overall processes that enable the device to determine blood pressure rather than a myopic focus on just the BP determination algorithm. The report showed that the process of extracting the oscillometric pulses could alter the shape of the pulse [11] [44]. They further proved that these alterations were not uniform across all patient groups proposing a possible explanation for their selective accurate. They also opined that it is unlikely to get a right analysis from oscillometric devices regardless of the accuracy of the algorithm if the input is erroneous. Thus, he proposed a validation technique that encompasses all aspects of the device function and not just the algorithms [11].

2.7 **Pulse Characterization using Sum of Sinusoids**

As expressed earlier, various attempts have been made to characterize pulses and determine blood pressure using quantitative and mathematical modeling measures [20] [48] [49]. Generally, physiological signals are difficult to reproduce because of their unique nature but advances in signal processing methods have been made to describe bio-signal components of pulses using transforms in such a way that numerical values can be attributed to them [17] [59]. The most common transforms are Fourier transforms and frequency analysis [17].

“Time-dependent functions of arterial pressure and flow relationships can be expressed in frequency domain using Fourier analysis.” [51]

The signals are pulsatile and exhibit wave propagation behaviors. “The shape of the pulse is determined by the cardiac output flow waveform and the vascular impedance [4]”. “The assumptions in the concept of impedance and wave transmission are that the system is linear and in steady state oscillation” [51].

2.7.1 The Validity of Fourier analysis of OMW

Expressing the heart signals as a sum of Fourier series requires that it satisfies the condition of linearity and periodicity [51] [53] [54]. These authors have established that time varying pulsatile physiological systems (circulatory & respiratory) produce signals whose periodic/oscillometric components can be analyzed by means of Fourier analysis of oscillatory time-dependent functions [54]. However, it is well known that arterial propagation properties caused by artery-cuff interaction, device component and respiratory additives alter frequencies and amplitude characteristic of pulses as the measurement progresses from systole to diastole [4] [11] [16] [48]. This behaviour is nonlinear, producing multiple oscillating harmonics and amplitude modulations [16] [29] [30] [40] [48] [52]. This begs the question of expressing pulse wave as a Fourier analysis. *W. Moer et al*. [52] and *K. Barbé et al*. [16] pointed out that it is clear that OMW exhibit multiple modulated amplitudes due to artefacts caused by nonlinearity because of heart rate and breathing activities. Stating that pressure pulses exhibit more than one harmonic thus, it is not ideally linear. In addition, a closer look at an oscillometric pulse shows that there are multiple maxima and minima, which is time varying and as such, the pulse is not absolutely periodic [16] [29]. Reports have expressed that the elastic nature of blood vessel does not allow circulatory signals obey the properties of linearity and steady state oscillation [51]. Attempts have been made to create linearized mathematical models of oscillometry [16] [52] [55].

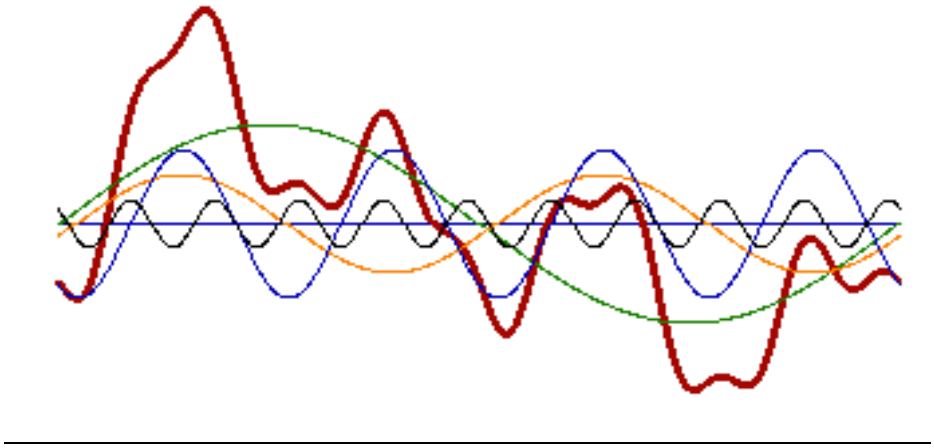

Figure 2-11: Figure of 4 harmonics of the blood pressure wave and the resultant sum. (SOURCE: Medical Instrumentation, Application and Design: [54] page 300 (Used with Modifications))

It is agreeable that linear behaving circulatory does not hold true. However, removing its non-linearity may not be practicable [16] [29] [51] [52] [59]. Nevertheless, research shows that under normal operating conditions the contribution of non-linearities is relatively negligible and therefore can be overlooked [59]. This implies that, if the assumptions are made, under normal operating conditions, blood pressure pulses can be dissected into sum of properly weighted sine and cosine functions of their proper frequency that when added together can reproduce the original complex waveform [59] . To further support the validity of this approach, [59] stated that the human heart generates beats, which occur at regular intervals. "The regularity of a heartbeat in terms of the length of an individual pulse, and its consistency over a long period of time can be regarded as a condition of steady state oscillation" [59].

These works introduce an advantage to characterizing of OMW properties in a quantitative manner, making it easy to compare corresponding harmonic pulses [51] [54]. *John G. Webster* [54] stated that "Analysis of the frequency component of pulse appear to have yielded more information on arterial properties than any other approach." He proposed that the arterial pulse be represented in terms of its frequency components.

For non-sinusoidal signal, the fundamental frequency is not sufficient to adequately reproduce it. Hence, other harmonics are needed to create a fair reproduction of the original signal [12] [54]. Figure 2.11 shows 6 harmonics of the blood pressure wave and the resultant sum. Three harmonics with the fundamental frequency are used in this research to reproduce individual oscillometric pulses.

2.7.2 Bio-Signal Representation by Sine Modelling

Time-varying waves exhibit regular amplitudes making them periodical and with basic sinusoidal components [58] [54]. A sinusoidal is a continuous moving waveform that has positive and negative half-cycles that are generally symmetrical with respect to a reference [58]. The waveform has a specified frequency in hertz and specified amplitude. The frequency components of these signals can be analyzed in frequency domain. Time-domain and frequency domain are related by the Fourier series and Fourier transforms [58]. Fourier series provide a summation of sinusoidal signals with the amplitudes, frequencies and phases to generate a periodic signal. The sum of sinusoids model expressed as a Fourier series can be represented as follows:

$$y = a_0 + \sum_{k=1}^{n}[a_k\, cos(k\omega t) + b_k\, sin(k\omega t)] \quad \text{-} \quad \textbf{\textit{Equation (2-1)}}$$

$$`y = a_0 + \sum_{k=1}^{n} a_k\, sin(kwt + \rho_k) \quad \text{-} \quad \textbf{\textit{Equation (2-1b)}}$$

where a_0 models a constant intercept (dc component); a_i is the amplitude; ω is the fundamental frequency; and i is the cosine and sine wave term. n is the number of harmonics in the series.

2.8 Mathematical Modelling of OMW

The modeling of OMW in this work takes a mathematical approach process. It involves using constrained non-linear optimization techniques with bounds. These procedures work in well-established mathematical programing applications such as MATLAB and their manner of

operation is explained in literature [60] [61] [65]. *T. F. Coleman* [60] considered various theorems for achieving convergence in non-linear minimization-optimization problems with bounds using an interior-reflective approach. We will determine on a pulse-to-pulse basis, the best possible parameters that optimizes the OMW pulses with respect to minimizing the least mean square error. The discrepancies between the original OMW (data) and the model sum of sinusoids is expressed as residuals and are the unknown parameters. The dc component, amplitude and phases on a pulse-to-pulse base would be determined using a least square optimization function. The frequency of the proper heart's operation is assumed to constantly be within a range of 0.7 – 3.0Hz and as such it is not considered to be among the unknowns.

2.8.1 Optimization Function

Optimization involves finding the best or most feasible solution to a computational problem such is: an equation, multiple objective functions, least-square or data fitting problems [62] [64]. Mathematically, it is often used in the sense of finding the maximum or minimum of some real function of n variables by systematically choosing the best elements with regards to some criteria. The input values is gotten from within an allowed set or constraints (model) and computing the values of the function [62]. The function, also known as an objective function is called the optimal solution and may be linear or nonlinear [64]. The aim is to measure the discrepancy between the model and the observation [62]. There are various ways of doing this, but by convention, the standard form of an optimization problem is stated in terms of minimization. The optimization tool in this work is the LSQ.

2.8.2 Least Square (LSQ) Optimization

Generally, Least Square problems have an objective function expressed as:

$$\min_{x} \quad \|F(x)\|_2^2 = \min_{x} (\sum_i F_i^2(x)) \quad - \quad \textbf{\textit{Equation (2-2)}}$$

where $lb \leq x \leq ub$. lb and ub are vectors which represents the lower and upper bounds. The aim is to find a vector x that is a local minimizer to a function that is a sum of squares [64]. The LSQ is used for many formulated parameterized models in various fields of Applied Mathematics for computational purposes [62]. It is a measure of the inconsistency between the model and the experimental data of the system in a curve fitting operation. By minimizing this function as expressed in equation 2.2, we solve for the *x*, where *x* is a vector which acts as a local minimizer. *x* selects values for the parameters that best match the model to the data. The minimizer in this LSQ problem is the parameter vector for which the sum of squares of the lengths of the discrepancies between the model and the observation is minimizes.

Fitting requires a parametric model that relates the response data to the predictor data with one or more coefficients [62]. The result of the fitting process is an estimate of the model coefficients. To obtain the coefficient estimates, the least squares method minimizes the summed square of residuals. The residual for the *i*-th data point ri is defined as the difference between the observed response value yi and the fitted response value ŷi, and is identified as the error associated with the data. The MATLAB *lsqcurvefit* solver is the function-handle for lsq bounded algorithms, having vectors which represents the upper and lower bound.

2.8.3 Prior Art

The concept of fitting data to model has often been used in mathematical computing for determining convergence properties, optimization, error estimation etc. [64]. Usually, as the data is fit to the model, sets of unknown parameters that define optimal conditions are derived [63].

In this approach, the amplitude and phase parameters of the fundamental frequency and harmonics of the signal were estimated and used to determine BP. What makes this work to be unique with respect to its contributions and other attempts to determine blood pressure

through mathematical modeling is that (to the best of our knowledge), there has not been any application of this technique for blood pressure estimation in literature. A similar works in [56] analyzed oscillometry in frequency using heart harmonics of the oscillometric waveform. [57] Harmonic estimation by Taylor-Fourier analysis was used to separate breathing frequencies from heart frequencies.

This proposed method has been mostly used in speech processing. In [69] and [66] to suppress co-channel talker interference in a situation in which the speech waveforms from both the desired talker and the interfering talker are vocalic. Other applications have been in the extraction of male and female voices for speech-to-text conversion [68].

2.8.4 Terminologies Describing Waves

A wave can be described by its frequency (f), amplitude (a), direction and velocity [12].

Circulation has a mean blood pressure (dc component) – MAP, about which the pulse pressure (ac component) fluctuates [4] [45]. The ac component is superimposed on a slowly varying dc component. A high-pass filter can be used to reduce the effect of the dc component [45].

Frequency: This describes the number of crests passing in a period of time. Expressed in Hertz [12]

Period: This is the time interval between each wave crest. It is expressed as $1/\text{frequency}$ [12].

Wave length: This is the distance between two consecutive wave crests [12].

Amplitude: The measure of the disturbance of the medium from its initial resting state [12].

Harmonics: A frequency of the signal that is an integer multiple of the fundamental frequency. E.g. Harmonics 2f, 3f, 4f would be first second and third harmonics of the fundamental frequency f [58].

Phase: The angular position of a signal within a cycle of the waveform.

Frequency and Time Domain: Fourier analysis relates Time and frequency domain of a signal.

Frequency domain is the expression of the strength of a signal in terms of frequency [58]. Dominant frequencies can be checked by a Power Spectrum Density analysis.

Time Domain: Analysis of a function as it occurs in nature, with respect to time [58].

Chapter 3: Methodology

In this chapter, the systematic procedures taken for this research is discussed along with the proposed approach and the reasons for choosing them. The data set used is discussed, as well as the data acquisition technique and the acquisition device.

3.1 Prototype Devices

The process is as described in [72]. Two blood pressure monitors were used for the data acquisition, the OMRON HEWM-790 ITCAN (Omron) and the InBeam [72]. OMRON HEWM-790 ITCAN is a commercially available oscillometric measurement device while the InBeanm device was developed at the School of Electrical Engineering and Computer Science (EECS) of the University of Ottawa [72]. This device records Electrocardiogram (ECG) and estimates BP sequentially. The ECG is used to determine period of occurrence of each pulse. Both devices are oscillometric devices.

3.1.1 Device Component

The main components in the InBeam are an analog ECG amplifier made by (Texas Instruments, Dallas, TX), a pressure transducer (Vernier Pressure Transducer BPS-BTA, Beaverton, OR, USA), a mini direct current (DC) air pump, and a key or control valve to allow manual control of the pressure valve.

3.1.2 Device Operation

The outputs of the ECGG amplifier and pressure transducer are fed into a National Instruments™ Series 9239 (NI-9239). The module is used for conditioning and sampling using a 24-bit delta-sigma analog-to-digital converter (ADC). The resultant digitized samples are then transmitted via Universal Serial Bus (USB) cable to a personal computer (PC-based) which runs an application (National InstrumentsTM LabVIEW) used for the

acquisition of ECG and cuff pressure signals. A sampling rate of 1000 Hz is used to sample all acquired signals. Further processing is done using MATLAB

3.2 Data Acquisition Setup Procedure

Two electrodes are required for the detection and acquisition of ECG signal [72]. The first is inserted within the side of the cuff that comes in contact with the arm of the subject. The cuff is worn on the subject's left arm. The other electrode is placed within a wristband, which is worn on the wrist of the subject's right hand [72]. Both electrodes were made of flexible conductive fabric.

The dataset used was gotten from volunteers at the University of Ottawa, by Dr. Saif Ahmad [72]. There were ten subjects with no history of cardiovascular or respiratory diseases, six are male and four are female. This research was authorized by the University of Ottawa Research Ethics Board and all participants were well informed of the procedures and were provided with consent forms [72].

Subjects were required to sit in an upright position such that their arms were at the same horizontal level as the heart. The subjects avoided all possible movements, breathed normally and did not cross their legs. The recording took a period of three different days. Each subject measured five times per day, per monitor.

The Omron cuff was wrapped around the subject's upper right arm. The InBeam cuff and the ECG conductive fabric were wrapped around the upper arm of the left hand and wrist of the left hand respectively. The Omron monitor recorded the first measurement followed by the InBeam monitor. A three-minute waiting time was observed between measurements as recommended by AAMI (Association for the Advancement of Medical Instrumentation, 2003). Then the process was repeated again sequentially until five pairs of measurements were recorded. The recordings were repeated a second and third day. Thirty measurements

(fifteen from Omron plus fifteen from InBeam) were collected from each of the ten healthy subjects, over a period of three different days. The total recordings were 300, 150 from each device. Both devices operate with the same principle using a deflating cuff.

3.3 Reference Algorithms & Reference Device

3.3.1 Maximum Amplitude Algorithm (MAA)

This is a height criteria ratio method of estimating blood pressure as described in section 2.4. The amplitude of the envelope of the peak-to-peak OMW is considered as OPI.

Blood pressure estimation using this MAA approach is compared to the proposed algorithm as our first reference.

In figure 3.1, the vertical lines represent the point estimates of SBP and DBP using the characteristic ratios (K_{SBP} and K_{DBP}). The points are mapped to the vertical pressure axis to find the pressure points. The SBP is on the left of maximum point of the MAP OPI, while the DBP is on the right.

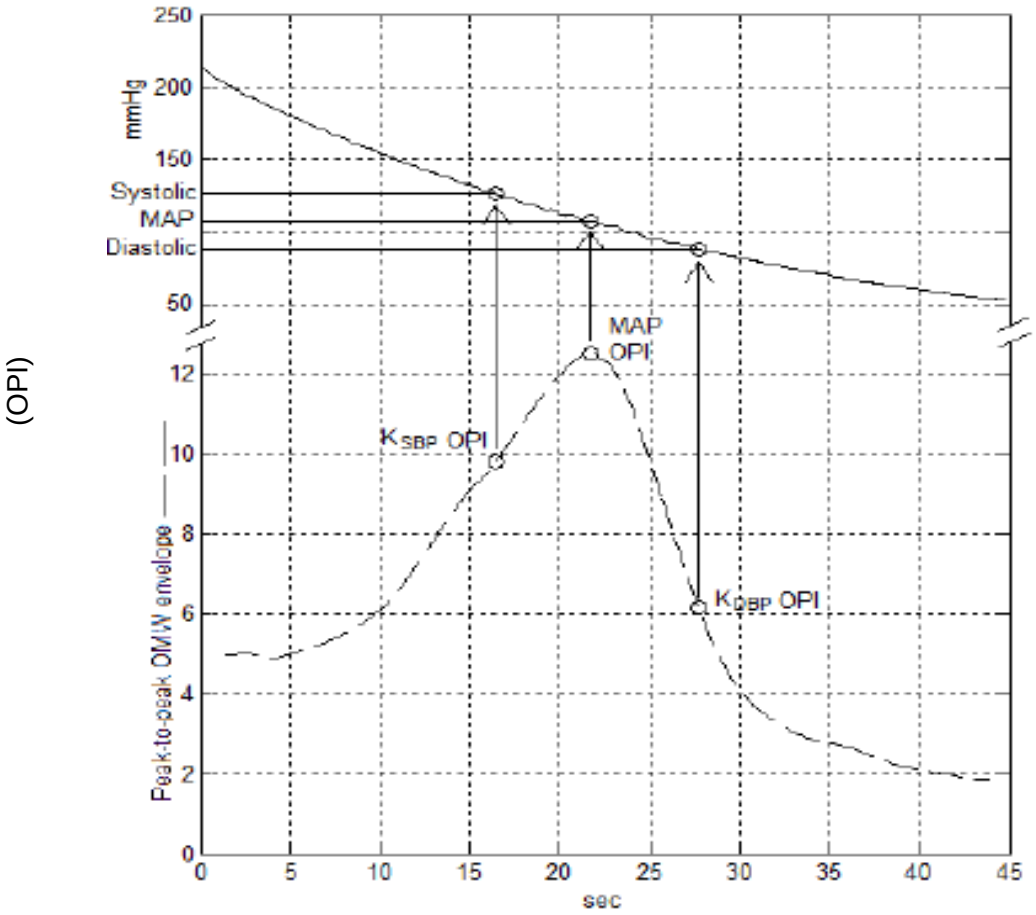

Figure 3-1: Illustration of the Maximum Amplitude Algorithm method of determining BP. The points are extrapolated to the cuff pressure on the y-axis to determine BP.
(SOURCE: S. Chen, V. Z. Groza, M. Bolic, H. R. Dajani, "Assessment of Algorithms for Oscillometric Blood Pressure Measurement", International Instrumentation and Measurement Technology Conference, pp. 3-1767, 2009 [19]; used with modification)

3.3.2 Pulse Morphology Parameters Algorithm (PMA)

Pulse morphology method makes use of parameters that describe pulses wave to estimate blood pressure in oscillometry. The parameters describe the featured contours on a typical oscillometric pulse [37] [20].

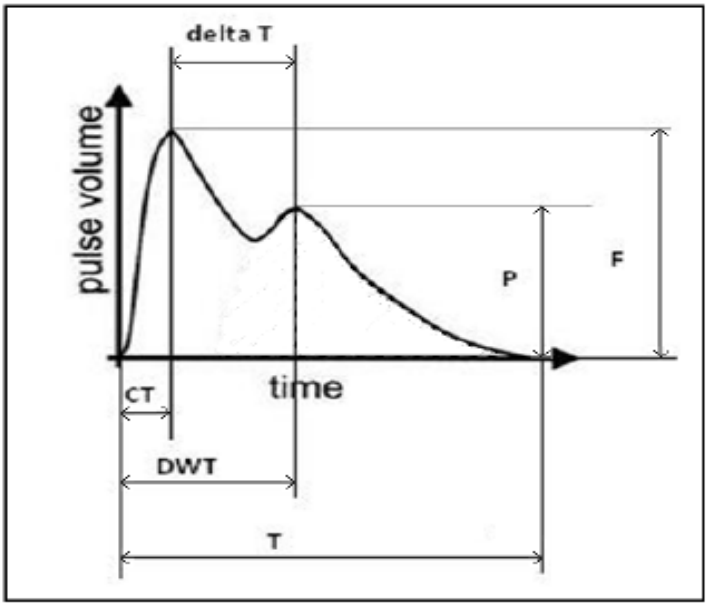

Figure 3-2: BP Pulse Parameters as described by pulse morphology method.
(SOURCE: Majid. M "Blood Pressure Estimation using Oscillometric Pulse Morphology" 2012 [20]; used with modification)

Figure 3.2 shows a typical oscillometric pulse with pulse wave evaluation indexes describing pulse peak volume and peak time-delay [36] [37]. These indexes are related to form parameters that describe the elastic state of the artery as it relates to the spreading and propagation of pulse waves (Pulse Wave Velocity (PWV)) in arterial systems as well as arterial blood pressure [27] [37]. Some indexes include: Augmentation Index (AI), Stiffness Index (SI), Reflective Index (RI) and Time-delay Index (ΔT/T). The parameters are briefly described as follows:

A.I – Refers to pressure increase within arteries caused by reflected wave [37] [47].

ΔT/T – time delay parameter which describes the time difference between the pressure wave from the roots of the aorta to the site of the reflected wave and back [37] [47]. It is responsible for the difference of central peripheral pulse wave.

R.I – Relates the degree of blood vessel constriction relative to its full dilated state (vascular tone) to the height of the first peak in the pulse wave [27] [37].

S.I – The stiffness index relates the pulse wave velocity in a large artery [37] [27]. Large artery stiffness can be described using the body height and the time delay of reflected wave (ΔT) [27] [47].

Table 3-1: Table of Pulse Morphology Indexes
(*Adapted from [20]: Majid. M "Blood Pressure Estimation using Oscillometric Pulse Morphology" 2012)*

Parameters	Description
Augmentation Index	Described as the percentile of the difference of the systolic peak (F) and second peak (P) divided by the systolic (F). $AI = \left[\frac{(F-P)}{F}\right] \times 100\%$
ΔT/T	T is the time of occurrence of the pulse. ΔT/T describes the change in T between the peaks of pulse waveform
Reflective Index	Described as a the percentile of the height of the second peak (P) relative to the height of the first peak (F) $RI = \left[\frac{P}{F}\right] \times 100\%$
Stiffness Index	Described as the height of the individual divided by the time difference between two peaks of BP pulse. $SI = \frac{h}{\Delta T}$

3.3.3 Reference Device

The reference device is the OMRON HEWM-790 ITCAN. The description of operation is as presented in section 3.1. The measurements were recorded under the same conditions and the recording instrument was sequentially alternated with the Inbeam prototype device. The results are compared to the presented method.

3.4 Proposed Algorithm

- **Process 1: Data Preparation**

Matlab is used to implement this algorithm. The recorded data is extracted and read by the program. The time stamps is expressed in milliseconds, the ECG is in volts, while the cuff pressure is in units of mmHg. The data is stored as arrays of values. The deflating cuff pressure waveform is shown as in Figure 2.2. The cuff pressure is acquired at a sampling rate of 100Hz and then it is time-interpolated at the sampling rate of 256 Hz. In the next process the OMW is extracted by subtracting the trend from the cuff pressure.

- **Process 2: Extraction of Oscillometric Waveform**

It is known that filtering method of extraction alters the shape of oscillometric waveform [11] [30] [44]. To investigate the effect of the extraction method on the shape of the oscillometric pulses and the accuracy of the proposed method, we have used two other baseline subtraction methods.

Method 1: The first method is the construction of baseline by the interpolation of the R-peak of the ECG of the subject. From literature [70], we understand that each pulse is triggered by and occurs within a trace of an R-peak of the ECG signal. The method identifies the origin of the oscillometric pulses by using the R-peak of the ECG signal QRS complex. The baseline is constructed by closely sampling the points between each R-peak at a sampling rate of 1KHz. To get the OMW ($P_P(t)$) the baseline ($P_v(t)$) is then subtracted from the cuff pressure ($P_c(t)$). Pulse amplitude characteristic is considered as baseline to peak. The resultant waveform is presented in figure 3.3.

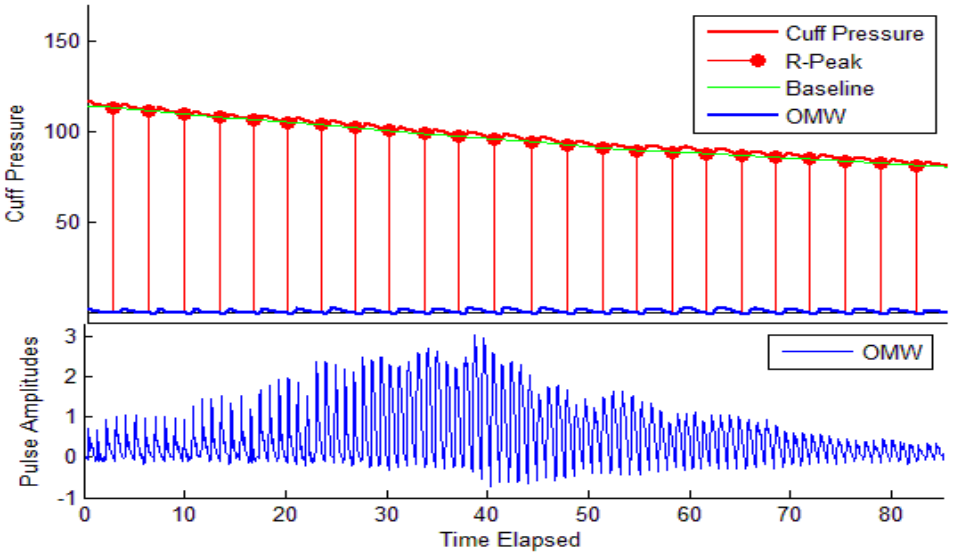

Figure 3-3: Illustration of the Baseline Construction Technique by Interpolation of the ECG R-Peak and the resultant OMW

Method 2: The second method involves the construction of the baseline using trapezoidal numerical integral. Pulse amplitude characteristic is considered as the area under curve. The gradient of the cuff pressure is determined and area under the cuff is estimated. The

equation of a line is used to construct the baseline for each pulse. This results in varying baseline per pulse. Figure 3.4 shows the plot of an arterial pulse (P_p) and the construction of the varying baseline.

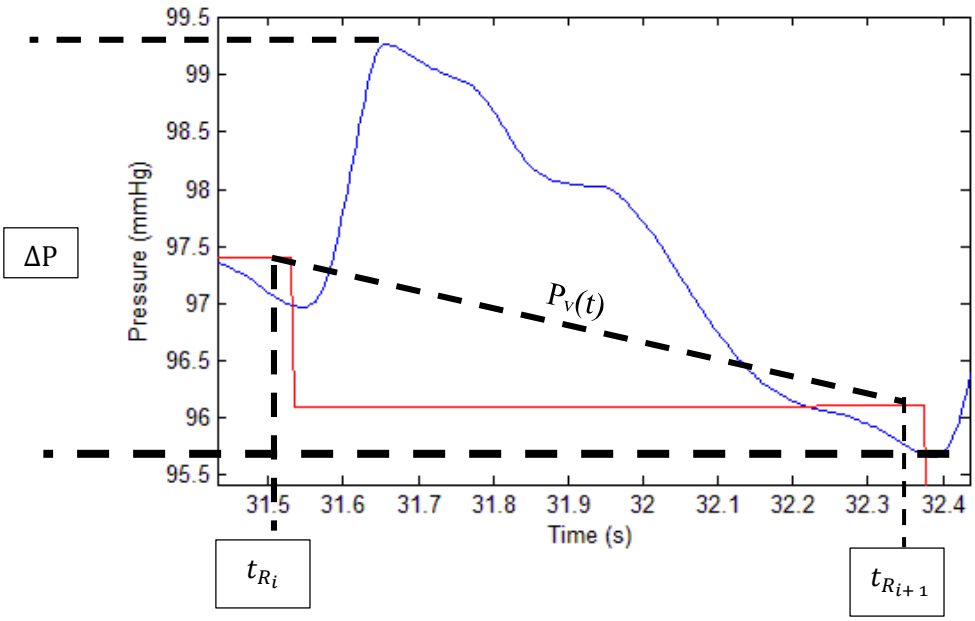

Figure 3.4: Construction of the varying baseline

$pc = cuff\ pressure;\ t_{R_i} = expresses\ the\ instantanious\ time;$ Pv $= baseline;$

$$\Delta P = Pc(t_{R_i}) - Pc(t_{R_{i+1}}) \qquad \text{- Equation 3-1}$$

$$gradiemt\ (m) of\ baseline\ (Pv)\ is\ expressed\ as$$

$$m = \frac{\Delta P}{t_{R_{i+1}} - t_{R_i}} \text{ - Equation 3-2b}$$

$$Pv(t) = mt + Pc(t_{R_i}) \qquad \text{- Equation 3-3c}$$

$$OMW = Pc(t) - Pv(t) \qquad \text{- Equation 3-4d}$$

The resultant oscillometric waveform is normalized by finding the origin of the pulse using the R-peak of the ECG signal as in method 1 and by removing the step offset introduced by each pulse level. The resultant OMW is leveled on the zero line as shown in figure 3.5b.

The advantage of this method is that it nullifies the input of dc component in the OMW by leveling the waveform on the zero line.

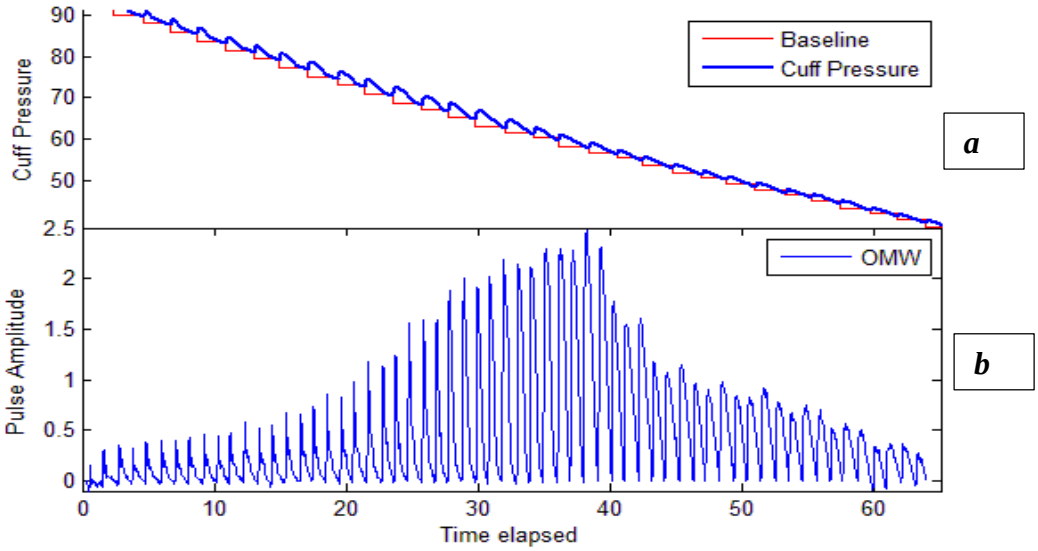

Figure 3-5: Illustration of the Baseline Construction Technique by Numerical Integral and the resultant waveform

Method 3: Oscillometric waveform extraction using a filter. A 2nd order Butterworth band-pass filter with cut-off frequencies of 0.5 Hz and 25 Hz was designed. The cuff pressure is filtered to remove the trend line and suppress higher frequency noise from the cuff pressure waveform. The resultant waveform is as shown in figure 3.6b.

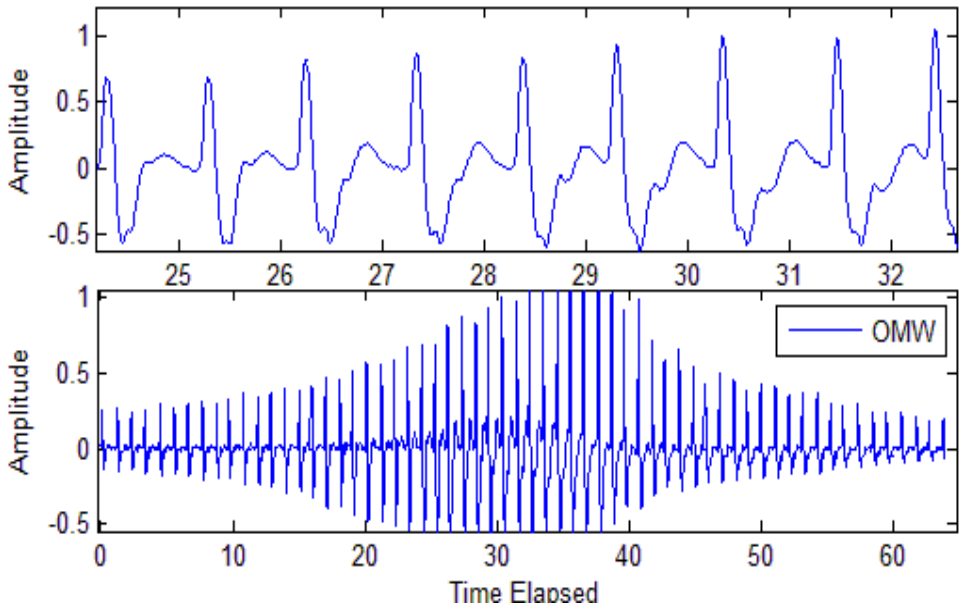

Figure 3-6: OMW Extracted by Band-Pass Filtering and the resultant waveform

- **Process 3: Extraction of Oscillometric Pulse**

The oscillometric waveform is split into individual pulses in this process. Pulse characteristic is regarded as a peak between two troughs. Because of the presence of multiple peaks, outliers, spikes and premature pulses, we made use of Pulse Transit Time (PPT) technique [70] as described in the OMW extraction. The same procedure is used to trace beat-to-beat pulse. Considering that the subjects are healthy individuals and it is expected that the pulse should occur between two ECG R-Peaks, we regarded a notable peak occurring between two ECG R-Peaks a pulse.

- **Process 4: Outlier Detection Correction**

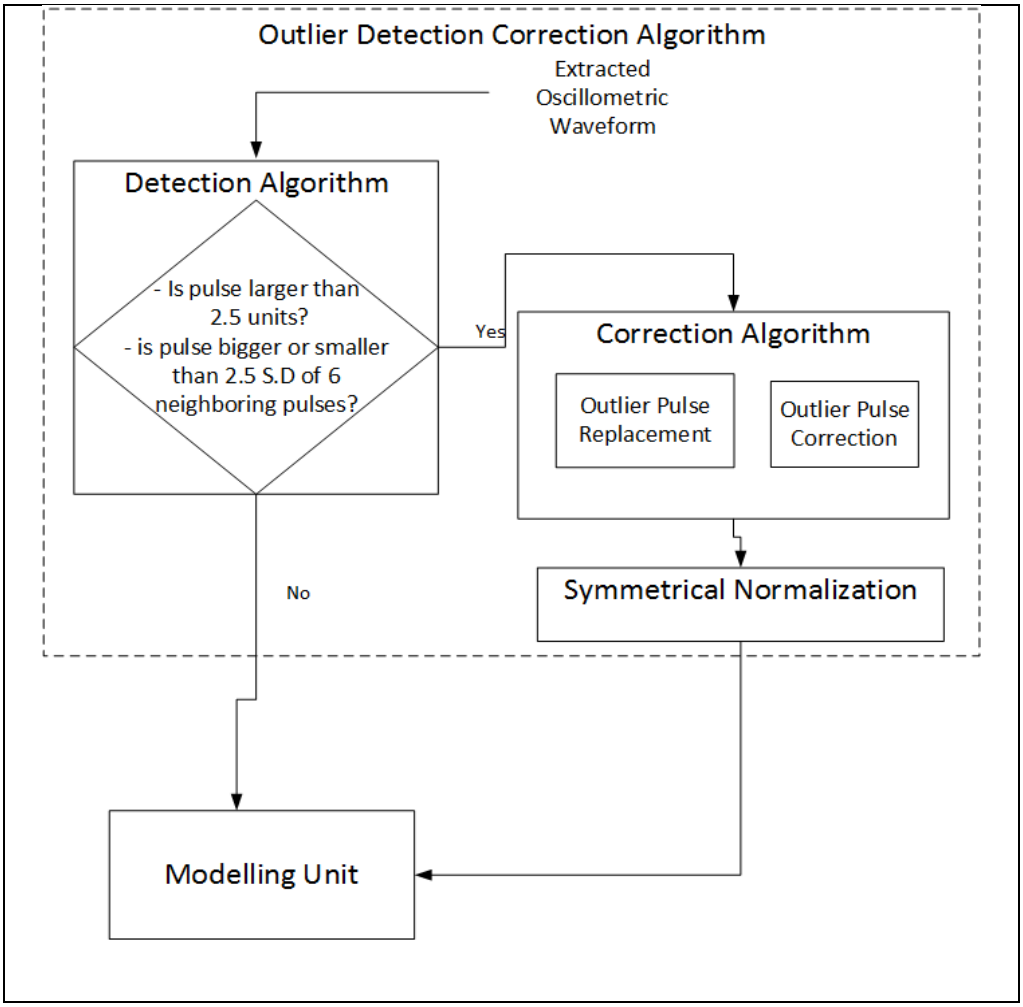

Figure 3-7: Block Diagram of Outlier Detection Algorithm

As mentioned above outliers affect the analysis of a dataset. The method of characterizing oscillometric pulses involves curve fitting modelling, attention has to be paid to remove data points that don't agree with the experimental dataset. For the purposes of this research we defined an outlier as either a spike or a premature pulse using various conditions:

- If the amplitude greater than 3.5mmHg it is a spike (figure 3.8).
- If the amplitude is greater than 2.5 times the standard deviation (SD) of neighboring pulses (figure 3.8).

- Condition 3 assumes an OMW is symmetrical. An outlier is a pulse that doesn't follow the symmetrical slope, incline or decline of neighboring pulses. An outlier in this definition can be a premature pulse or a spike (figure 3.8).

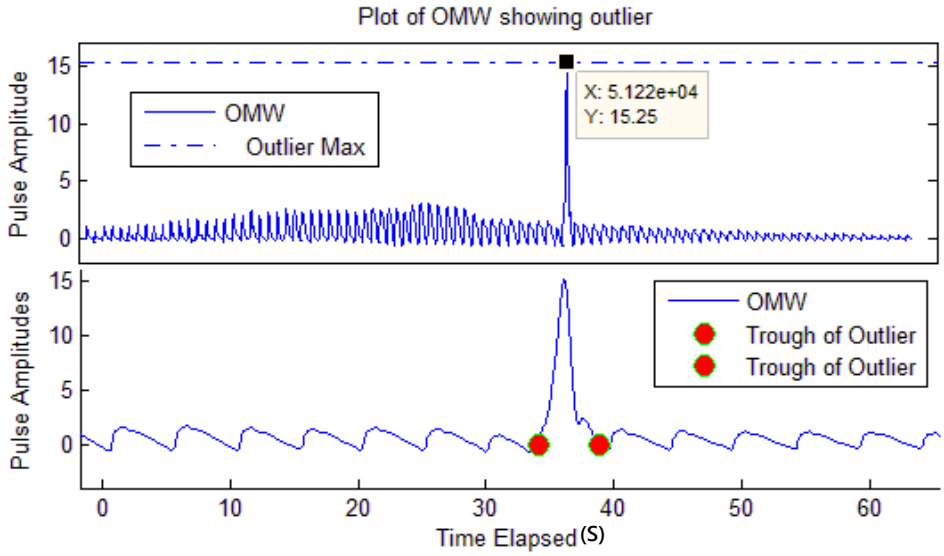

Figure 3-8: Outlier Detection Mechanism showing the roots of the Outlier pulse at the ECG R-Peak points

To solve the problem of outliers, we used our algorithm to identify pulses using the conditions listed above. Two methods were used to resolve an outlier pulse.

Outlier Correction Method 1: We segment an OMW into the systolic and diastolic segment. The systolic segment is on the left side of the peak point, while the diastolic is on the right side of the peak point. If the outlier is found on the diastolic segment, the algorithm removes the pulse and finds a pulse with the same number of samples as the outlier pulse from the same segment. The outlier is then replaced by this pulse figure 3.9. Because the pulse may have a bigger or smaller amplitude than neighbouring pulses in the segment, the pulse is normalized to the slope or trend of neighbouring pulses.

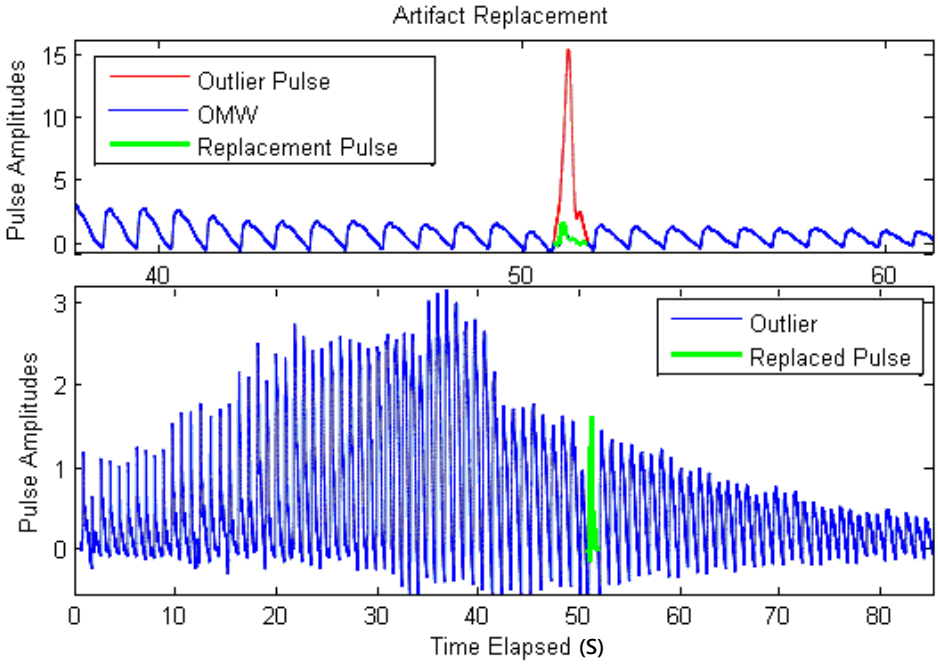

Figure 3-9: Illustration of Outlier Pulse Replacement

Outlier Correction Method 2: A correction factor is used to estimate a value which is used to multiply or divide the outlier pulse to a value that is less than 2.5 the SD of six neighbouring pulses. The resultant pulse may be smaller or bigger than the neighbouring pulse. It is then normalized to the trend of the neighbouring pulses as the above method. Figure 3.10 shows the resultant waveform.

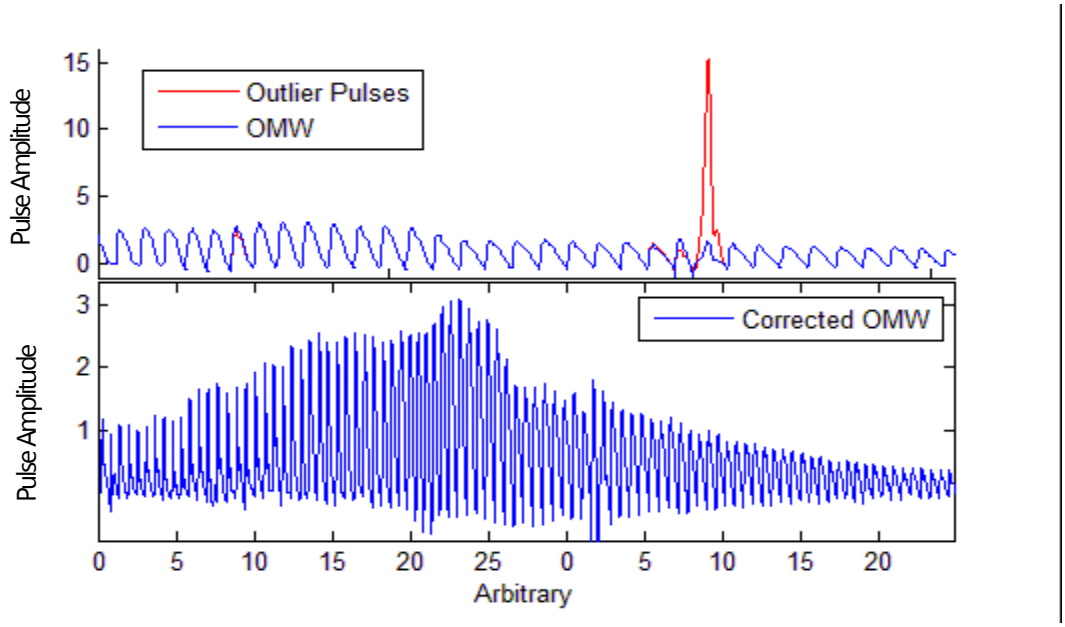

Figure 3-10: Outlier Pulse Correction Method

- **Process 5: Modelling of Pulses**

Individual pulses are fitted using a model. The fitting model is a weighted sum of sinusoids, to the fourth harmonic. The number of harmonics was derived by finding the power density spectrum of the signal, which gives a value of four. Matlab function *lsqcurvefit* is used as a model handle or error estimator. The resultant model is described/estimated as a series of quantitative measures of amplitudes and phases. Research shows that the first six harmonics can give a fairly good replicable bio-signal [53] [54] [58].

The simplest form of the model function is expressed as:

$$\boldsymbol{Y = dc + A_0 * sin(2 * pi * f * t) + Phi_0} \qquad \textbf{- Equation (3-5)}$$

$\boldsymbol{where}$: $\boldsymbol{dc = dc\ component}$; 0

$\boldsymbol{A_0 = Amplitude}$;

$\boldsymbol{pi = 3.14157}$;

$\boldsymbol{f = Heart\ frequency}$;

$\boldsymbol{t = Time}$;

$\boldsymbol{Phi_0 = Phase}$;

- **Process 6: Extraction of Model Parameters**

The response data model is given as:

$$\boldsymbol{Y = dc + A_0 * sin(2 * pi * f * t) + A_1 * sin(4 * pi * f * t + Phi_1) + A_2 * sin(6 * pi * f * t + Phi_2) + A_3 * sin(8 * pi * f * t + Phi_3)} \quad \textbf{- Equation (3-6)}$$

Where coefficients A_0 A_1 A_2 and A_3 represent the amplitudes, dc is the dc component of the signal and phi_1 phi_2 phi_3 are phases. Phase phi_0 is assumed to be zero as such it is not part of the estimation parameters.

After modeling the individual pulses, the coefficients were extracted for individual pulses and the changes with respect to deflating cuff pressure were determined. Figures 4.1 – 4.8 show graph of the coefficients plotted against average pulse number. Further signal

processing is done to estimate systolic (SBP), diastolic (DBP), and mean arterial pressures (MAP) from the parameters.

Table 3-2: Table of Parameters Proposed Algorithm. Adopted from MATLAB Manual [64] [63]

Parameter	Description
Problem Type	Nonlinear Curve Fitting
Objective Function Formula	$\boxed{\min_{x}} \ \|F(x, xdata) - ydata\|_2^2$
Constrain Bounds	Lb ≤ x ≤ Ub
Solver	lsqcurvefit
Estimation Parameters	A_0, A_1, A_2, A_3, Phi_1 Phi_2 Phi_3 Dc
Lb	Lower Bounds
Ub	Upper Bound
x0	Starting point

3.5 **Multiple Oscillation in Oscillometric Pulse Modeling**

Oscillometric waveform exhibit multiple oscillations which make them difficult to model using their frequency function.

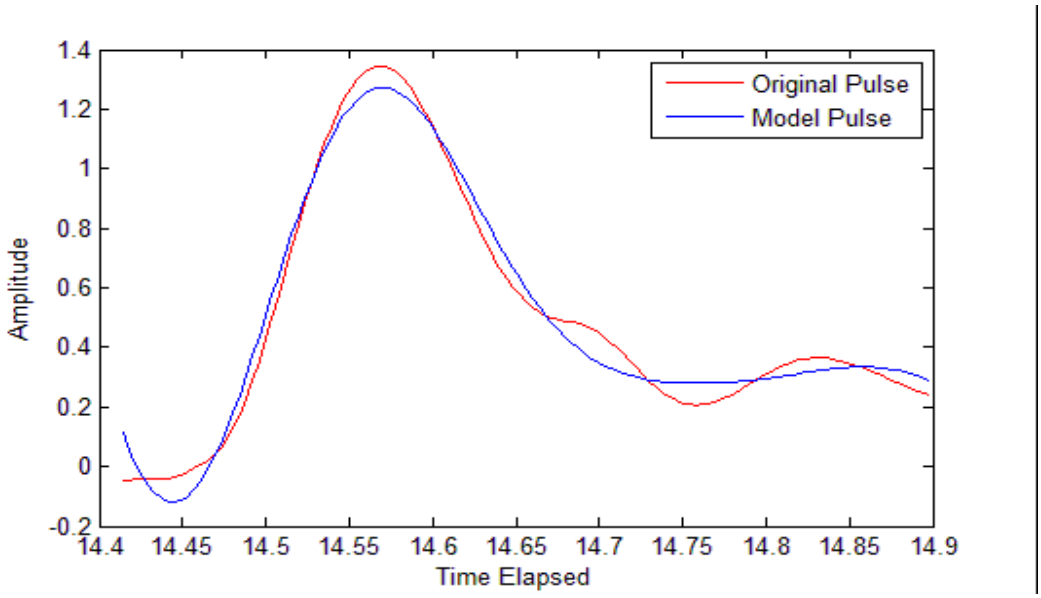

Figure 3-11: Illustration of a modelled pulse after removing multiple oscillation.

This is due to complex interaction between the cuff and the arm. Multiple oscillations make the modelling function skewed. In an attempt to make the waveform easier to model we linearize oscillometric waveform by removing multiple components of the reverse wave leaving only the systolic peak. Figure 3.11 shows an illustration of the model using the algorithm function. The end result proved to be better for our model. The assumption is that the inherent information in the pulse is provided in the systolic peak.

3.6 Error Estimation and Analysis

The errors in a least square problem is assumed to be normally distributed because the normal distribution often provides an adequate approximation to the distribution of many measured quantities [62].

A constant variance in the data implies that the "spread" of errors is constant. Data that has the same variance is sometimes said to be of equal quality. The assumption that the random errors have constant variance is not implicit to weighted least squares regression [62] [63]. Instead, it is assumed that the weights provided in the fitting procedure correctly indicate the differing levels of quality present in the data.

Comparison of results was done with Mean Absolute Error and Standard Deviation. These estimation measures are often used in statistical analysis for deviation estimation and comparison [14].

MAE is the mean of how much the data varies from the mean of the absolute error. The error is calculated as$|(x - \bar{y})|$. Where y is the reference value (omron).

The standard Deviation (SD) is the spread or variation from the mean. It is estimated as the square root of the summation of the variance divided by the degree of freedom. The SD is estimated using Excel spreadsheet.

Student t-tests checked if the averages of two sets of data are reliably different from each other. It tells us in inferential statistical sense about the sample we don't have. Thus, we can generalize our finding. Three types of t- tests exist. The Independent-sample t-test, paired t-test, and one-sample t-test. Paired t-tests was used for the purpose of comparing the proposed method with the reference data.

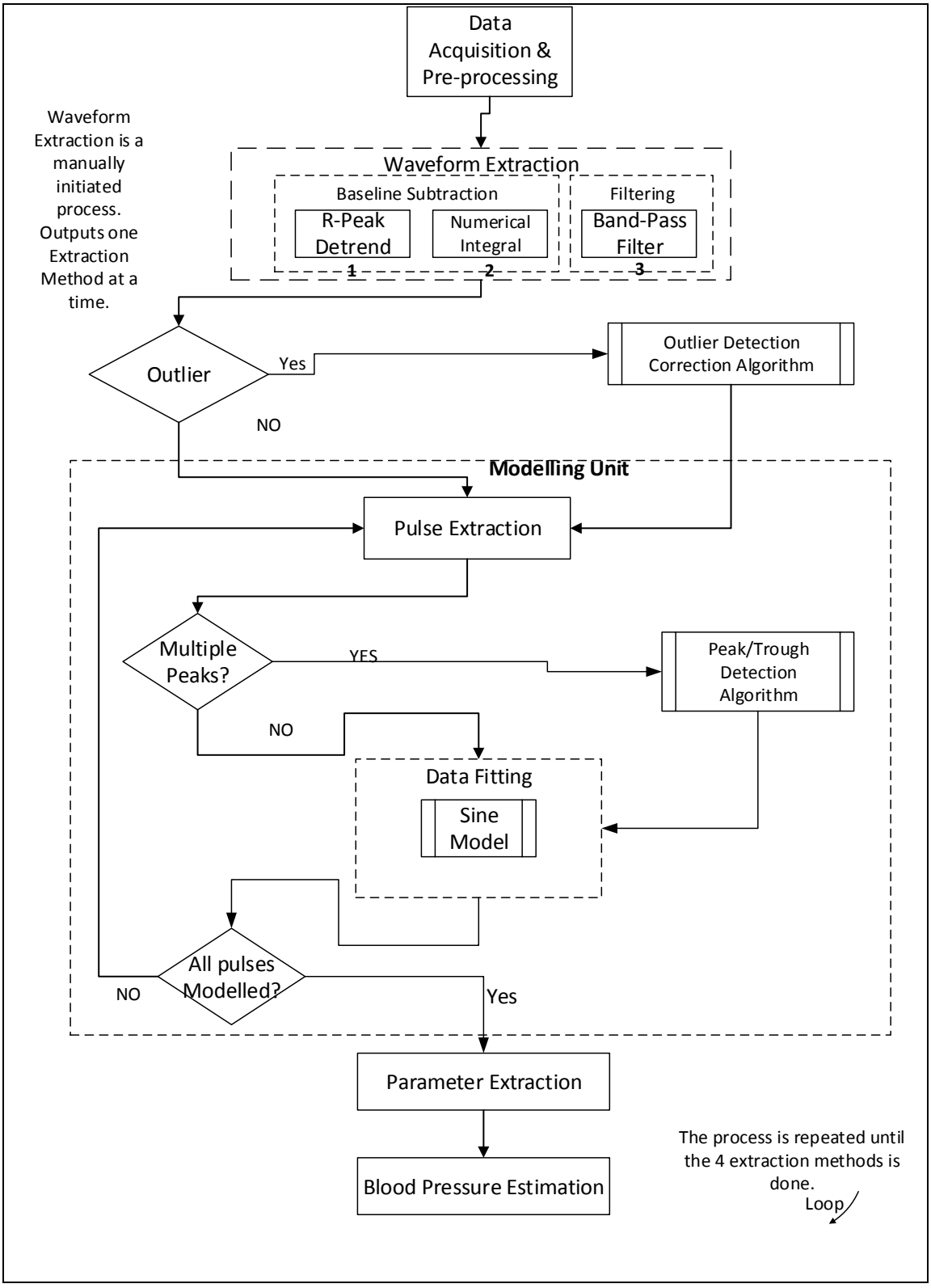

Figure 3-12: Block diagram of the proposed method

Chapter 4: Results and Analysis

The first part of the presented experiment was for the modelling section. Extraction of oscillometric waveform was done primarily using a baseline subtraction detrending technique. Each waveform is then separated into its component pulses as explained earlier in chapter 3. Optimized values of the model parameters are obtained.

The amplitude, phase, and dc component parameters presented in Section 3.7 are obtained from the individual pulses for all 10 subject. Amplitude and phase changes occur in pulses as the cuff pressure changes. The behavior of phase parameter changes are unique and different from that of amplitude parameter across the different pressure regions. In this section the Parameters of pulse waveform as they vary with changing cuff pressure across the pressure regions is presented.

4.1 Pulse Harmonic Parameters and Varying Cuff Pressure

The frequency component of oscillometric pulses can be used to estimate SBP, MAP and DBP. Using the curve fitting function, it can be observed that the amplitude and phasor parameters change as pulse morphology changes. These changes occur as steep increase or decrease and peaks in the shape of the parameters when plotted for all pulses. Four amplitude parameters, three phase parameters and the dc component were extracted as discussed in the previous chapter: The amplitudes are identified as A_0, A_1, A_2, A_3, while the phases are Phi_1, Phi_2, and Phi_3. The DC component is represented as DC. These values were obtained for each pulse in the OMW and the changes are used to estimate BP. They represent the optimally derived values which when put together can be used to best characterize or reproduce the pulse. Figures 4.2 to 4.9 shows the plot of the eight parameters for one subject. The x-axis represents the pulse number each. Y-axis represents the parameter index.

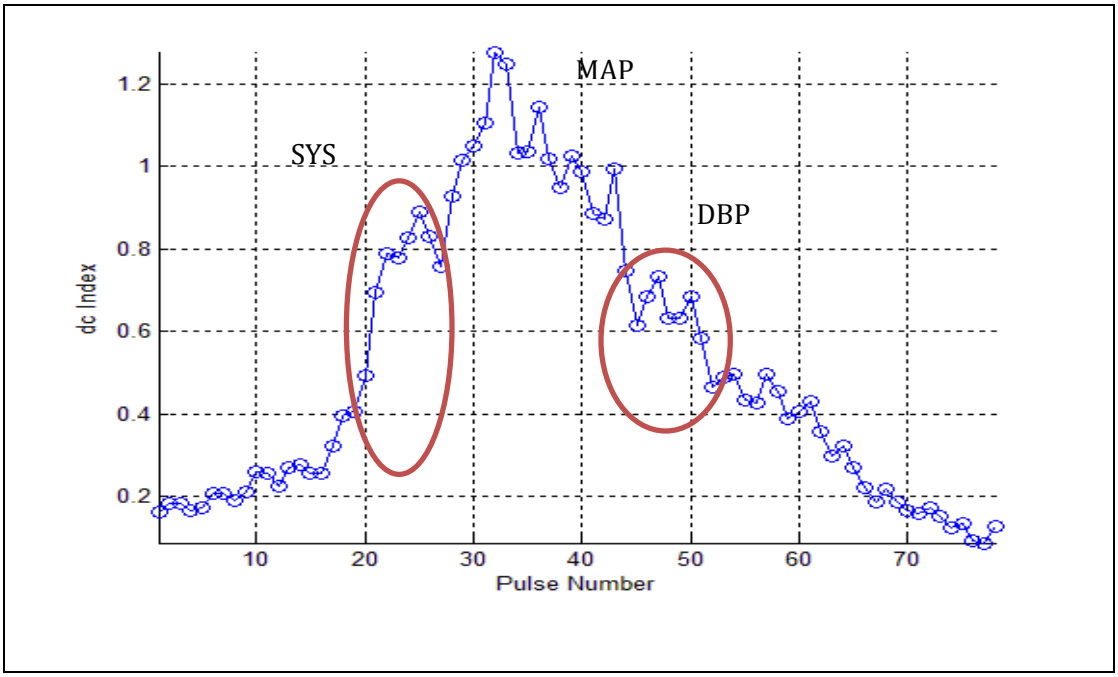

Figure 4-1: Plot of DC Component

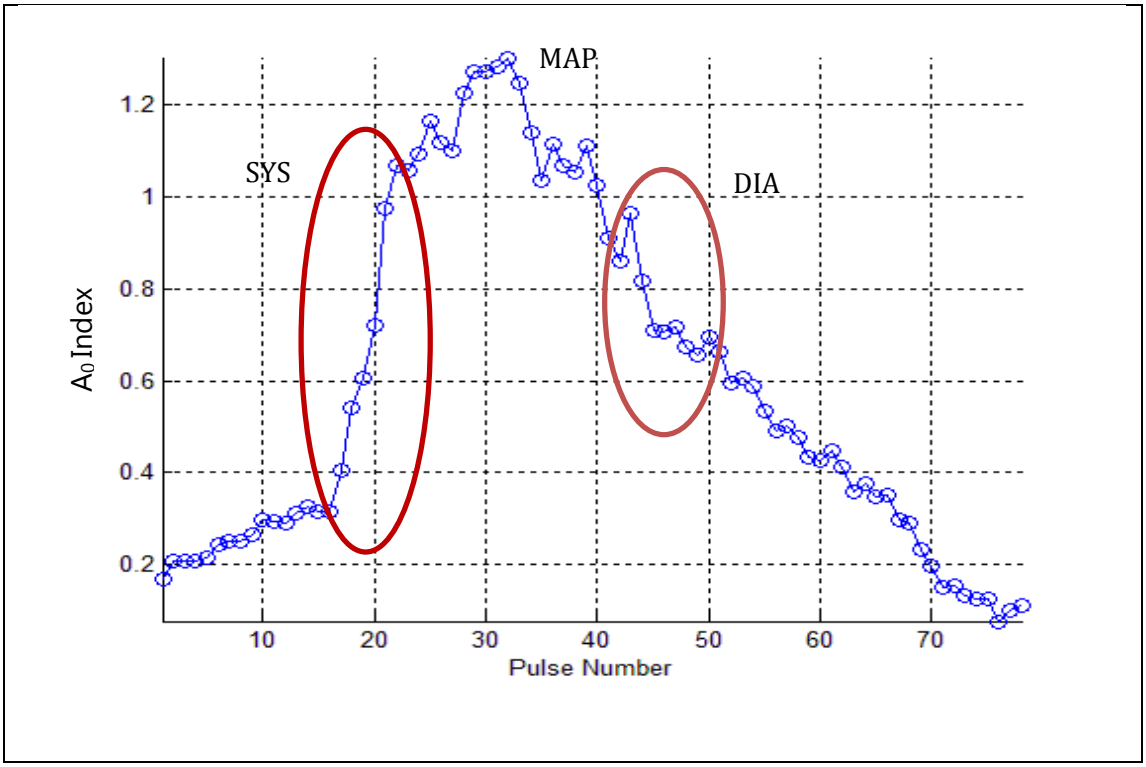

Figure 4-2: Plot of Amplitude Changes (A_0)

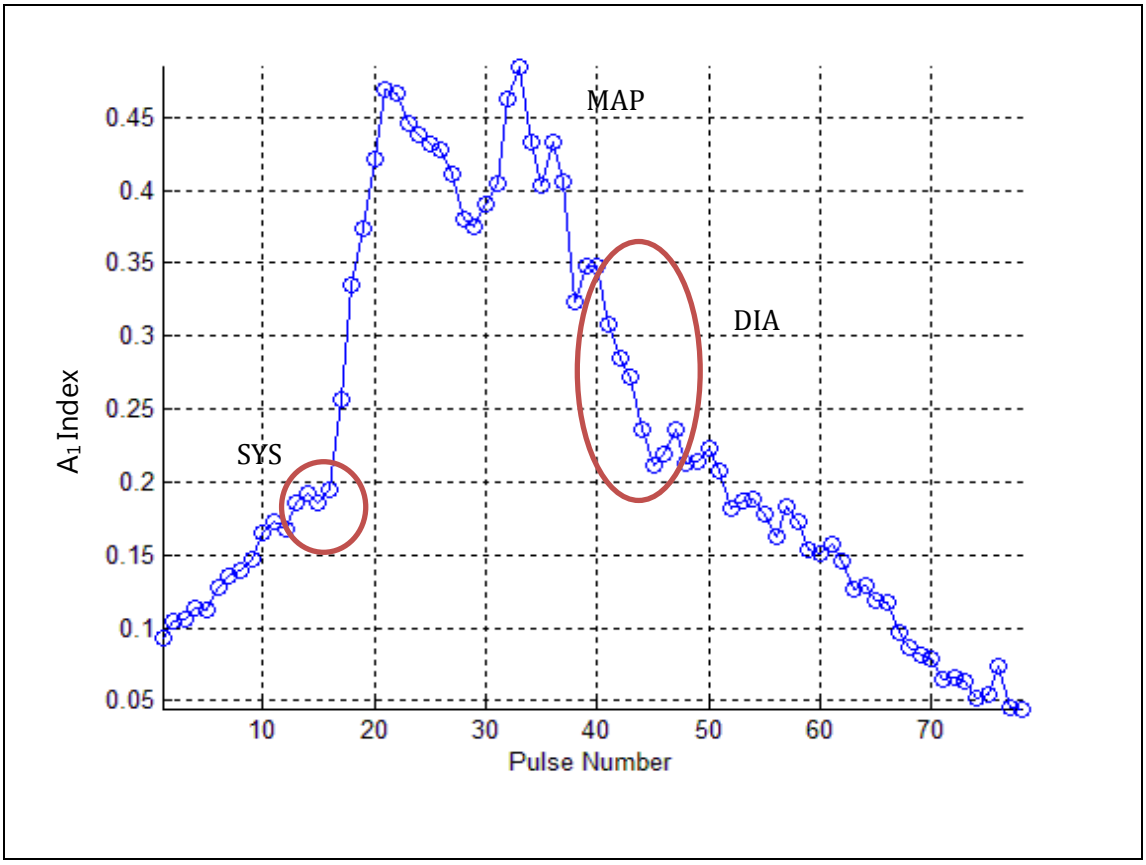

Figure 4-3: Plot of Amplitude Changes (A_1)

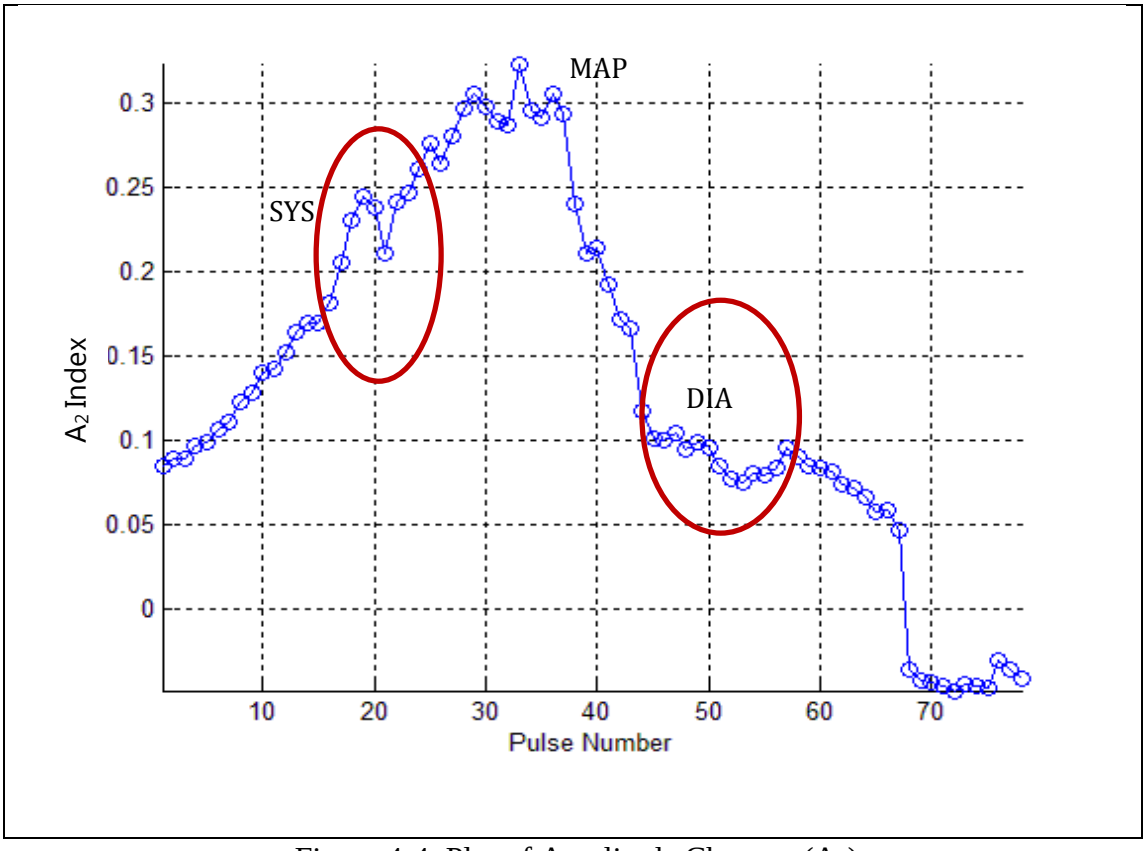

Figure 4-4: Plot of Amplitude Changes (A_2)

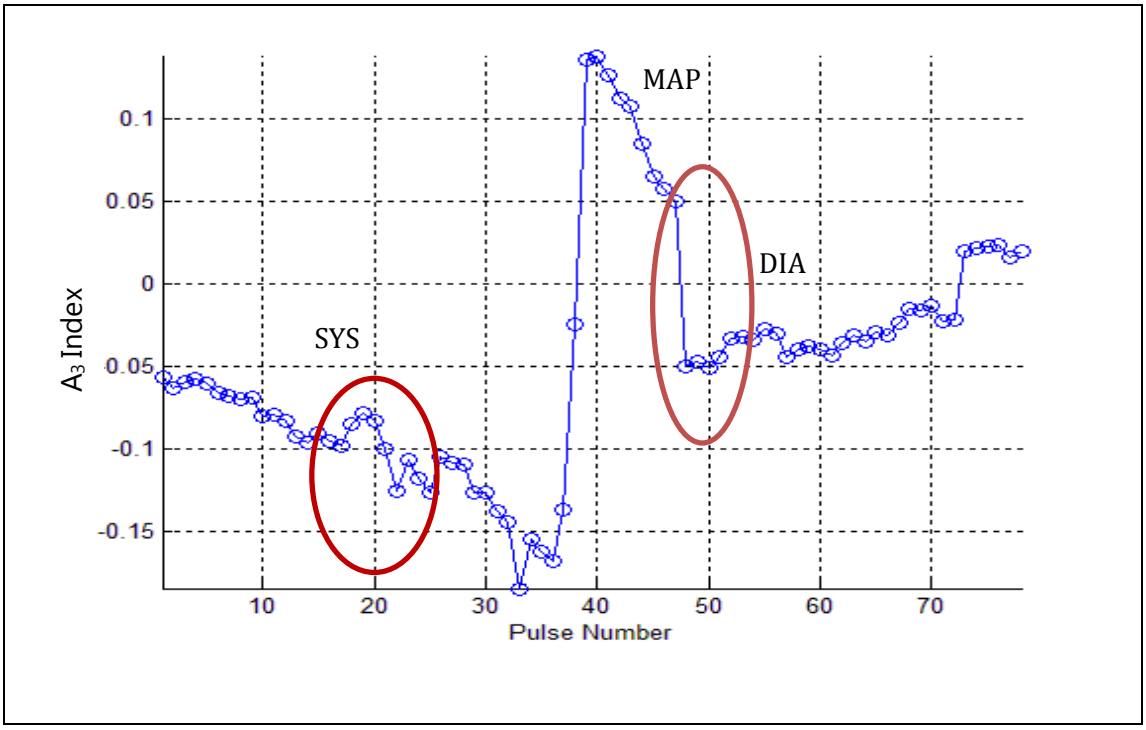

Figure 4-5: Plot of Amplitude Changes (A_3)

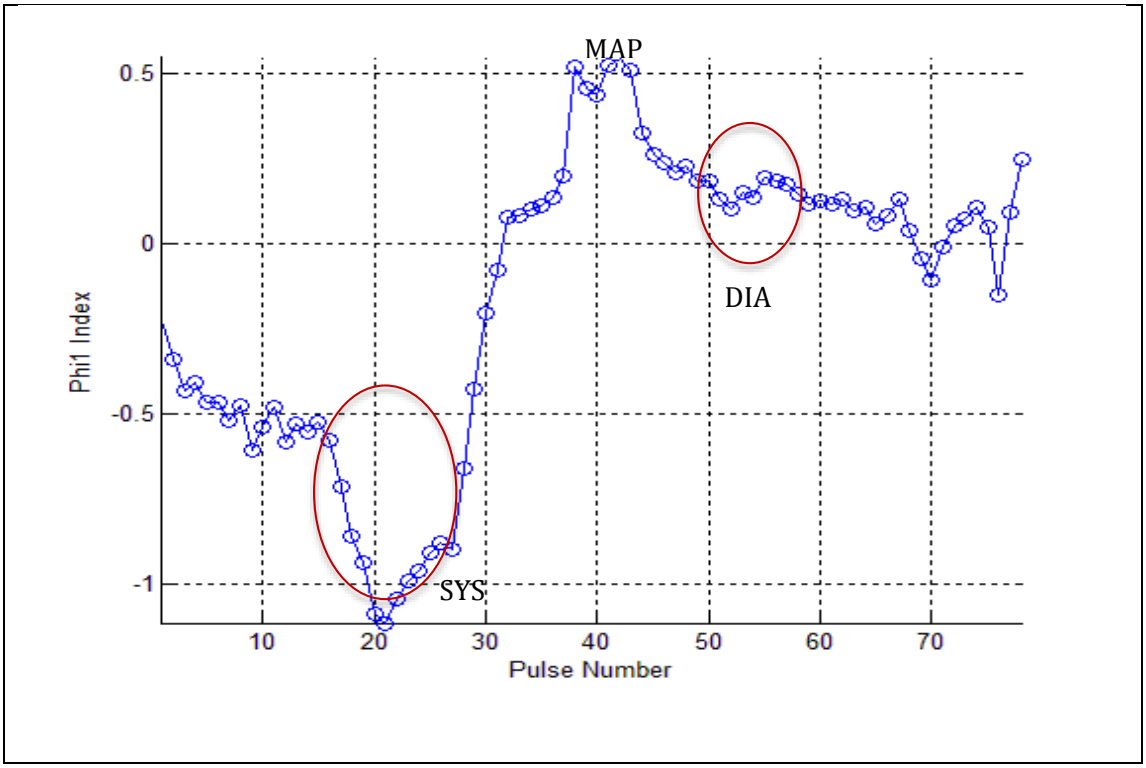

Figure 4-6: Plot of Phase Changes (Phi_1)

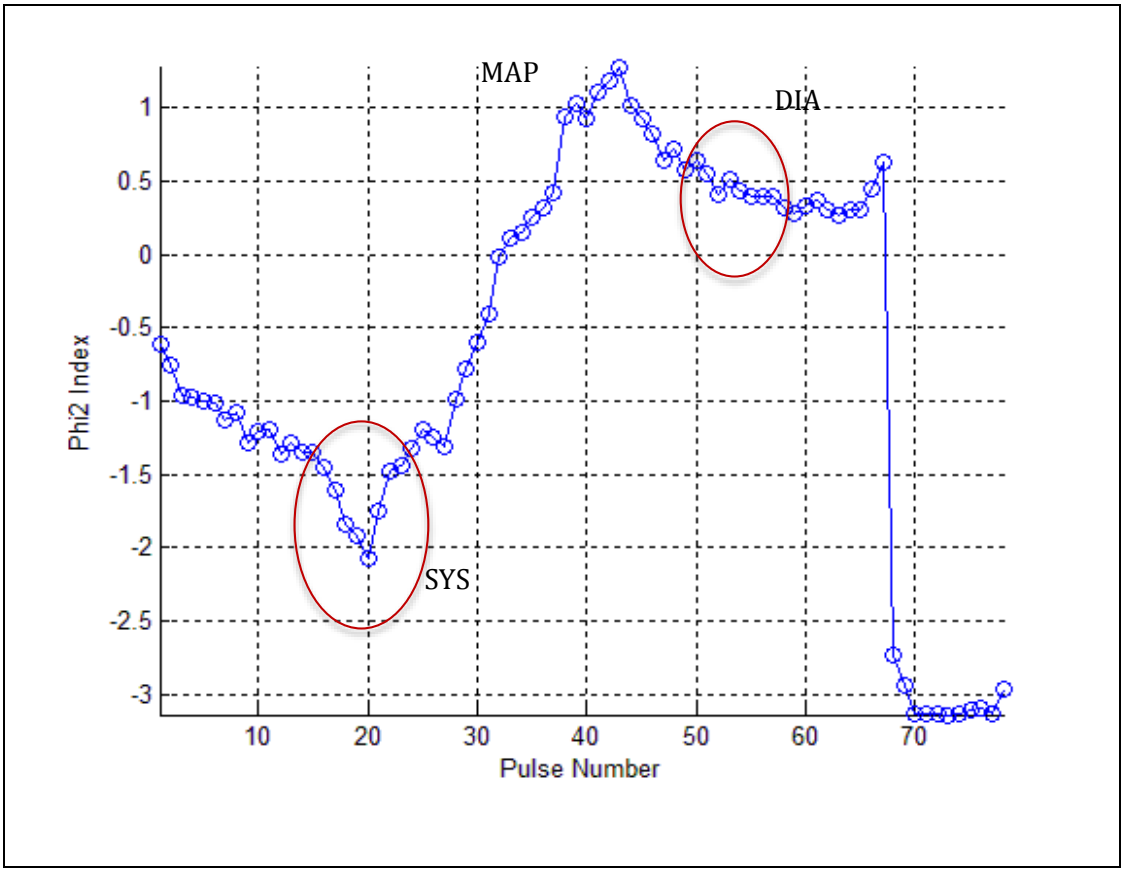

Figure 4-7: Plot of Phase Changes (Phi_2)

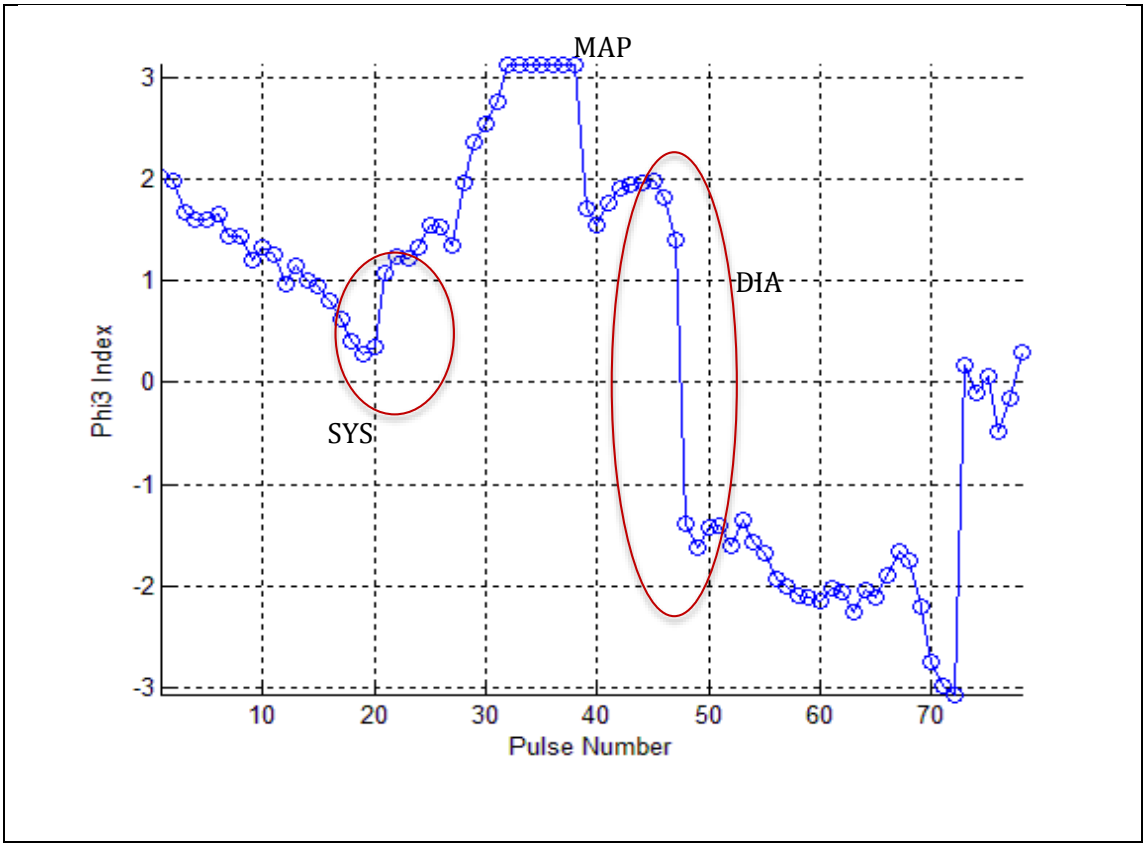

Figure 4-8: Plot of Phase Changes (Phi_3)

The figures 4.1 to 4.8 as presented; represent the behavior of each parameters across the pressure regions. This was done for all pulses in the waveform for all ten subject. Estimated diastolic and systolic occurrence regions is circled in red. Our algorithm identifies the region with the most prominent slope and/or most prominent peak as the region of interest. The plots of the DC and amplitude A1 were similar in all cases. Amplitude A3 showed a big phase change just before the maximum point. The phase graphs were similar in the three cases. Maximum and minimum values for the phases were constantly 3.14 and -3.14 respectively which represents the upper and lower bound limits of pi (Π). These values were observed to occur mostly at the origin and the end of the blood pressure measurement.

4.2 **Determination of Blood Pressure using sine function**

Estimated SBP and DBP occur in the region after or before a major phase or amplitude jumps. For the SBP region in a concave behaving graph it can be observed that the major phase jump is an increase slope. The region after that becomes concave.

The opposite occurred in a DBP region. The Research shows that the pressure at which the maximum oscillation appears corresponds to the mean arterial pressure (MAP) [5] [22 - 24]. In chapter 2 we defined MAP as the average of the total arterial pressure during one cardiac cycle. Maximum amplitude occurs at this point by a phenomenon known as vascular unloading [22 - 24].

In terms of arterial compliance, at MAP point, external pressure (cuff pressure) equals the internal arterial pressure and, the arterial wall does not contain any stress. This implies that, transmural pressure is zero and arterial compliance is maximum [11] [13]. To determine MAP using the amplitudes and DC component, the waveform of the OMW pulse parameter is

smoothen and the maximum is extrapolated to the cuff pressure corresponding to the location of the MAP.

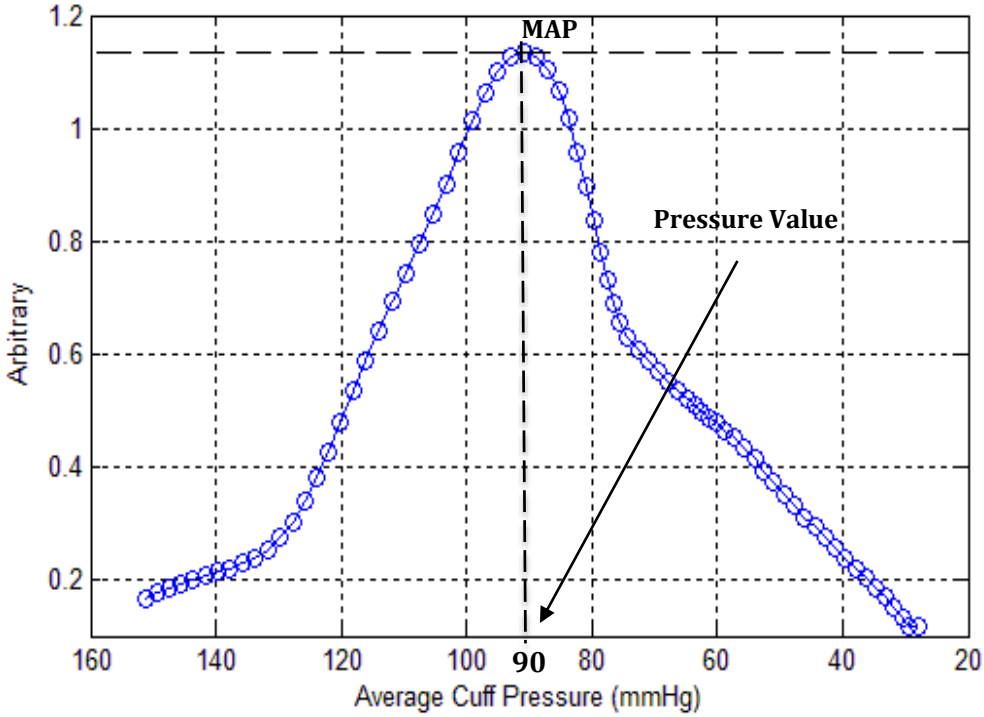

Figure 4-9: Smoothened Parameter showing a distinct peak. The peak represents the MAP. Pressure value at this point is shown on the x-axis

Using the phases, outliers are first removed. We indexed an outlier at MAP as values higher than 3. This is because at normal operation of the fitting function without any rapid changes the phase value is at 3.14 which represents PI (Π). After the outliers are removed, the plot is smoothened; the signal is interpolated and the maximum value is determined. The pulse number is mapped to the cuff pressure to determine the pressure value in mmHg.

It is known that the MAP occurs between the SBP and DBP. This knowledge was useful in the determination of SBP and DBP.

To determine SBP and DBP we divided the waveform into three regions, systolic, diastolic and MAP regions (Fig 4.10). The idea is to isolate the search area of our algorithm to the specific pressure region.

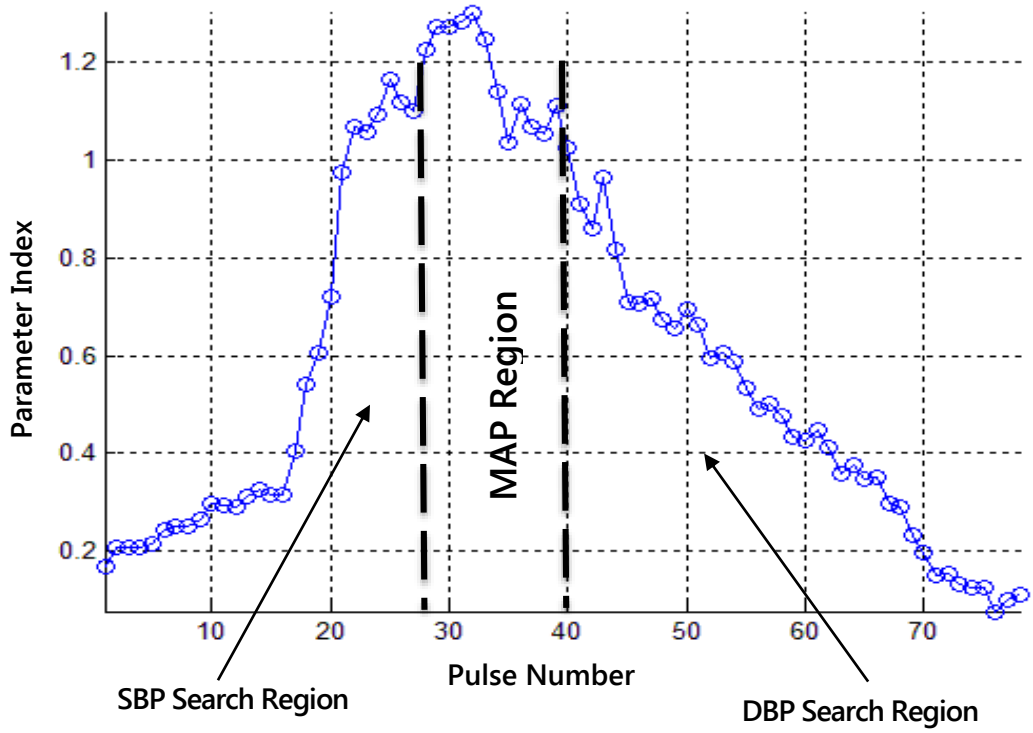

Figure 4-10: Illustration of the SBP and DBP search regions.

The SBP search region is limited to about one-third of the total pulse number, observed from the beginning of the recording. The search for DBP is limited to about the third one-third of the total pulse number, observed from the beginning of the recording (Ref: Fig 4.10).

Further processing is done to remove border peaks in the systolic region for phases and for inverted waveform. Every waveform has multiple maximas and minima [29]. We hypothesized that the most prominent local maxima and slope in SBP and DBP search regions are identified as the SBP and DBP points respectively. For better accuracy, 3 prominent peaks are found per region and the average of the cuff pressure values are used.

A cuff pressure value is assigned to each pulse within a waveform. This was derived by finding the average of the multiple cuff pressure sample points within a pulse and the cuff deflates. The values of the estimated parameters are presented in tables 4.1 to 4.3 for all parameters at the important pressure points.

Blood pressure estimation is done by extrapolating the estimated pressure point to the cuff pressure to determine the pressure value. The SD and MAE result for all the parameters at the pressure regions is presented in tables. Comparison is made with the Omron value by estimating the mean absolute error (MAE) and the standard deviation (SD).

Table 4-1: Mean Absolute Error with OMRON results at DBP; Comparison with Pulse Morphology and MAA

MAE	Pulse Harmonic Parameters								Reference Algorithms				
									Pulse Morphology				Ref
DBP	DC	A_0	A_1	A_2	A_3	Phi_1	Phi_2	Phi_3	AI	ΔT/T	SI	RI	MAA
mmHg	4.6	3.2	3.8	4.7	4.2	9.4	11.9	9.3	5.3	4.1	5.1	4.1	5.8

Table 4-2: Mean Absolute Error with OMRON results at MAP; Comparison with Pulse Morphology and MAA

MAE	Pulse Harmonic Parameters								Reference Algorithms				
									Pulse Morphology				Ref
MAP	DC	A_0	A_1	A_2	A_3	Phi_1	Phi_2	Phi_3	AI	ΔT/T	SI	RI	MAA
mmHg	3.1	2.9	2.9	5.3	5.7	3.9	4.3	2.9	3.9	5.0	4.3	4.3	4.8

Table 4-3: Mean Absolute Error with OMRON results at SBP Comparison with Pulse Morphology and MAA

MAE	Pulse Harmonic Parameters								Reference Algorithm				
									Pulse Morphology				Ref
SBP	DC	A_0	A_1	A_2	A_3	Phi_1	Phi_2	Phi_3	AI	ΔT/T	SI	RI	MAA
mmHg	7.0	6.9	7.9	5.7	5.0	4.5	5.2	3.9	6.6	6.3	6.3	5.9	4.0

Table 4-4: Comparison of the proposed method with Omron and Pulse Morphology at DIA

	Pulse Harmonic Parameters								Reference Algorithms: Pulse Morphology				Reference Algorithms: MAA	Ref Device
SD-DBP	DC	A_0	A_1	A_2	A_3	Phi_1	Phi_2	Phi_3	AI	ΔT/T	SI	RI	MAA	Omron
mmHg	72±5	74±4	69±7	70±5	69±6	76±5	80±6	82±5	72±7	74±7	74±7	75±5	69±3	73±4

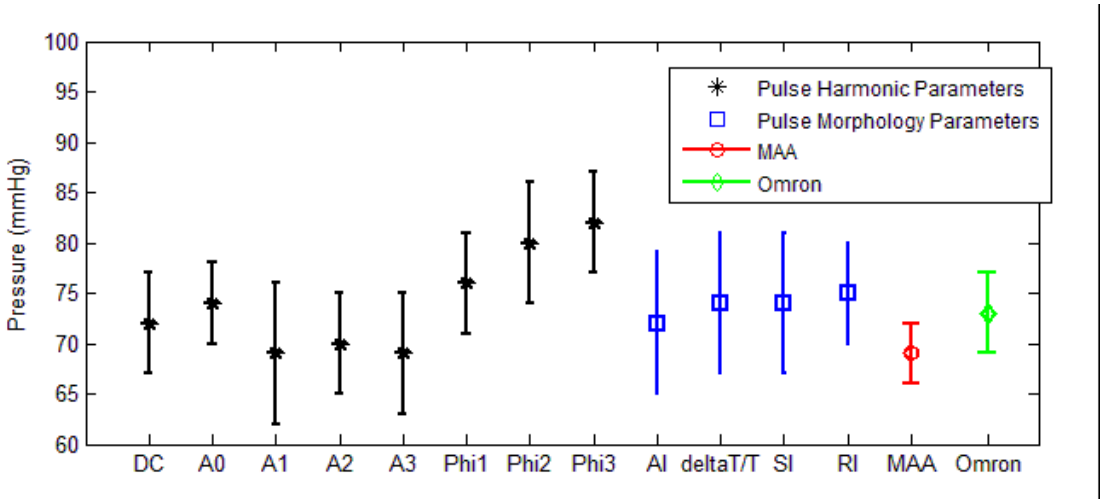

Figure 4-11: Error-Bar Plot of the Comparing the Proposed method with Omron and Pulse Morphology and Showing Deviation Error at DBP

Table 4-5: Comparison of the proposed method with Omron and Pulse Morphology at MAP

	Pulse Harmonic Parameters								Reference Algorithms: Pulse Morphology				Reference Algorithms: MAA	Ref Device
SD-MAP	DC	A_0	A_1	A_2	A_3	Phi_1	Phi_2	Phi_3	AI	ΔT/T	SI	RI	MAA	Omron
mm Hg	94±3	94±3	94±3	97±4	97±4	96±3	96±4	94±4	87±5	87±6	90±5	90±6	89±6	92±5

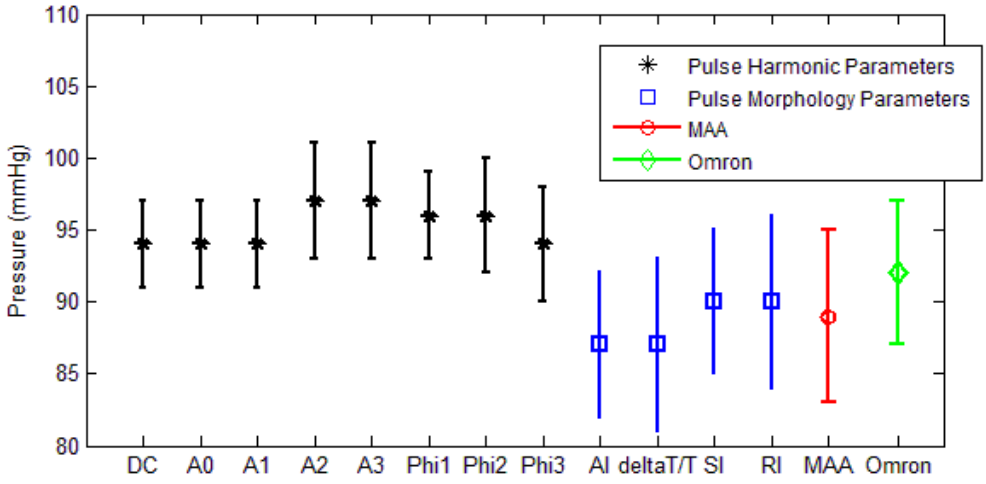

Figure 4-12: Error-Bar Plot of the Comparing the Proposed method with Omron and Pulse Morphology and Showing Deviation Error at MAP

Table 4-6: Comparison of the proposed method with Omron and Pulse Morphology Method at SYS

	Pulse Harmonic Parameters								Reference Algorithms					Ref Device
									Pulse Morphology				MAA	
SD-SBP	DC	A_0	A_1	A_2	A_3	Phi_1	Phi_2	Phi_3	AI	ΔT/T	SI	RI	MAA	Omron
mmHg	105±4	104±3	104±3	109±7	109±6	109±7	109±7	110±5	121±8	121±8	123±7	124±7	121±5	123±6

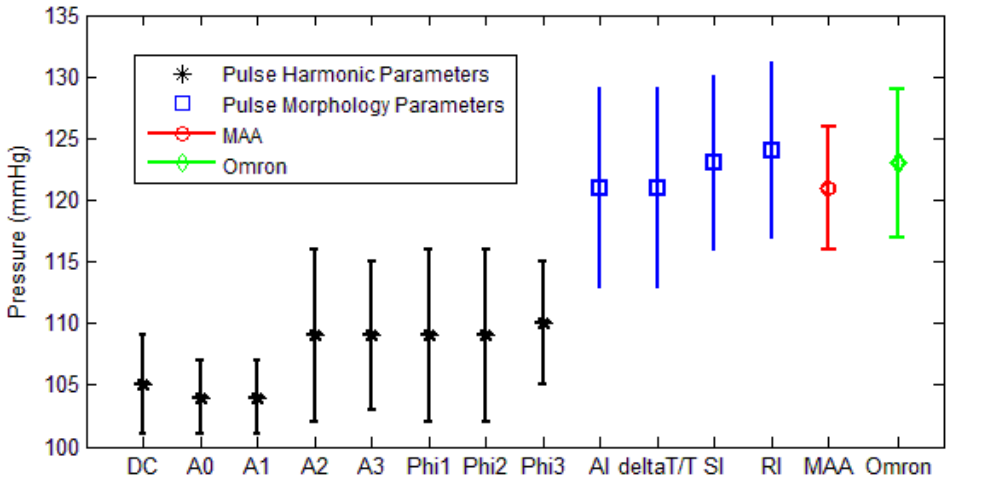

Figure 4-13: Error-Bar Plot of the Comparing the Proposed method with Omron and Pulse Morphology and Showing Deviation Error at SBP

A couple of differences were observed between the OMW for the subject groups. To test the behavior of the algorithm between subject groups, the SD and MAE of the estimated BP values between male and female subjects were compared.

Table 4-7: Comparison of the proposed method amongst subject groups with Omron results at DBP.

DBP	DC-SD	A_0-SD	A_1-SD	A_2-SD	A_3-SD	Phi_1-SD	Phi_2-SD	Phi_3-SD	Omron
Men	74.2±3.9	73.6±4.0	69.6±6.1	71.7±6.0	74.4±3.7	80.9±3.9	80.8±3.9	79.7±4.6	77.2±3.9
Women	69.1±5.8	69.5±6.5	69.3±3.8	69.6±5.6	68.2±4.7	79.6±4.0	78.4±2.5	78.8±3.5	74.9±2.4

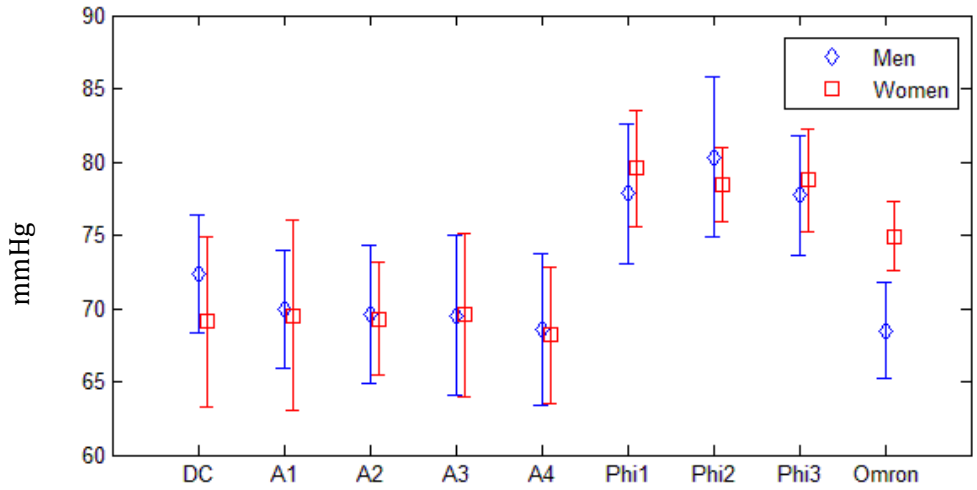

Figure 4-14: Error-Bars comparison the SD between Subject groups at DBP

Table 4-8: Comparison of the proposed method amongst subject groups comparison with Omron results at MAP

MAP	DC-SD	A_0-SD	A_1-SD	A_2-SD	A_3-SD	Phi_1-SD	Phi_2-SD	Phi_3-SD	Omron
Men	88.3±3.3	94.9±3.7	95.3±3.3	95.3±3.3	95.7±4.0	96.4±3.2	94.7±5.1	94.9±5.1	97.4±4.5
Women	86.3±1.8	95.1±2.2	94.9±2.3	94.9±2.3	96.3±3.8	95.1±2.9	95.5±4.0	96.8±2.5	97.5±3.9

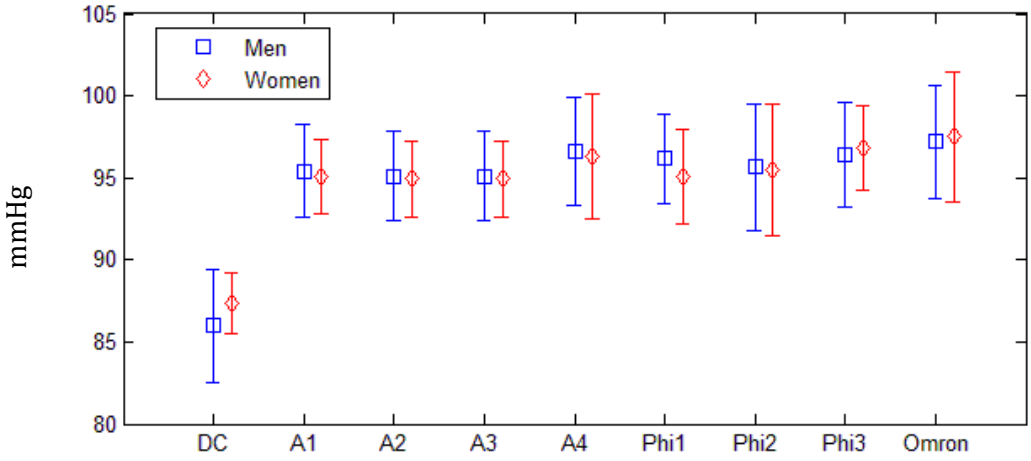

Figure 4-15: Error-Bars comparison the SD between Subject groups at MAP

Table 4-9: Comparison of the proposed method amongst subject groups comparison with Omron results at SBP

SBP	DC-SD	A_0-SD	A_1-SD	A_2-SD	A_3-SD	Phi_1-SD	Phi_2-SD	Phi_3-SD	Omron
Men	113.2±4.3	106.8±4.7	106.8±4.7	108.9±5.5	110.0±5.8	110.8±5.8	109.0±5.1	111.3±4.9	114.3±3.9
Women	109.5±3.7	107.0±3.6	107.3±3.6	109.1±4.7	107.7±4.0	107.6±3.5	108.3±4.1	106.8±5.5	109.2±3.4

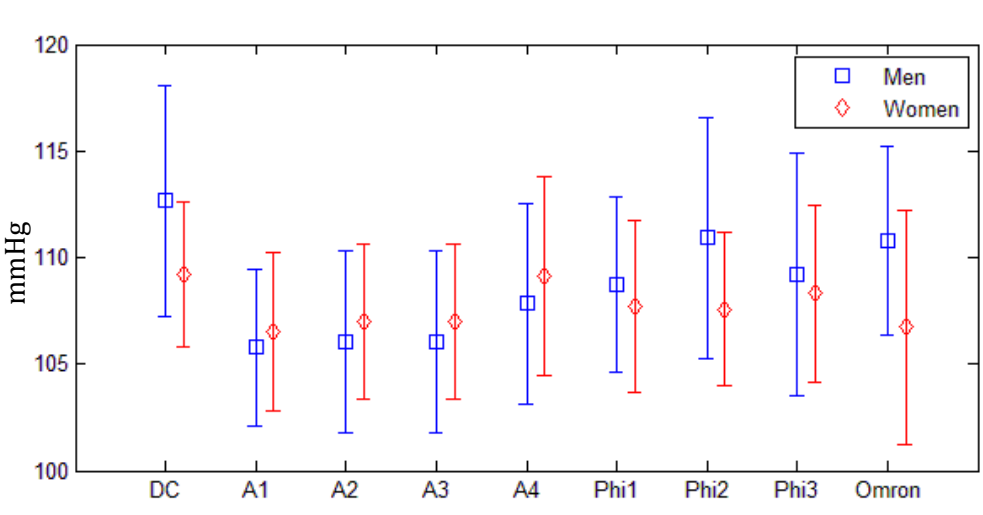

Figure 4-16: Error-Bars comparison the SD between Subject groups at SBP

4.3 **Bland Altman Test**

Bland Altman difference test tells us how well the data fits the normal expectation of agreement. I.e. the upper and lower limits. The confidence limit is defined as the standard deviation (SD) of the difference multiplied by 1.96 and added to the mean difference for the upper limit. The mean difference is subtracted for the lower limits. The limits of agreements estimates the interval that a given proportion of differences between different methods/measures is likely to lie within.

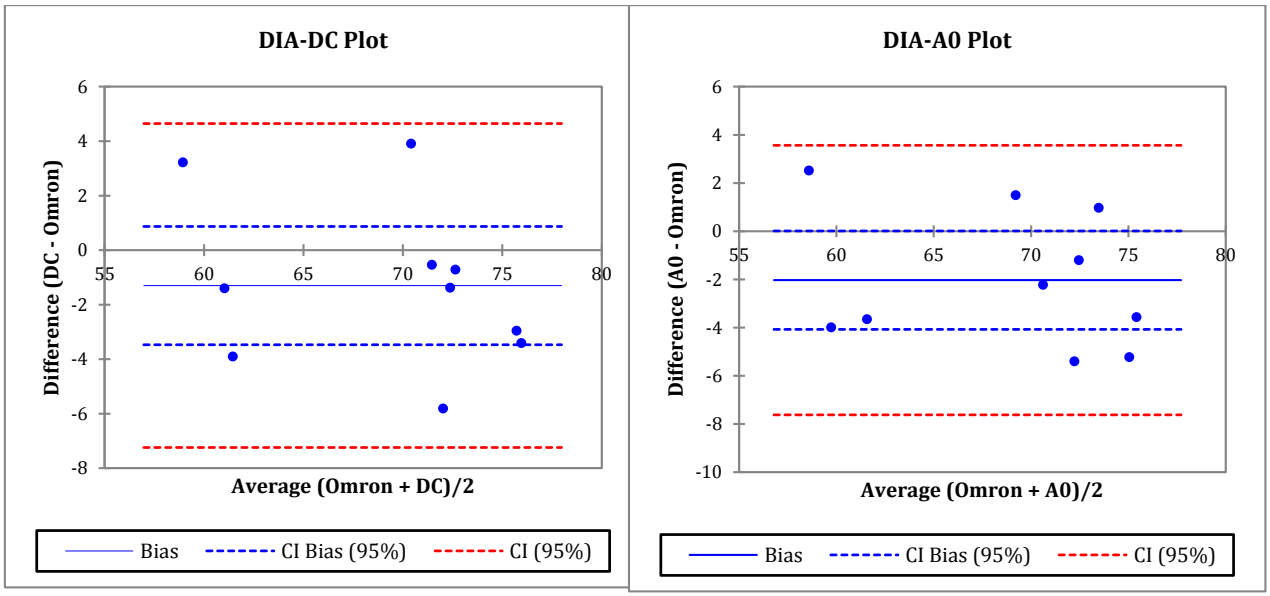

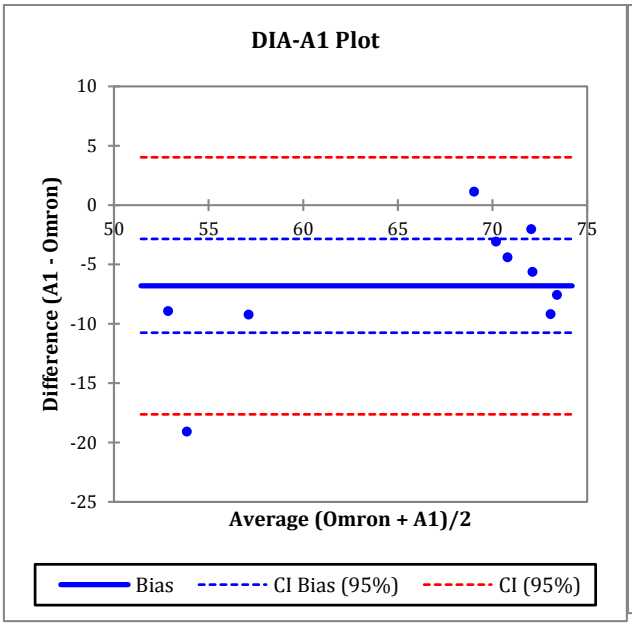
DIA-A1 Plot
Difference (A1 - Omron)
Average (Omron + A1)/2
Bias
CI Bias (95%)
CI (95%)

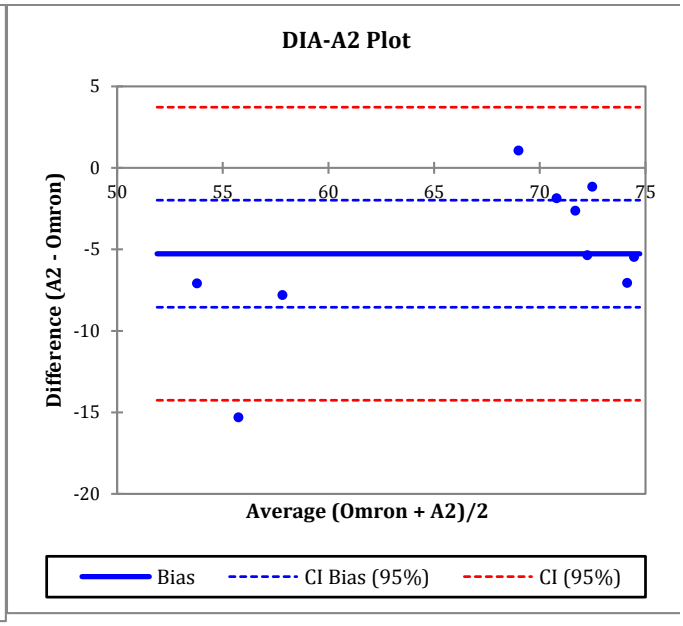
DIA-A2 Plot
Difference (A2 - Omron)
Average (Omron + A2)/2
Bias
CI Bias (95%)
CI (95%)

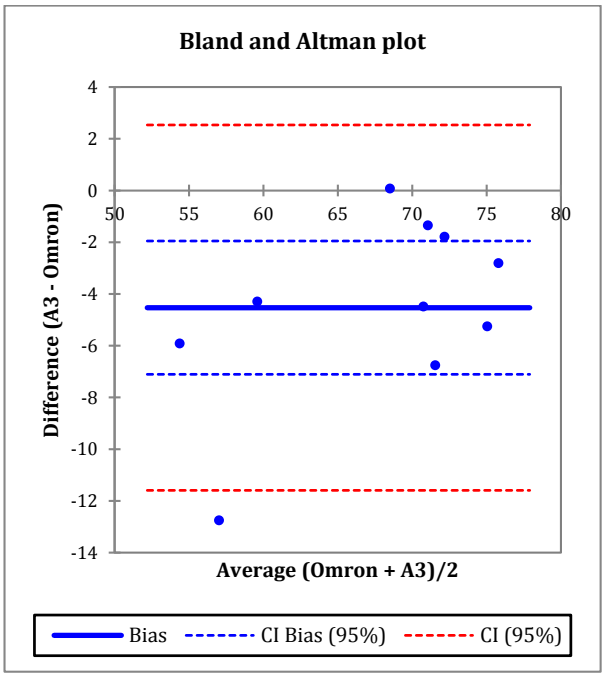
Bland and Altman plot
Difference (A3 - Omron)
Average (Omron + A3)/2
Bias
CI Bias (95%)
CI (95%)

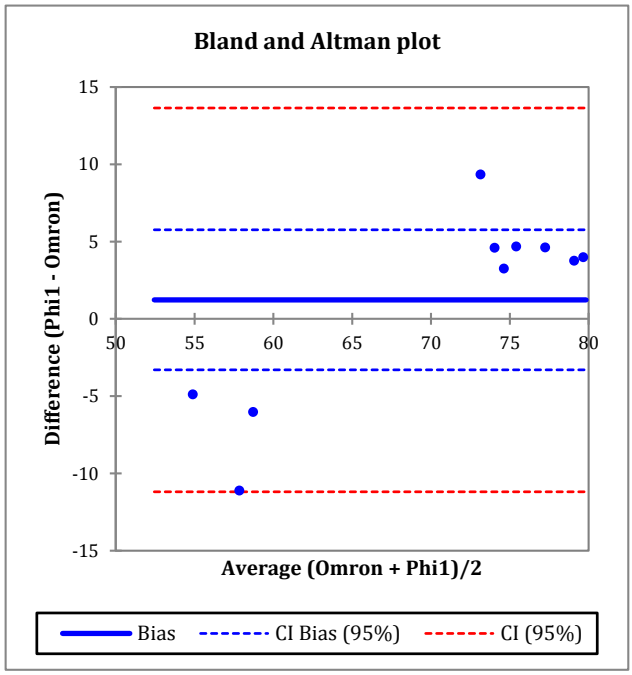
Bland and Altman plot
Difference (Phi1 - Omron)
Average (Omron + Phi1)/2
Bias
CI Bias (95%)
CI (95%)

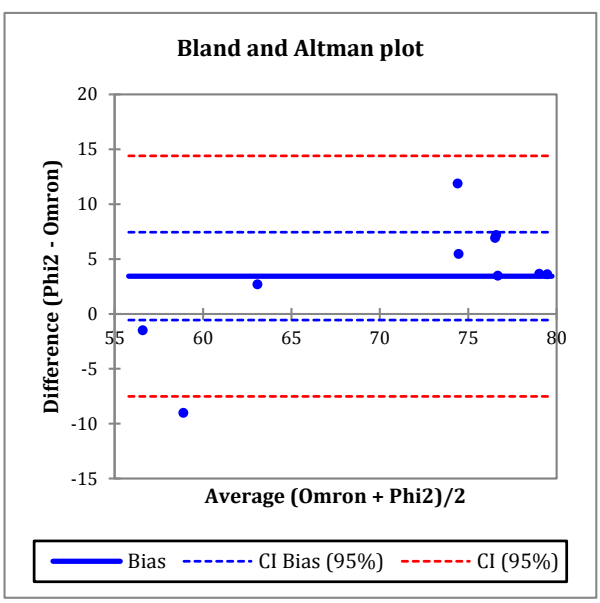

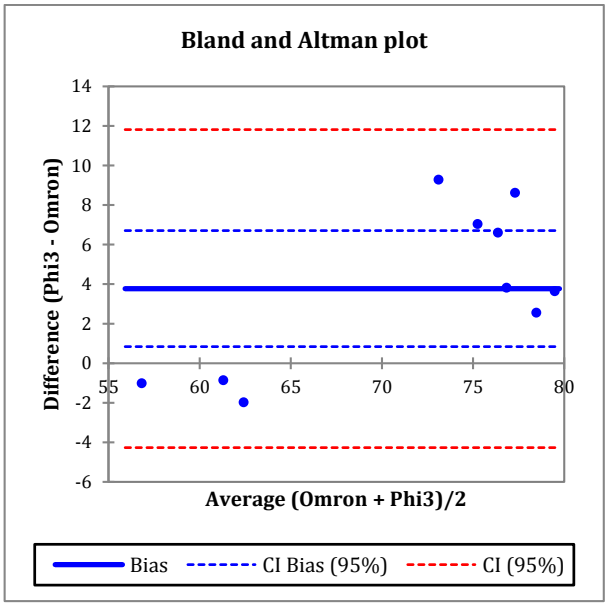

Figure 4-17: Bland Altman Difference vs Average Test at DBP

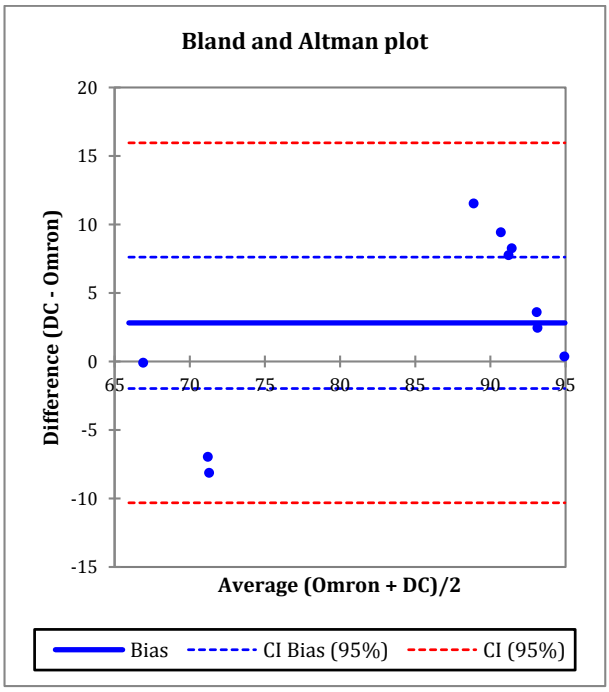

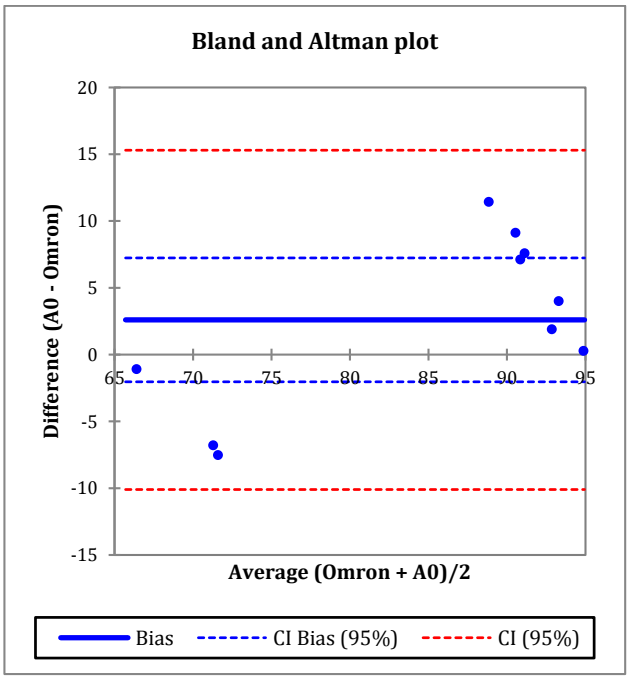

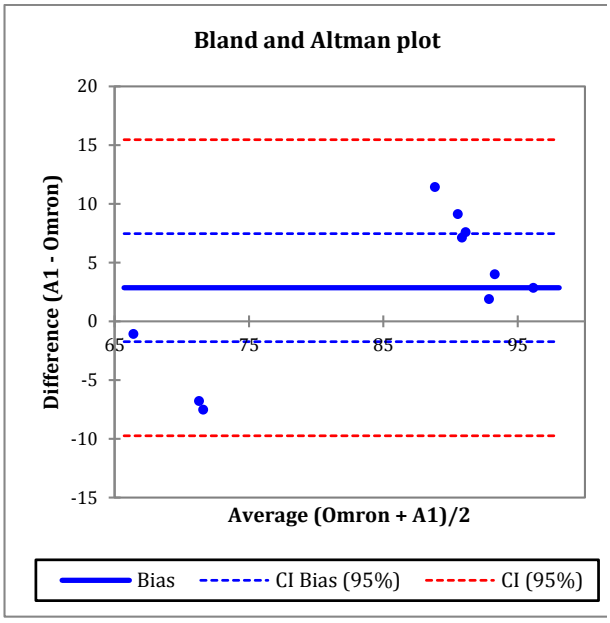
Bland and Altman plot
Difference (A1 - Omron)
Average (Omron + A1)/2
Bias
CI Bias (95%)
CI (95%)

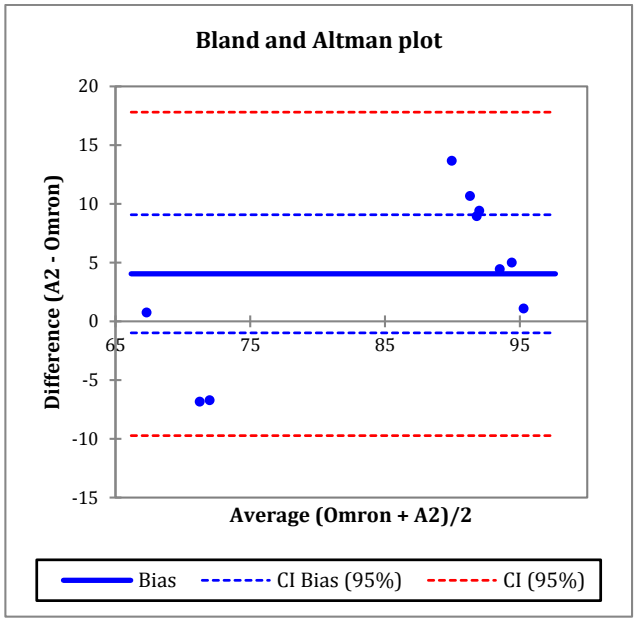
Bland and Altman plot
Difference (A2 - Omron)
Average (Omron + A2)/2
Bias
CI Bias (95%)
CI (95%)

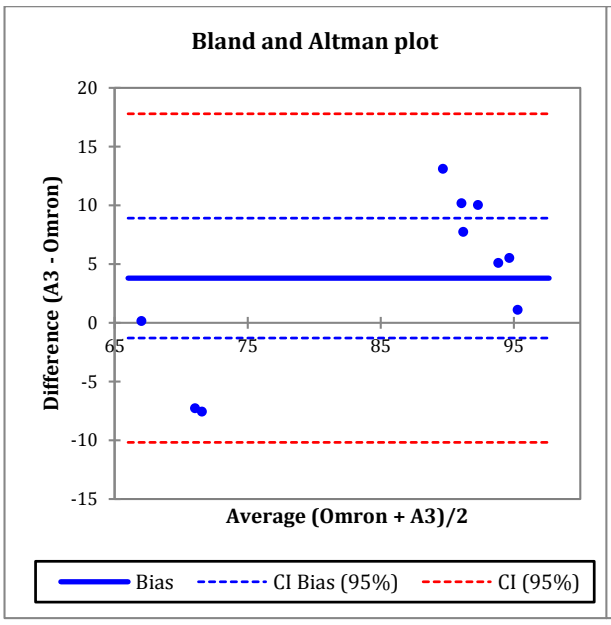
Bland and Altman plot
Difference (A3 - Omron)
Average (Omron + A3)/2
Bias
CI Bias (95%)
CI (95%)

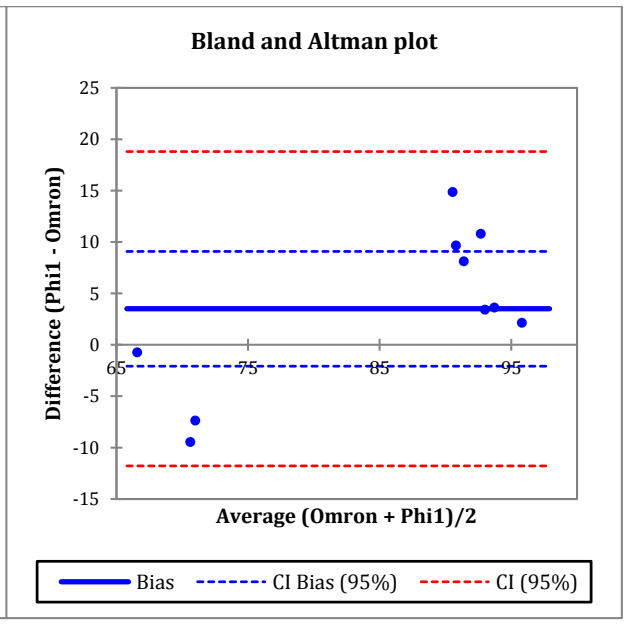
Bland and Altman plot
Difference (Phi1 - Omron)
Average (Omron + Phi1)/2
Bias
CI Bias (95%)
CI (95%)

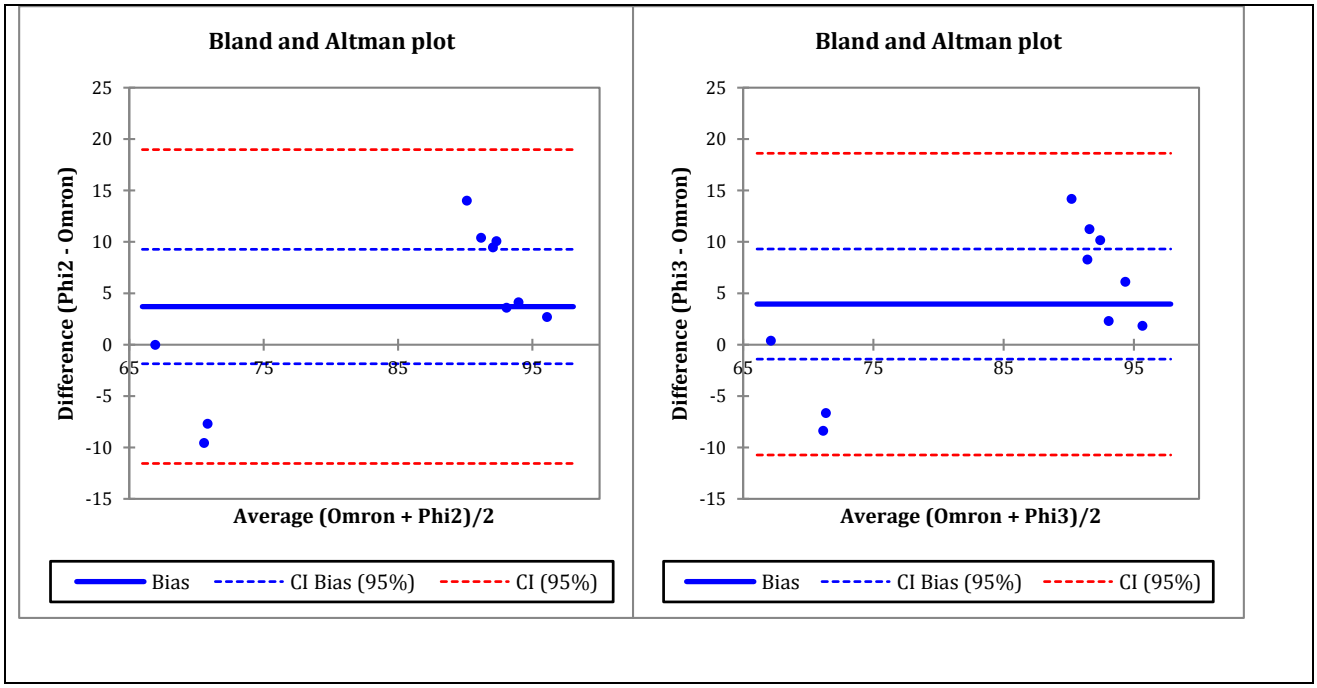

Figure 4-18: Bland Altman Difference vs Average Test at MAP

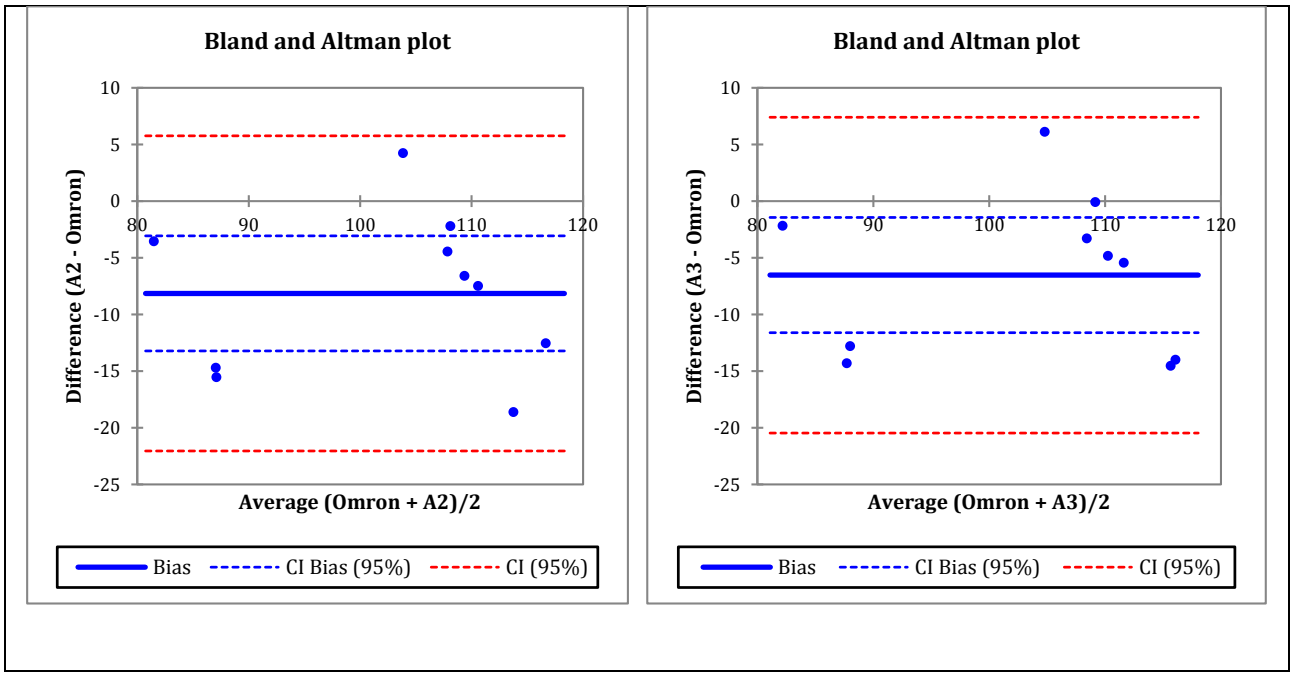

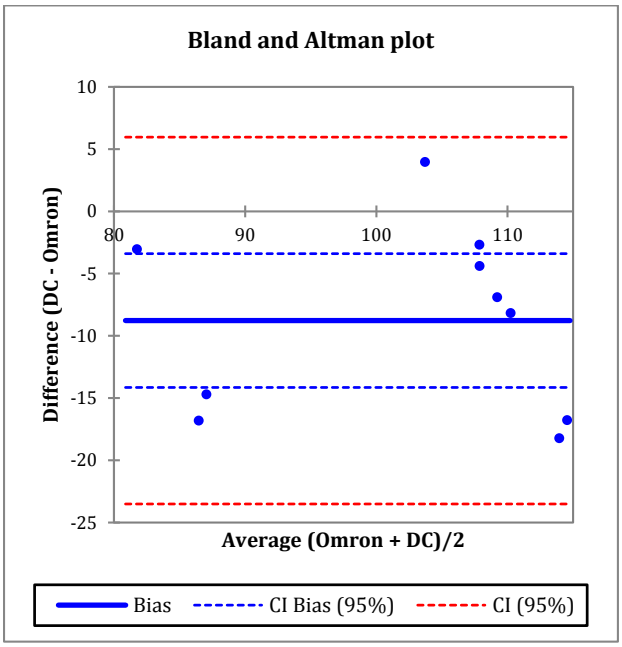
Bland and Altman plot
Difference (DC - Omron)
Average (Omron + DC)/2
Bias
CI Bias (95%)
CI (95%)

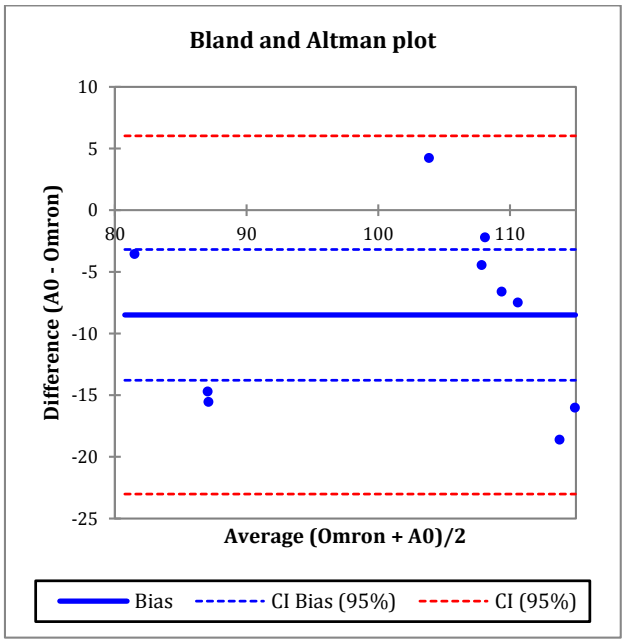
Bland and Altman plot
Difference (A0 - Omron)
Average (Omron + A0)/2
Bias
CI Bias (95%)
CI (95%)

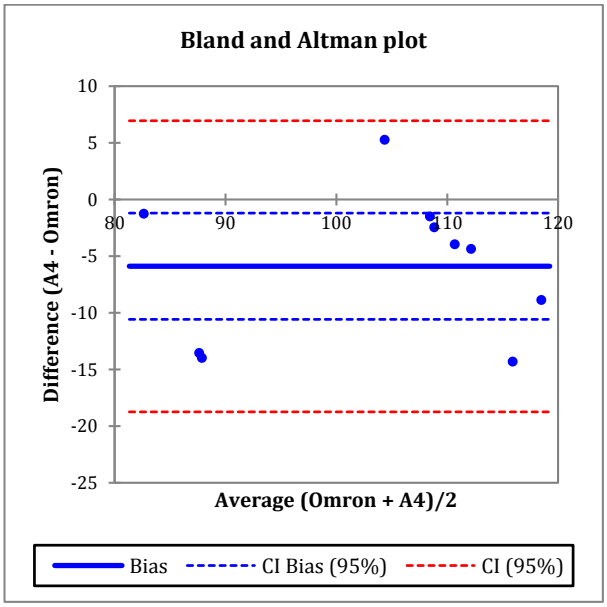
Bland and Altman plot
Difference (A4 - Omron)
Average (Omron + A4)/2
Bias
CI Bias (95%)
CI (95%)

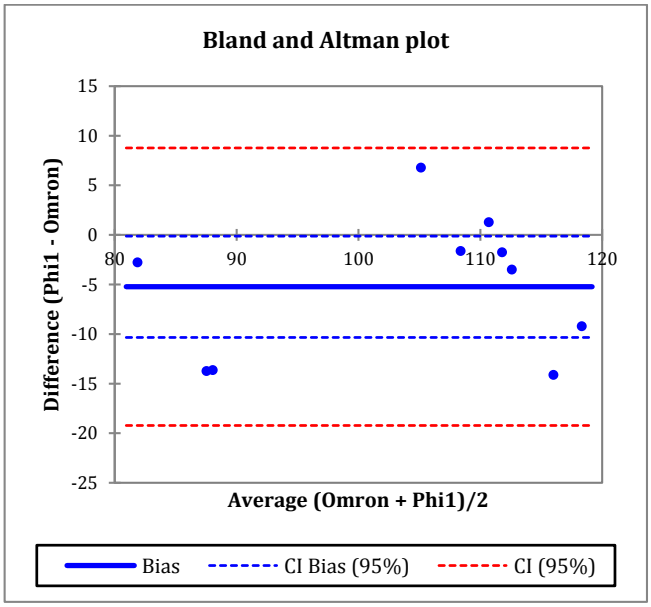
Bland and Altman plot
Difference (Phi1 - Omron)
Average (Omron + Phi1)/2
Bias
CI Bias (95%)
CI (95%)

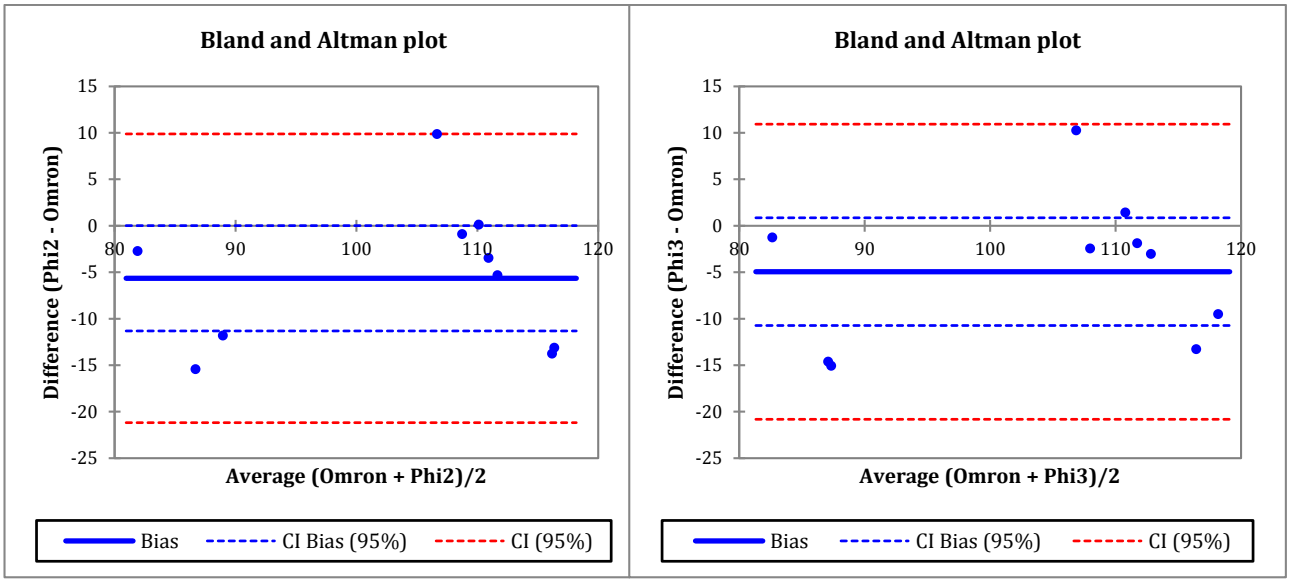

Figure 4-19: Bland Altman Difference vs Average Test at SBP

The limits can be used to determine if the methods can be applied interchangeably or the new method can replace the old, without changing the interpretation of the results. The Bland Altman test is done for all amplitude and phase parameters for one subject at SBP, DBP and MAP using the proposed method and the OMRON recording. Figures 4.16- 4.18 show the plots of results of the test. The solid horizontal lines represent the mean difference while the broken line represents the limits of agreements. Each plot has a key that further explains the properties. The presented plots is the grouped bland Altman test of the 10 subject with 15 trials. A point on the plot represents an average of the recording for one subject.

The plot shows most of the data points close to the mean difference and few points outside the limits of agreements. This is interpreted as having more similarity between the estimated BP with proposed method and OMRON results.

The estimation parameters show small oscillations which may be due to breathing and in some instances major movements in the limbs occur as spikes in the signal. These might be responsible for the large deviation between the BP estimation using the proposed method and OMRON device (Ref: Tables 4.4 – 4.6)

Chapter 5 further discusses the results presented, outlining possible options to the proposed method. The different extraction techniques used in this project, as well as results of further statistical tests and analysis are also presented.

Chapter 5: Comparisons of Methods and Algorithms

In the previous chapter, we presented the proposed method of determining blood pressure by characterizing oscillometric pulses using eight frequency parameters of the pulse waveform. We compared the different results for the amplitude and phase components.

Maximum amplitude is considered to be the mean arterial pressure (MAP). Since the Omron device does not estimate the mean pressure, we estimated the mean arterial pressure using the equation presented by *M. Razminia et al*, [71]. This formula takes into consideration the heart rate and deflation rate of the cuff. It is proven to be more accurate than the precious formula written as 33 percent MAP formula. DC and amplitude parameters showed the least deviation from the reference value as compared to the phases.

The presented results showed that various components had better agreements for different blood pressure values. The result shows that all parameters performed well at MAP. DC and A_0 performed well at DBP, MAP and SBP. Phases Phi_1, Phi_2 and Phi_3 had high deviation values of ±7 at SBP and ±5 at DBP Ref to tables 4.1 – 4.3.

In comparison with the reference algorithms Pulse Morphology algorithm, MAA and Omron, the proposed parameters had less deviation values than MAA, Omron and PMA at MAP. Parameters DC and A_0 and A_1 performed better at SBP than the reference algorithm and device having lower deviation. At DBP, Omron and MAA had better performances. However, the proposed method fared better with less deviation than pulse morphology algorithm.

Comparison amongst subject groups in tables 4.7 – 4.9: the proposed algorithm showed better results for women at SBP and MAP as compared to men. At DBP it showed tendencies to overestimate or underestimate the values for women as compared to men.

The diastolic pressure showed the least agreement for all parameters. The lower and higher standard deviation values were ±4 and ±6. The guess is: because diastole occur close to the end of the measurement, the frequency change is high at this point as such large amplitude and phase changes were recorded.

From the observation of women subjects, the oscillometric waveform for women appear to be shorter as compared to men, with less than 70 pulses in most cases. However, the cuff was inflated to 140mmHg before deflation began. Giving a range of about 40mmHg above the estimated, before systolic blood pressure instead of the recommended 20 – 30 mmHg in many cases. This had negative effect on the determination of the systolic pressure using the proposed algorithm.

The effect of artifact on the performance of the proposed method is also worth consideration. An observation of the plots of the parameters shows there is an oscillatory component in the parameters. We suspect it is due to breathing arrhythmia, affecting the details of the frequency parameters. The presence of these factors makes it difficult to observe the changes at the important pressure points, making pressure extraction difficult. Likewise is the contributions dc component to the inaccuracy of the modelled oscillometric pulses cannot be discarded.

5.1 Student T-Tests

The estimated Blood pressure using the proposed method is compared to the OMRON reference using the t-test.

The t-test helps to test a hypothesis based on reliability of the difference between their mean. It checks for the variance between the groups and compares it to the difference within the groups. The comparison is regarded as the t values. Every t-value has a p-value. The result of the t-test determines if the method being tested can be used interchangeably with the existing method or not. The exiting method is referred to as the '**null**' hypothesis (H0). While the new method is the '**alternative**' hypothesis (H1).

A p-value is the probability that the pattern produced by a data can be produced by a random data. This tells us if the difference between our groups is real or it is a fluke. A p-value of 5% (0.05) means, there is a 5 percent chance that we will get these results with random data. For the purpose of this research we considered a p-value of 0.05 as statistically reliable. The results of the comparisons are presented in tables 5.1 to 5.3. The table shows which of the hypothesis is accepted using the 5% p-value.

Table 5-1: Student t-test, Results at DBP

DBP (T-test)	DC	A_0	A_1	A_2	A_3	Phi_1	Phi_2	Phi_3
Difference	-1.2993	-2.0287	-6.7999	-5.2675	-4.5293	1.2264	3.4374	3.7704
p-value	0.0051	0.0001	< 0.0001	< 0.0001	< 0.0001	0.0992	< 0.0001	< 0.0001
H0(0.05)/H1	H1	H1	H1	H1	H1	H0	H1	H1

Table 5-2 Student t-test, Results at MAP

MAP (T-test)	DC	A_0	A_1	A_2	A_3	Phi_1	Phi_2	Phi_3
Difference	2.8195	2.6036	2.8595	4.0372	3.8015	3.5023	3.7059	3.9449
p-value	< 0.0001	< 0.0001	< 0.0001	< 0.0001	< 0.0001	< 0.0001	< 0.0001	< 0.0001
H0(0.05)/H1	H1	H1	H1	H1	H1	H1	H1	H1

Table 5-3 Student t-test, Results at SBP

SBP (T-test)	DC	A_0	A_1	A_2	A_3	Phi_1	Phi_2	Phi_3
Difference	-8.7749	-8.4920	-8.1453	-6.5331	-5.8954	-5.2283	-5.6527	-4.9408
p-value	< 0.0001	< 0.0001	< 0.0001	< 0.0001	< 0.0001	< 0.0001	< 0.0001	< 0.0001
H0(0.05)/H1	H1	H1	H1	H1	H1	H1	H1	H1

H0 - indicates that the null hypothesis cannot be rejected at the 5% significant level, and when H1- indicates that the null hypothesis can be rejected at the 5% level.

At DBP, amplitude parameters DC, A_0, A_1, A_2, A_3 and phase parameters Phi_2 and Phi_3 had p-values less than 0.05 as such showed better agreement than Phi_1.

At MAP and SBP, all parameters had p-values less than 0.05 as such they showed that they are reasonable values and could not have been gotten by fluke. In all cases the null hypothesis can be rejected except in Phi_1 at DBP.

5.2 Effect of Extraction Method on Oscillometric pulses

In order to investigate the effect of the extraction method on the shape of oscillometric pulses, oscillometric waveform was extracted using three methods. Two are baseline subtraction methods while the third makes use of a filter (Ref section 3.4).

The resultant waveform for the three processes are presented in the precious chapter. Each waveform is then separated into its component pulses. Samples of pulses are selected from the three important pressure regions and compared. The aim is to observe the effect of the extraction procedure on the shape of the pulses. Figure 5.4 shows nine randomly selected pulses. The left column are pulses from the systolic region for the three extraction methods. The middle column are pulses occurring the middle of the recording, while the right column shows pulses from the diastolic region.

It can be observed that the dicrotic notch was mostly visible around SBP region on cuff deflation pressure waveform and became less visible moving from SBP region to DBP region. In the diastolic region, (Fig 5.1 column 3) multiple peaks can be observed. This may be due to higher blood flow as the recording approach the end of the cuff deflation.

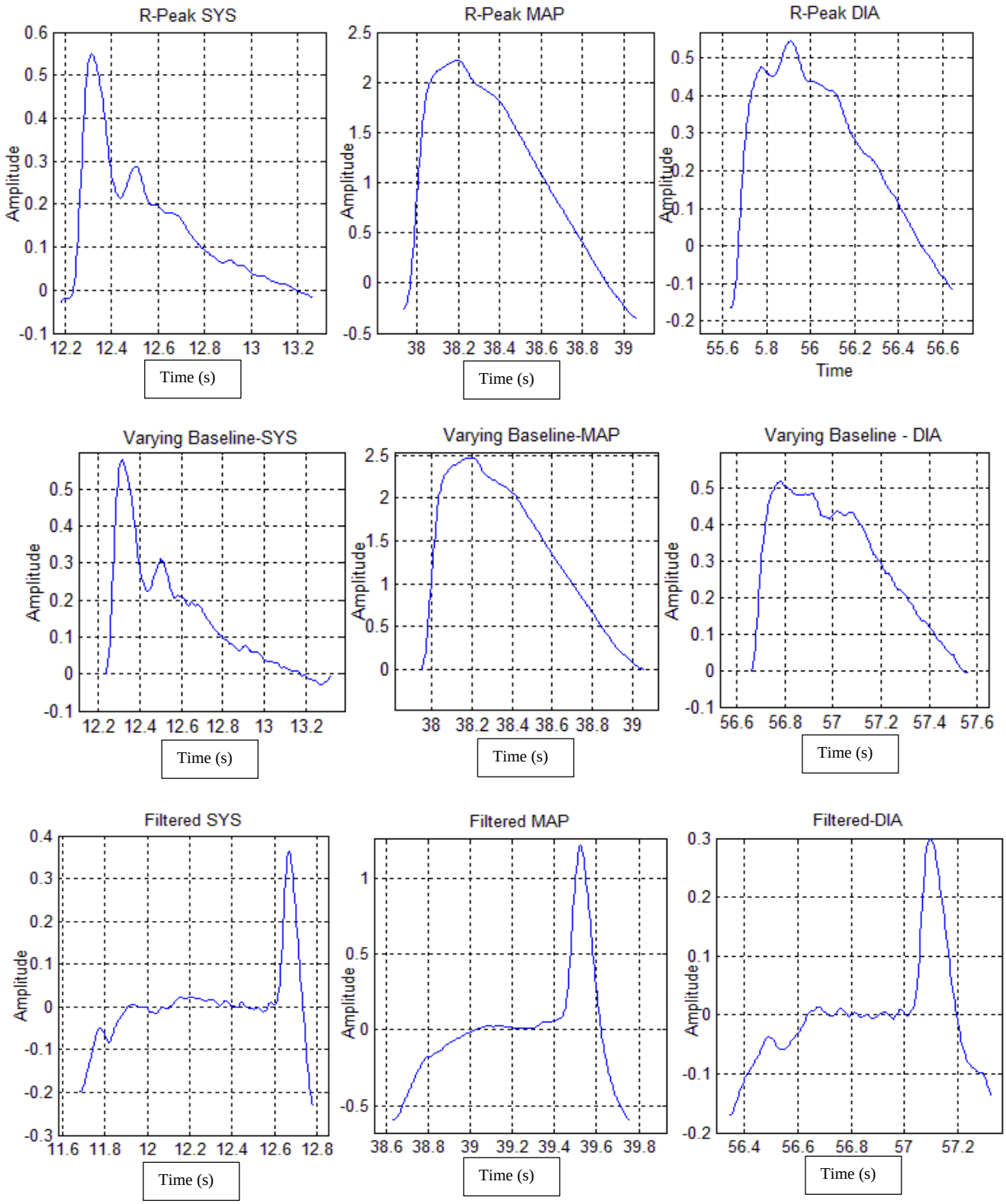

Figure 5-1: Samples of pulses from systolic, diastolic and MAP region for different extraction methods.

Pulses from the filter extracted waveform, (Fig 5.1 row 3) appeared to be inverted and distorted with the forward wave occurring in the later part of the pulse.

In the MAP region (Fig 5.1 column 2), pulses from the baseline extracted OMW had higher amplitudes than the pulses from the filtered OMW. Therefore, characteristics and shape of the pulses changed with extraction techniques and at different pressure points.

The frequency component of all pulses for every individual at SBP, MAP and DBP was computed and the difference is observed such that we can determine what extraction method is preferred for the proposed method. The plot of the estimation components are as presented in the previous chapter. Here we compare the derived blood pressure values according to the extraction methods.

Table 5-4: Comparison of the Proposed Method using different extraction method with OMRON at DIA

SD-DIA	DC	A_0	A_1	A_2	A_3	Phi_1	Phi_2	Phi_3	Omron
R-Peak	74.2±3.9	73.6±4.0	69.6±6.0	71.7±6.1	74.4±3.7	81.0±3.0	80.8±4.0	79.8±4.7	77.2±3.9
Filtering	81.5±5.4	82.6±5.1	82.8±5.1	81.0±6.0	79.7±6.6	90.8±4.0	91.2±3.9	90.5±6.1	77.2±3.9
Varying Baseline	72.6±4.7	72.7±4.0	69.4±5.4	71.7±5.4	72.3±5.0	80.6±3.6	81.2±4.1	80.6±3.6	77.2±3.9

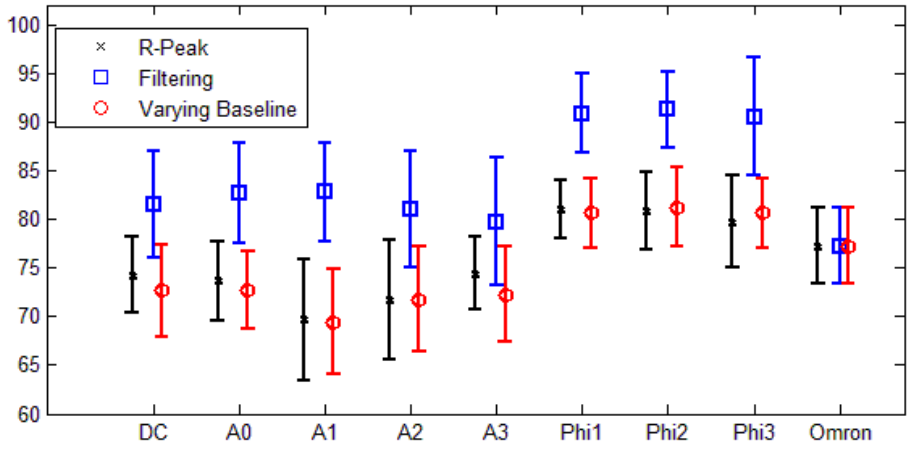

Figure 5-2: Error bar plot for the Proposed Method using Different Extraction Methods Compared to Omron. Results at DBP.

Table 5-5: Comparison of the proposed method using different extraction method with OMRON at MAP

SD-MAP	DC	A_0	A_1	A_2	A_3	Phi_1	Phi_2	Phi_3	Omron

R-Peak	94.9±3.7	95.3±3.3	95.3±3.3	95.7±4.0	96.4±3.2	94.7±5.1	94.9±5.1	97.4±4.5	91.3±3.3
Filtering	87.3±3.5	86.1±2.9	86.1±2.9	87.0±3.3	86.1±3.8	85.0±4.6	87.0±4.4	86.2±3.0	91.3±3.3
Varying Baseline	94.5±4.9	94.7±2.6	96.3±3.4	96.9±3.4	96.1±3.9	97.1±4.7	95.0±5.0	97.2±4.7	91.3±3.3

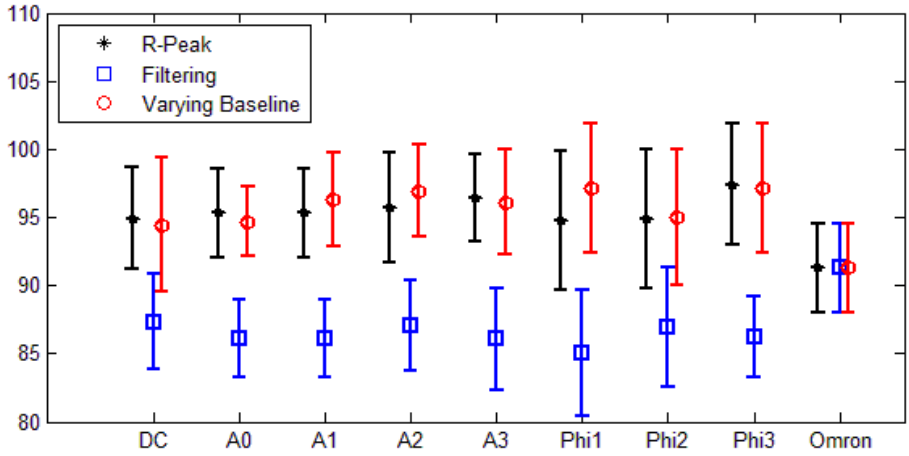

Figure 5-3: Error bar plot for the Proposed Method using Different Extraction Methods Compared to Omron. Results at MAP.

Table 5-6: Comparison of the Proposed Method using different extraction method with OMRON at SBP

SD-SYS	DC	A_0	A_1	A_2	A_3	Phi_1	Phi_2	Phi_3	Omron
R-Peak	106.2±4.3	106.8±4.7	106.8±4.7	108.9±5.5	110.0±5.8	110.8±5.8	109.0±5.1	111.3±4.9	114.3±3.9
Filtering	109.5±5.5	109.6±4.4	109.6±4.4	109.6±4.6	108.9±5.9	115.1±3.4	109.3±6.3	106.8±5.0	114.3±3.9
Varying Baseline	107.9±4.5	106.9±4.2	109.9±4.4	109.6±5.0	109.1±3.7	111.2±4.7	110.3±5.4	111.2±4.7	114.3±3.9

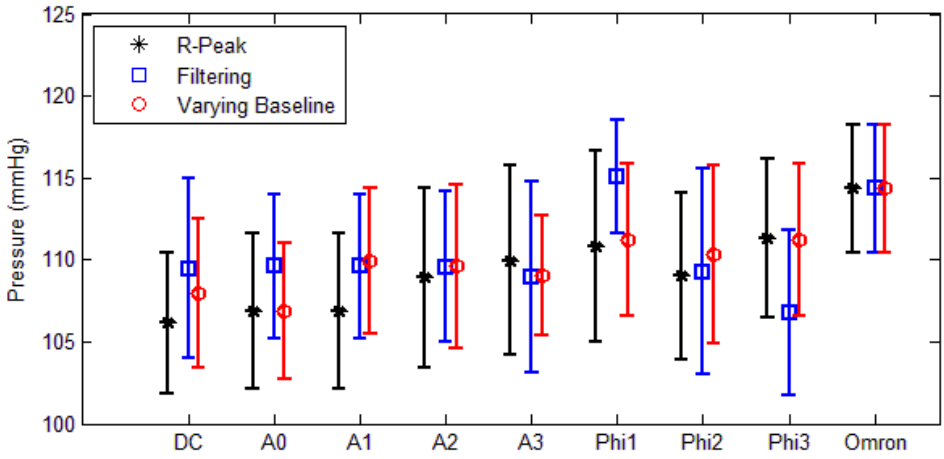

Figure 5-4: Error bar plot for the Proposed Method using Different Extraction Methods Compared to Omron. Results at SBP.

It is obvious that filtering alters the shape of oscillometric pulses. We observed the most distorted are pulses from the filtering method. The varying baseline method and the R-peak baseline method showed similar results with slight difference in amplitude at MAP. The results presented in tables 5.4 - 5.6 shows that there is no significant difference using the proposed algorithm combined with the different extraction methods. The varying baseline detrending method performed best at SBP with least deviation. Filtering performed best at MAP with little improvement over the baseline methods. At DBP, the baseline methods performed better than filtering. From this analysis we can find the combination of methods that give the best results.

Chapter 6: Summary and Conclusions

Blood pressure measurement is an important aspect of clinical medicine. The determination of blood pressure is affected by many factors some of which are not well understood. Mathematical modelling techniques have been used to analyze factors affecting the accurate determination of blood pressure. Pulse morphological studies have been found to tell us more about the state of the cardiovascular system.

This work is intended to further the studies on pulse morphological analysis by mathematically characterizing oscillometric pulses. By frequency analysis of oscillometric waveform, we used the fundamental frequency and its harmonics to characterize individual pulses at different pressure points. The pulses were analyzed by cuff-fitting using a non-linear sum of sinusoid model.

Eight model parameters were used to obtain the SBP MAP and DBP of all subjects. The subjects were divided into two groups male and female and the performance was compared.

MAP was determined by cuff smoothening SBP and DBP were determined by finding the most prominent peak in the region.

The effect of extraction method was examined on the proposed method and on the shape of pulses. Three methods were used to extract the oscillometric waveform. Blood pressure was determined using the proposed method. The performance of the algorithm using the different extraction methods was presented. We found what extraction method coupled with the proposed algorithm would produce the best results.

The effect of multiple harmonics oscillations was observed on the proposed method, pulses with multiple oscillations were truncated after the second peak. The performance was tested and presented.

Testing and analysis using statistical tools was done by comparing the proposed method to reference algorithms, pulse morphology [20] and the OMRON HEWM-790 ITCAN device.

6.1 Contributions

The contributions of this work are as follows:

- Development of a novel method of estimating blood pressure using the parameters of the fundamental frequency and harmonic characteristics of pulses.
- In-depth characterization of pulse waveforms using frequency analysis.
- Analysis of amplitude and phase behavior of pulse waveforms at important pressure points.
- Analysis of various methods of extracting oscillometric waveforms on oscillometric pulses and the performance accuracy of each using the proposed method to determine what extraction method best works with the proposed algorithm.
- Development of pulse outlier correction algorithm technique to reduce the effect of respiration artifact.
- Comparing the robustness of the proposed method to BP values estimated with OMRON, MAA and Pulse Morphology Algorithm.

6.2 Limitations and Future Works

A few limitations were encountered in this work. The most pressing of them is the lack listed as follows:

- Lack of proper validation method. An ideal validation for this work would have been with the auscultatory method of non-invasive blood pressure measurement. However, it was done with Omron device and other algorithms.
- Limitation of number of test subjects. The method was tested on 10 subjects. A larger dataset would allow better testing for statistical forecasting.
- Using the proposed method, it was clear that dataset had breathing artifact. Advanced signal processing techniques can be used to remove the breathing component; however, this is outside the scope of this research. Future studies should include removal of respiratory component.
- The model was done using bounded nonlinear optimization tool with objective function of minimizing the least square error. Constrained optimization tools can be used to further the work done.
- This work estimated blood pressure using individual amplitude and phase parameters individually. Amplitude parameters were found to be better at MAP than at SBP and DBP. In future studies a fusion of phase and amplitude parameters can be used to get better result.
- Attempts have been made in literature to linearize oscillometry by finding the best possible amplitude modulation for the envelope. Complex arterial interactions may be lost in the residual using this approach. Further studies can consider using our approach of removing multiple oscillation components in the pulses leaving the forward and reflected wave.

Appendix A: BP Estimated by 8 Harmonic Parameters of Pulse Waveform

Subject 1 DBP	Omron	DC	A0	A1	A2	A2	Phi1	Phi2	Phi3
Trial 1	76	76	70	76	75	75	79	79	79
Trial 2	76	73	73	61	69	76	79	81	79
Trial 3	80	78	74	78	78	73	81	80	85
Trial 4	78	73	76	76	67	68	78	78	80
Trial 5	78	77	76	78	78	76	87	86	86
Trial 6	81	78	77	63	65	65	85	77	74
Trial 7	79	70	78	61	61	77	83	85	71
Trial 8	78	76	67	76	69	77	84	85	83
Trial 9	79	79	79	64	79	79	78	88	88
Trial 10	84	79	79	64	75	75	77	77	74
Trial 11	80	71	71	71	71	74	83	83	79
Trial 12	76	70	71	70	61	74	83	83	79
Trial 13	69	68	69	70	74	77	80	80	83
Trial 14	71	78	69	69	78	78	77	75	80
Trial 15	73	69	75	68	76	72	79	76	78

Subject 1 MAP	Omron	DC	A1	A2	A3	A4	Phi1	Phi2	Phi3
Trial 1	91	94	94	94	97	95	93	96	96
Trial 2	87	96	95	95	93	101	90	90	90
Trial 3	91	94	94	94	95	96	89	89	105
Trial 4	93	102	91	91	94	100	102	102	102
Trial 5	93	96	99	99	94	96	98	103	99
Trial 6	95	95	95	95	102	100	90	92	92
Trial 7	92	89	93	93	101	93	91	101	89
Trial 8	92	89	103	103	90	90	89	91	100
Trial 9	94	92	94	94	95	98	90	90	98
Trial 10	97	100	99	99	102	94	94	90	99
Trial 11	92	93	95	95	94	92	93	93	93
Trial 12	91	100	95	95	92	101	102	102	102
Trial 13	85	94	90	90	94	96	96	91	99
Trial 14	86	95	98	98	91	96	102	98	98
Trial 15	89	94	94	94	101	96	99	94	98

Subject 1 SBP	Omron	DC	A1	A2	A3	A4	Phi1	Phi2	Phi3

Trial 1	115	110	112	112	106	108	110	110	110
Trial 2	106	110	110	110	114	116	119	115	115
Trial 3	110	110	110	110	107	116	105	107	115
Trial 4	119	102	102	102	115	105	102	109	107
Trial 5	118	101	101	101	114	101	103	103	116
Trial 6	117	108	111	111	115	117	116	112	112
Trial 7	112	111	104	104	101	117	117	103	107
Trial 8	115	99	117	117	100	106	110	115	108
Trial 9	119	106	108	108	110	112	113	109	109
Trial 10	119	108	108	108	102	110	112	112	119
Trial 11	111	99	107	107	109	102	108	115	113
Trial 12	115	110	104	104	111	102	102	102	104
Trial 13	112	106	99	99	117	115	112	102	118
Trial 14	111	104	104	104	109	111	114	116	104
Trial 15	116	108	105	105	104	111	119	105	113

Subject 2 DBP	Omron	Dc	A1	A2	A3	A3	Phi1	Phi2	Phi3	MAA
Trial 1	84	69	68	77	77	68	75	74	77	78
Trial 2	80	77	77	67	67	67	79	77	77	80
Trial 3	77	75	75	66	67	74	73	73	75	78
Trial 4	79	76	76	63	67	73	89	87	87	76
Trial 5	76	77	76	64	61	77	86	78	86	81
Trial 6	80	79	79	79	75	78	85	87	85	85
Trial 7	79	78	78	65	77	77	80	85	72	86
Trial 8	76	74	74	62	65	66	82	85	75	84
Trial 9	79	78	79	75	74	74	80	74	77	80
Trial 10	86	77	61	78	77	63	83	84	83	83
Trial 11	71	63	69	63	77	71	79	77	87	69
Trial 12	78	73	67	63	63	76	83	84	85	74
Trial 13	75	75	75	71	77	78	84	84	87	74
Trial 14	74	73	66	65	68	73	81	83	82	75
Trial 15	71	71	66	69	69	72	87	87	86	76

Subject 2 MAP	Omron	Dc	A1	A2	A3	A3	Phi1	Phi2	Phi3	MAA
Trial 1	104	91	94	103	98	99	95	94	94	90
Trial 2	99	95	94	98	97	97	94	98	98	92
Trial 3	97	96	96	95	96	97	99	99	99	91
Trial 4	94	92	92	98	97	101	99	99	95	88
Trial 5	97	96	97	94	92	92	92	100	97	95
Trial 6	99	91	91	94	96	97	95	103	98	100
Trial 7	97	91	92	94	99	97	95	93	95	97
Trial 8	92	91	91	92	91	102	99	99	94	97

Trial 9	94	96	96	100	96	96	96	96	96	92
Trial 10	101	94	97	96	94	92	94	92	94	96
Trial 11	88	98	97	100	96	90	98	95	96	80
Trial 12	93	101	100	94	100	96	99	101	97	88
Trial 13	90	98	98	101	95	94	103	97	97	87
Trial 14	89	98	94	102	94	92	99	99	98	86
Trial 15	87	100	96	103	96	95	96	96	100	87

Subject 2 SBP	Omron	Dc	A1	A2	A3	A3	Phi1	Phi2	Phi3	MAA
Trial 1	136	115	115	113	121	122	115	121	121	123
Trial 2	129	109	100	100	100	118	118	100	118	122
Trial 3	130	104	104	116	116	117	102	102	102	119
Trial 4	119	114	122	113	103	109	121	115	121	120
Trial 5	132	108	100	112	115	122	101	101	100	121
Trial 6	131	110	110	108	111	114	111	103	111	127
Trial 7	127	101	101	119	118	123	115	101	113	124
Trial 8	120	102	101	113	107	109	121	117	107	123
Trial 9	119	107	107	108	108	123	118	100	116	121
Trial 10	126	104	123	111	104	121	104	103	119	122
Trial 11	116	106	106	112	112	105	105	120	120	114
Trial 12	117	101	101	118	103	110	118	101	101	116
Trial 13	115	103	103	103	104	109	121	121	121	115
Trial 14	114	105	105	106	103	100	123	123	123	112
Trial 15	113	103	103	103	101	107	112	119	108	115

Subject 3 DBP	Omron	DC	A1	A2	A3	A4	Phi1	Phi2	Phi3	MAA
Trial 1	73	66	70	76	72	79	87	82	83	63
Trial 2	74	66	77	70	69	79	72	70	72	66
Trial 3	74	66	76	77	69	66	74	77	81	66
Trial 4	74	74	74	62	70	70	71	70	71	66
Trial 5	71	64	79	74	73	72	71	85	83	68
Trial 6	75	78	74	78	77	77	79	80	88	69
Trial 7	71	75	62	67	63	64	73	73	85	67
Trial 8	78	78	75	77	66	66	77	86	86	70
Trial 9	85	78	75	61	75	68	86	86	82	73
Trial 10	75	78	73	61	69	65	84	80	83	69
Trial 11	69	75	75	60	74	60	73	85	85	71
Trial 12	69	78	77	69	61	64	76	88	87	74
Trial 13	67	72	72	73	69	61	75	82	81	69
Trial 14	70	67	77	62	73	74	74	77	74	74

Trial 15	70	70	73	62	77	62	73	83	83	73

Subject 3 MAP	Omron	DC	A1	A2	A3	A4	Phi1	Phi2	Phi3
Trial 1	91	91	91	91	102	93	92	95	93
Trial 2	92	94	95	95	91	102	94	94	94
Trial 3	94	93	91	91	103	90	94	103	90
Trial 4	94	91	91	91	99	100	94	94	94
Trial 5	90	97	92	92	93	97	93	93	93
Trial 6	95	90	90	90	99	94	99	90	90
Trial 7	92	95	96	96	101	96	101	98	91
Trial 8	97	91	91	91	91	103	100	102	92
Trial 9	102	99	99	99	99	100	99	95	99
Trial 10	97	97	91	91	95	95	99	96	94
Trial 11	86	92	91	91	96	98	94	95	91
Trial 12	85	95	95	95	95	95	99	95	95
Trial 13	85	96	96	96	91	97	94	94	97
Trial 14	89	99	99	99	97	98	91	95	95
Trial 15	89	97	99	99	101	103	91	101	104

Subject 3 SBP	Omron	DC	A1	A2	A3	A4	Phi1	Phi2	Phi3	MAA
Trial 1	121	103	104	104	114	112	110	109	101	120
Trial 2	121	100	105	105	118	114	118	118	115	121
Trial 3	126	106	103	103	103	115	107	103	109	117
Trial 4	126	103	103	103	108	110	119	103	114	111
Trial 5	122	102	102	102	101	104	105	112	110	130
Trial 6	127	102	102	102	105	116	101	101	101	125
Trial 7	127	110	106	106	104	110	101	101	101	123
Trial 8	130	103	104	104	117	113	106	117	117	124
Trial 9	130	112	100	100	115	102	102	106	109	123
Trial 10	132	104	104	104	117	116	102	117	106	128
Trial 11	114	101	111	111	104	101	118	112	111	125
Trial 12	113	104	104	104	108	106	111	115	111	123
Trial 13	115	110	109	109	100	102	118	118	114	118
Trial 14	122	104	104	104	104	101	103	104	112	118
Trial 15	120	107	105	105	116	109	112	102	116	114

Subject 4 DBP	Omron	DC	A1	A2	A3	A4	Phi1	Phi2	Phi3
Trial 1	68	70	69	70	67	78	73	88	75
Trial 2	68	78	68	65	72	71	79	88	79
Trial 3	67	74	69	71	61	66	77	77	72

Trial 4	62	69	71	79	73	62	85	85	81
Trial 5	73	77	77	71	72	67	77	81	79
Trial 6	70	79	72	72	67	67	74	85	84
Trial 7	71	73	77	69	64	63	71	73	75
Trial 8	70	72	67	64	75	76	82	74	81
Trial 9	71	74	66	64	78	69	72	76	74
Trial 10	73	65	67	76	66	72	76	86	73
Trial 11	72	75	73	71	62	62	85	83	80
Trial 12	65	69	69	70	65	69	79	79	71
Trial 13	66	67	73	69	78	69	74	82	82
Trial 14	66	69	69	61	71	75	77	75	82
Trial 15	65	75	62	73	73	62	85	73	79

Subject 4 MAP	Omron	DC	A1	A2	A3	A4	Phi1	Phi2	Phi3
Trial 1	88	98	92	92	96	98	91	103	95
Trial 2	84	97	97	97	91	91	91	92	91
Trial 3	82	99	98	98	95	99	99	100	96
Trial 4	81	91	97	97	94	96	98	94	103
Trial 5	86	96	96	96	97	93	97	93	99
Trial 6	89	96	91	91	99	94	98	97	91
Trial 7	90	94	97	97	92	92	91	96	103
Trial 8	90	95	95	95	102	96	102	99	97
Trial 9	88	93	97	97	96	98	98	96	96
Trial 10	92	97	95	95	102	95	97	97	96
Trial 11	88	97	92	92	96	99	90	95	100
Trial 12	85	91	90	90	99	99	98	98	98
Trial 13	82	96	95	95	98	98	95	93	97
Trial 14	82	100	100	100	95	98	98	93	98
Trial 15	84	91	94	94	98	97	91	100	98

Subject 4 SBP	Omron	DC	A1	A2	A3	A4	Phi1	Phi2	Phi3
Trial 1	117	103	103	103	104	103	103	107	115
Trial 2	109	104	110	110	112	107	117	113	109
Trial 3	104	103	101	101	118	106	114	100	105
Trial 4	110	101	101	101	104	105	118	118	115
Trial 5	105	107	105	105	109	116	113	113	113
Trial 6	118	106	101	101	109	106	109	108	108
Trial 7	119	114	111	111	112	114	104	104	103
Trial 8	119	106	109	109	103	106	106	106	107
Trial 9	113	108	115	115	113	110	116	112	112
Trial 10	120	101	104	104	102	106	113	101	117
Trial 11	112	101	106	106	105	108	113	113	109

Trial 12	116	108	102	102	106	111	113	106	106
Trial 13	107	111	111	111	106	109	106	105	113
Trial 14	107	108	108	108	111	109	118	118	118
Trial 15	114	106	105	105	103	116	101	115	113

Subject 5 DIA	Omron	DC	A1	A2	A3	A4	Phi1	Phi2	Phi3
Trial 1	72	68	67	65	76	69	71	72	74
Trial 2	69	69	68	78	68	77	73	80	88
Trial 3	71	71	71	70	75	73	81	81	72
Trial 4	68	64	68	72	71	64	72	71	74
Trial 5	70	72	70	67	76	70	80	74	80
Trial 6	75	72	75	77	73	72	77	87	79
Trial 7	76	78	78	70	77	74	72	80	86
Trial 8	73	73	74	74	78	73	83	83	85
Trial 9	73	73	76	73	73	73	71	89	76
Trial 10	73	71	72	76	65	71	83	73	86
Trial 11	73	72	72	73	67	67	80	79	80
Trial 12	74	71	71	62	78	71	77	77	77
Trial 13	77	75	75	62	64	73	86	88	87
Trial 14	73	71	67	70	68	69	83	78	75
Trial 15	79	74	73	77	69	75	77	87	77

Subject 5 MAP	Omron	DC	A1	A2	A3	A4	Phi1	Phi2	Phi3
Trial 1	86	91	91	91	100	100	103	95	91
Trial 2	83	95	99	99	90	92	96	100	99
Trial 3	85	96	98	98	101	99	98	97	101
Trial 4	80	99	97	97	94	99	99	98	94
Trial 5	83	100	91	91	97	103	103	91	91
Trial 6	90	98	91	91	97	90	93	102	99
Trial 7	92	95	95	95	90	96	97	96	96
Trial 8	89	91	92	92	98	95	97	101	95
Trial 9	90	93	95	95	100	93	99	96	93
Trial 10	89	93	91	91	94	102	101	98	101
Trial 11	87	91	91	91	99	97	93	97	91
Trial 12	90	91	93	93	91	102	94	93	94
Trial 13	89	97	95	95	103	100	97	98	98
Trial 14	85	103	99	99	97	92	102	98	99
Trial 15	89	100	99	99	97	100	100	102	91

Subject 5 SBP	Omron	DC	A1	A2	A3	A4	Phi1	Phi2	Phi3

Trial 1	109	102	102	102	101	104	113	113	117
Trial 2	106	111	110	110	112	103	108	118	117
Trial 3	108	111	107	107	107	110	107	115	107
Trial 4	99	112	112	112	112	112	112	112	111
Trial 5	105	100	104	104	100	103	111	111	116
Trial 6	113	106	106	106	100	106	110	111	115
Trial 7	118	103	101	101	103	101	114	114	108
Trial 8	115	106	105	105	106	105	101	102	115
Trial 9	118	103	103	103	110	103	103	103	115
Trial 10	114	104	113	113	106	102	116	117	117
Trial 11	111	108	108	108	106	111	114	106	110
Trial 12	117	104	104	104	110	113	109	110	113
Trial 13	109	110	102	102	103	108	116	116	108
Trial 14	104	104	105	105	117	114	117	102	102
Trial 15	105	102	102	102	108	117	118	102	102

Subject 6 DBP	Omron	DC	A1	A2	A3	A4	Phi1	Phi2	Phi3
Trial 1	58	60	58	32	58	60	57	40	42
Trial 2	57	58	56	58	58	48	53	62	58
Trial 3	58	62	60	30	50	50	49	66	66
Trial 4	55	62	60	60	57	62	48	64	48
Trial 5	55	62	62	62	62	41	41	57	61
Trial 6	55	63	63	63	50	63	60	71	73
Trial 7	57	63	63	61	32	63	64	41	51
Trial 8	52	61	59	59	59	56	50	64	72
Trial 9	57	60	63	37	59	34	55	46	47
Trial 10	57	62	60	31	60	60	50	72	47
Trial 11	55	59	63	32	42	46	52	57	59
Trial 12	61	62	55	62	30	30	42	40	45
Trial 13	60	62	61	42	34	62	70	52	71
Trial 14	63	57	53	37	42	61	45	55	57
Trial 15	60	57	62	61	61	35	52	52	46

Subject 6 MAP	Omron	DC	A1	A2	A3	A4	Phi1	Phi2	Phi3
Trial 1	70	67	65	65	71	65	65	65	67
Trial 2	67	66	64	64	64	70	64	64	70
Trial 3	68	68	68	68	71	66	64	68	68
Trial 4	66	65	65	65	69	71	65	65	65
Trial 5	65	64	64	64	66	66	64	68	68
Trial 6	64	69	66	66	66	66	68	68	68
Trial 7	67	66	65	65	70	68	70	70	65
Trial 8	62	66	66	66	67	67	64	67	66

Trial 9	66	69	67	67	64	69	67	67	67
Trial 10	66	69	69	69	68	67	69	69	69
Trial 11	66	67	65	65	70	63	65	65	65
Trial 12	69	68	68	68	65	65	65	67	67
Trial 13	69	69	67	67	67	69	65	65	67
Trial 14	72	65	64	64	69	67	69	69	69
Trial 15	68	65	65	65	69	67	69	67	69

Subject 6 SBP	Omron	DC	A1	A2	A3	A4	Phi1	Phi2	Phi3
Trial 1	90	80	75	75	84	81	75	75	77
Trial 2	84	79	82	82	85	84	74	82	87
Trial 3	84	82	82	82	83	79	74	82	82
Trial 4	84	81	81	81	83	81	87	85	84
Trial 5	82	84	74	74	79	80	85	78	78
Trial 6	80	82	80	80	76	88	88	81	81
Trial 7	85	76	86	86	82	81	80	84	87
Trial 8	79	76	82	82	80	88	83	82	86
Trial 9	80	79	77	77	81	82	81	77	87
Trial 10	81	81	81	81	75	79	79	82	81
Trial 11	85	81	80	80	83	82	80	80	75
Trial 12	83	82	82	82	84	83	85	77	81
Trial 13	84	82	77	77	77	81	75	83	80
Trial 14	86	78	74	74	83	80	79	79	82
Trial 15	82	82	84	84	83	81	83	82	83

Subject 7 DBP	Omron	DC	A1	A2	A3	A4	Phi1	Phi2	Phi3
Trial 1	66	59	59	31	59	59	41	40	49
Trial 2	62	64	60	58	64	42	47	47	72
Trial 3	66	47	44	47	41	63	52	57	52
Trial 4	65	58	58	32	38	58	48	51	69
Trial 5	64	57	62	57	56	31	51	51	51
Trial 6	62	58	61	33	31	31	58	50	71
Trial 7	67	53	60	58	30	61	40	57	68
Trial 8	66	64	64	33	33	54	70	57	71
Trial 9	66	62	62	62	61	61	42	42	45
Trial 10	68	63	63	33	32	39	58	67	72
Trial 11	58	60	60	34	32	64	62	59	74
Trial 12	61	58	58	31	59	40	51	72	62
Trial 13	62	61	61	61	61	61	45	45	45
Trial 14	58	63	58	30	63	63	69	73	73
Trial 15	60	64	64	64	61	33	51	48	48

Subject 7 MAP	Omron	DC	A1	A2	A3	A4	Phi1	Phi2	Phi3
Trial 1	79	68	70	70	71	68	65	65	68
Trial 2	73	67	67	67	70	64	64	64	65
Trial 3	77	65	70	70	68	68	66	65	65
Trial 4	77	67	69	69	67	69	64	70	69
Trial 5	78	67	67	67	70	72	65	65	70
Trial 6	73	69	68	68	70	69	69	67	68
Trial 7	77	67	68	68	67	68	65	65	65
Trial 8	76	67	67	67	67	66	70	67	67
Trial 9	78	66	66	66	69	69	64	68	68
Trial 10	80	67	68	68	68	66	66	66	67
Trial 11	72	67	67	67	71	67	64	64	65
Trial 12	73	67	66	66	69	67	70	65	66
Trial 13	75	69	69	69	71	67	67	67	67
Trial 14	70	69	69	69	65	67	65	65	65
Trial 15	72	66	66	66	67	70	65	65	70

Subject 7 SBP	Omron	DC	A1	A2	A3	A4	Phi1	Phi2	Phi3
Trial 1	99	83	83	83	83	79	75	85	82
Trial 2	90	77	75	75	81	84	74	84	75
Trial 3	96	75	88	88	76	76	81	82	75
Trial 4	96	81	81	81	77	87	85	81	87
Trial 5	102	80	80	80	80	85	88	83	82
Trial 6	91	78	85	85	83	87	78	78	76
Trial 7	92	77	78	78	85	82	86	85	85
Trial 8	92	77	77	77	78	75	80	80	82
Trial 9	98	77	77	77	80	84	85	83	78
Trial 10	99	78	78	78	78	83	76	81	78
Trial 11	96	77	77	77	85	77	84	85	76
Trial 12	93	77	76	76	77	77	81	84	76
Trial 13	96	77	77	77	82	78	77	80	77
Trial 14	91	81	81	81	84	79	85	88	85
Trial 15	92	76	76	76	77	80	85	87	83

S8

Subject 8 DBP	Omron	DC	A1	A2	A3	A4	Phi1	Phi2	Phi3
Trial 1	77	67	64	65	68	67	78	79	78
Trial 2	76	61	67	73	68	61	83	75	83
Trial 3	77	62	76	65	64	62	82	84	84
Trial 4	77	60	60	65	73	64	76	77	76

Trial 5	75	77	77	66	77	66	82	77	82
Trial 6	76	72	67	71	62	74	80	80	75
Trial 7	78	67	63	73	67	65	78	77	75
Trial 8	73	71	77	74	61	70	81	80	74
Trial 9	74	70	64	69	72	64	74	74	80
Trial 10	76	63	64	63	64	66	76	77	76
Trial 11	70	68	77	71	71	76	78	81	81
Trial 12	71	73	73	68	68	73	83	81	81
Trial 13	77	72	62	73	78	70	88	78	82
Trial 14	74	76	76	73	72	72	82	80	82
Trial 15	73	79	76	72	79	74	73	77	74

Subject 8 MAP	Omron	DC	A1	A2	A3	A4	Phi1	Phi2	Phi3
Trial 1	91	93	90	90	100	98	98	100	104
Trial 2	89	97	97	97	99	91	93	99	97
Trial 3	87	93	93	93	94	96	91	94	97
Trial 4	88	95	95	95	92	95	95	95	98
Trial 5	89	97	96	96	92	90	97	97	90
Trial 6	86	93	99	99	100	93	95	100	100
Trial 7	88	94	96	96	98	96	88	96	102
Trial 8	85	95	95	95	100	97	100	97	97
Trial 9	86	98	98	98	93	90	102	96	102
Trial 10	89	97	97	97	104	97	100	97	100
Trial 11	86	100	96	96	95	100	92	99	93
Trial 12	85	96	94	94	98	97	100	100	98
Trial 13	89	95	93	93	92	97	91	96	99
Trial 14	86	91	93	93	92	95	95	93	91
Trial 15	85	95	92	92	97	93	95	92	95

Subject 8 SBP	Omron	DC	A1	A2	A3	A4	Phi1	Phi2	Phi3
Trial 1	115	98	112	112	108	109	102	104	109
Trial 2	112	104	104	104	116	100	107	107	104
Trial 3	105	109	105	105	117	107	110	110	110
Trial 4	108	114	110	110	107	111	104	104	101
Trial 5	113	100	100	100	108	107	109	117	107
Trial 6	105	109	107	107	109	105	111	105	105
Trial 7	106	108	115	115	108	108	111	108	102
Trial 8	107	108	108	108	105	105	111	114	111
Trial 9	109	105	105	105	105	108	105	105	102
Trial 10	113	106	104	104	106	109	104	110	100
Trial 11	114	106	105	105	108	106	112	107	117
Trial 12	109	107	104	104	108	107	112	108	112

Trial 13	109	105	105	105	101	102	107	106	101
Trial 14	106	108	109	109	112	114	104	104	104
Trial 15	107	109	109	109	118	115	104	115	115

Subject 9 DBP	Omron	DC	A1	A2	A3	A4	Phi1	Phi2	Phi3
Trial 1	77	77	77	61	64	65	74	72	80
Trial 2	73	72	68	68	66	68	76	76	77
Trial 3	71	68	67	69	61	72	72	72	74
Trial 4	68	73	73	72	75	66	80	80	81
Trial 5	79	74	74	70	70	74	73	78	85
Trial 6	75	72	68	60	70	75	81	81	75
Trial 7	73	71	71	62	77	71	78	79	79
Trial 8	70	72	72	71	72	71	82	82	82
Trial 9	75	65	60	73	76	73	72	77	81
Trial 10	71	65	65	65	65	70	74	76	75
Trial 11	67	69	69	71	78	64	74	74	72
Trial 12	68	76	73	71	75	76	87	86	86
Trial 13	68	78	73	73	64	69	76	73	74
Trial 14	70	68	68	68	64	66	73	78	74
Trial 15	71	68	64	77	72	77	72	72	87

Subject 9 MAP	Omron	DC	A1	A2	A3	A4	Phi1	Phi2	Phi3
Trial 1	88	94	92	92	98	102	102	101	101
Trial 2	83	91	97	97	91	99	100	100	101
Trial 3	81	92	92	92	96	92	100	102	92
Trial 4	78	96	95	95	98	97	102	93	96
Trial 5	91	91	91	91	97	97	91	91	91
Trial 6	86	97	97	97	102	100	102	102	98
Trial 7	86	94	92	92	92	90	101	101	99
Trial 8	83	97	97	97	95	99	97	97	97
Trial 9	85	93	93	93	97	101	99	101	102
Trial 10	83	101	101	101	98	95	99	96	103
Trial 11	78	100	100	100	99	97	94	98	99
Trial 12	81	91	91	91	103	94	100	99	99
Trial 13	81	96	96	96	92	92	92	92	92
Trial 14	82	92	92	92	97	93	92	92	92
Trial 15	81	95	94	94	97	96	99	92	98

Subject 9 SBP	Omron	DC	A1	A2	A3	A4	Phi1	Phi2	Phi3
Trial 1	105	113	114	114	105	105	104	113	116

Trial 2	100	104	104	104	114	104	102	115	115
Trial 3	98	110	111	111	110	104	116	115	115
Trial 4	96	113	112	112	100	105	110	113	115
Trial 5	110	101	101	101	110	113	105	110	100
Trial 6	103	104	105	105	106	104	108	114	114
Trial 7	108	105	103	103	103	113	109	101	112
Trial 8	105	102	102	102	105	105	100	116	116
Trial 9	102	103	103	103	114	101	107	103	111
Trial 10	102	112	116	116	111	105	106	106	106
Trial 11	96	102	102	102	102	100	115	109	113
Trial 12	102	101	101	101	109	115	109	109	112
Trial 13	102	102	101	101	115	117	113	119	119
Trial 14	101	102	104	104	103	103	109	115	115
Trial 15	96	112	112	112	110	110	114	116	100

Subject 10 DBP	Omron	DC	A1	A2	A3	A4	Phi	Phi0	Phi1
Trial 1	67	73	76	60	68	58	59	56	100
Trial 2	67	80	77	61	71	61	67	56	23
Trial 3	66	78	77	61	81	69	59	56	13
Trial 4	62	70	27	59	77	66	18	63	18
Trial 5	61	75	75	58	79	68	66	68	66
Trial 6	59	73	72	80	80	69	17	77	136
Trial 7	62	71	74	61	68	58	137	64	98
Trial 8	60	73	73	77	87	77	75	73	87
Trial 9	58	75	70	76	71	61	61	56	18
Trial 10	59	76	78	63	80	68	136	75	29
Trial 11	61	74	75	54	95	78	100	61	105
Trial 12	63	75	74	79	84	65	17	58	96
Trial 13	59	75	67	53	71	63	141	67	98
Trial 14	61	75	71	57	88	83	133	71	46
Trial 15	61	79	69	62	70	60	86	69	104

Subject 10 MAP	Ref	DC	A1	A2	A3	A4	Phi	Phi0	Phi1
Trial 1	77	74	80	72	69	69	66	97	115
Trial 2	77	81	79	71	71	71	78	119	75
Trial 3	76	93	77	72	81	80	69	118	56
Trial 4	73	73	74	70	78	75	68	116	68
Trial 5	70	84	76	70	80	77	103	90	86
Trial 6	72	81	76	74	74	83	58	73	119
Trial 7	75	72	67	88	79	82	117	110	70
Trial 8	72	84	90	75	68	69	103	75	119
Trial 9	71	78	77	67	99	109	119	92	113

Trial 10	72	81	74	90	102	78	72	108	63
Trial 11	78	89	89	76	93	77	93	102	57
Trial 12	78	73	65	73	69	72	119	68	105
Trial 13	76	97	73	87	83	87	95	71	103
Trial 14	76	76	89	75	75	67	59	120	61
Trial 15	77	80	85	88	85	85	94	64	64

Subject 10 SBP	Ref	DC	A1	A2	A3	A4	Phi	Phi0	Phi1
Trial 1	93	103	100	106	106	104	100	102	109
Trial 2	93	101	103	105	101	97	99	103	99
Trial 3	92	106	102	106	107	102	100	102	101
Trial 4	91	104	95	106	106	103	100	102	100
Trial 5	85	103	101	104	106	102	100	101	101
Trial 6	91	100	103	105	108	101	98	101	90
Trial 7	95	100	103	106	110	102	99	103	110
Trial 8	91	99	103	110	103	103	104	102	105
Trial 9	92	102	103	104	109	101	97	101	89
Trial 10	92	104	102	104	108	101	99	102	106
Trial 11	102	99	103	104	104	98	90	103	87
Trial 12	100	96	101	103	108	100	96	99	106
Trial 13	100	97	87	106	108	97	106	99	99
Trial 14	98	97	110	100	94	106	87	102	100
Trial 15	101	98	99	105	110	100	94	101	91

Reference

[1] John G. Webster, “Harmonic Analysis of Blood Pressure Waveform,” in *Medical Instrumentation Application and Design*, 4th ed., 2010, pp. 293 – 299.

[2] M. Ward and J. A. Langton, "Blood pressure measurement," *Continuing Education in Anaesthesia, Critical Care & Pain*, vol. 7, pp. 122-126, 2007..

[3] T. Dieterle, “Blood pressure measurement - an overview,” *Swiss Med. Wkly.*, no. January, pp. 1–9, 2012.

[4] H. W. SHIRER, *Blood pressure measuring methods*," *IRE TRANSACTIONS ON B1O-MEDICAL ELECTRONICS" vol 4. BME-9"*. 1962.

[5] J. Penaz, “Automatic noninvasive Measurement of Arterial blood pressure,” *IEEE Instrum. Meas. Soc.*, no. February, 2011.

[6] “H. Sorvoja and R. Myllyla, "Noninvasive blood pressure measurement methods," *Molecular and Quantum Acoustics*, vol. 27, pp. 239-264, 2006.

[7] Leslie A. Geddes, “Requirement for Reproduction of the Blood Pressure Wave,” in *The Direct and Indirect Measurement of Blood Pressure*, 1st ed., Chicago: Year Book Medical Publishers, 1970, pp. 46 – 48.

[8] B. M. Egan, Y. Zhao, and R. N. Axon, “US Trends in Prevalance, Awareness, Treatment and Control of Hypertension , 1988-2008,” *Jama*, vol. 303, no. 20, pp. 2043–2050, 2010.

[9] K.G. Ng, C.F. Small, “Survey of Automated Noninvasive Blood Pressure Monitors,” *Journal of Clinical Engineering*, Vol. 33, Dec. 1994, pp. 452-475.

[10] W. a Littler and B. Komsuoglu, “Which is the most accurate method of measuring blood pressure?,” *Am. Heart J.*, vol. 117, no. 3, pp. 723–728, 1989.

[11] J. N. Amoore, “Oscillometric sphygmomanometers: a critical appraisal of current technology.,” *Blood Press. Monit.*, vol. 17, no. 2, pp. 80–8, 2012.

[12] John Brunner, “Fundamentals: Waves, Horns, Estuaries and weighty words,” in *Handbook of Blood Pressure Monitoring*, 2nd ed., Massachusetts: PSG Publishing Company, 1978, pp. 3 – 13.

[13] G. Drzewiecki, R. Hood, and H. Apple, “Theory of the oscillometric maximum and the systolic and diastolic detection ratios,” *Ann. Biomed. Eng.*, vol. 22, no. 1, pp. 88–96, 1994.

[14] J. C. T. B. Moraes, M. Cerulli, and P. S. Ng, “A strategy for determination of systolic, mean and diastolic blood pressures from oscillometric pulse profiles,” *Comput. Cardiol. 2000 Vol27 Cat 00CH37163*, pp. 211–214, 2000.

[15] J. Jilek and T. Fukushima, “Oscillometric blood pressure measurement: The methodology, some observations, and suggestions,” *Biomed. Instrum. Technol.*, vol. 39, no. 3, pp. 237–241, 2005.

[16] K. Barbé, W. V. Moer, and L. Lauwers, “Oscillometric blood pressure measurements: A signal analysis,” *J. Phys. Conf. Ser.*, vol. 238, p. 012052, 2010.

[17] E. Balestrieri, University of Sannio and P. Daponte University of Sannio, “Open Questions on Unified Approach for Calibration of Oscillometric Blood Pressure Measurement Devices,” *Differences*, pp. 206–211, 2009.

[18] M. Forouzanfar, S. Member, S. Ahmad, I. Batkin, H. R. Dajani, S. Member, V. Z. Groza, and M. Bolic, “Coefficient-Free Blood Pressure Estimation Based on Pulse Transit Time – Cuff Pressure Dependence,” vol. 60, no. 7, pp. 1814–1824, 2013.

[19] S. Chen, V. Z. Groza, M. Bolic, and H. R. Dajani, “Assessment of algorithms for oscillometric blood pressure measurement,” *2009 IEEE Intrumentation Meas. Technol. Conf. I2MTC 2009*, no. May, pp. 1763–1767, 2009.

[20] M. Mafi, S. Rajan, M. Bolic, V. Z. Groza, and H. R. Dajani, “Blood pressure estimation using oscillometric pulse morphology,” *Proc. Annu. Int. Conf. IEEE Eng. Med. Biol. Soc. EMBS*, pp. 2492–2496, 2011.

[21] S. H. Song, D. K. Kim, J. S. Lee, Y. J. Chee, and I. Y. Kim, “Mean arterial pressure estimation method using morphological changes in oscillometric waveform,” *Comput. Cardiol. 2009*, no. c, pp. 737–739, 2009.

[22] R. Raamat and J. Talts, “Accuracy of some algorithms to determine the oscillometric mean arterial pressure: a theoretical study,” *Blood Press. …*, vol. 18, no. 1, pp. 50–6, 2013.

[23] J. Liu, J. O. Hahn, and R. Mukkamala, “An initial step towards improving the accuracy of the oscillometric blood pressure measurement,” *IEEE Eng. Med. Biol. Conf.*, pp. 4082–4085, 2013.

[24] M. Ursino and C. Cristalli, “A mathematical study of some biomechanical factors affecting the oscillometric blood pressure measurement,” *IEEE Trans. Biomed. Eng.*, vol. 43, no. 8, pp. 761–778, 1996.

[25] M. Aboy, J. McNames, R. Hornero, T. Thong, D. Cuesta, D. Novak, and B. Goldstein, “A novel statistical model for simulation of arterial and intracranial pressure.,” *Conf. Proc. Annu. Int. Conf. IEEE Eng. Med. Biol. Soc. IEEE Eng. Med. Biol. Soc. Conf.*, vol. 1, pp. 129–132, 2004.

[26] M. Forouzanfar, H. R. Dajani, V. Z. Groza, M. Bolic, and S. Rajan, “Feature-Based Neural Network Approach for Oscillometric Blood Pressure Estimation,” *IEEE Trans. Instrum. Meas.*, vol. 60, no. 8, pp. 2786–2796, 2011.

[27] M. Mafi, M. Bolic, V. Z. Groza, H. R. Dajani, and S. Rajan, “Oscillometric blood pressure pulse morphology,” *MeMeA 2011 - 2011 IEEE Int. Symp. Med. Meas. Appl. Proc.*, 2011.

[28] J. N. Amoore, Y. Lemesre, I. C. Murray, S. Mieke, S. T. King, F. E. Smith, and A. Murray, “Automatic blood pressure measurement: the oscillometric waveform shape is a potential contributor to differences between oscillometric and auscultatory pressure measurements.,” *J. Hypertens.*, vol. 26, no. 1, pp. 35–43, 2008.

[29] K. Barbé and W. Van Moer, “An innovative oscillometric blood pressure measurement: Getting rid of the traditional envelope.” 2012.

[30] R. Raamat, J. Talts, K. Jagomägi, and J. Kivastik, “Errors of oscillometric blood pressure measurement as predicted by simulation.,” *Blood Press. Monit.*, vol. 16, no. 5, pp. 238–245, 2011.

[31] J. N. Amoore, E. Vacher, I. C. Murray, S. Mieke, S. T. King, F. E. Smith, and A. Murray, “Effect of the shapes of the oscillometric pulse amplitude envelopes and their characteristic ratios on the differences between auscultatory and oscillometric blood pressure measurements.,” *Blood Press. Monit.*, vol. 12, no. 5, pp. 297–305, 2007.

[32] G. Jeon, J. Jung, I. Kim, A. Jeon, S. Yoon, J. Son, J. Kim, S. Ye, J. Ro, D. Kim, and C. Kim, “A Simulation for Estimation of the Blood Pressure using Arterial Pressure-volume Model,” *World Acad. Sci. Eng. Technol.*, vol. 1, no. 6, pp. 416–421, 2007.

[33] J. U. of T. Talt, R. R. U. of Tartu, J. U. of Tartu, and J. K. of Tartu, “Accuraccy of the Oscillomet Fixed- Ratio Bloood Pressure Measurement Using Different Methods of Characterization of Oscillometric Pulses,” *Ifmebe Proc.*, pp. 3–6, 2013.

[34] R. R. Joshi, “Automatic detection of pulse morphology patterns & cardiac risks,” *J. Biomed. Sci. Eng.*, vol. 05, no. 06, pp. 315–322, 2012.

[35] J. Jilek and T. Fukushima, “Blood flow under wrist cuff, in hand alters oscillometry waveforms during blood pressure measurement,” *Biomed. Instrum. Technol.*, vol. 41, no. 3, pp. 238–243, 2007.

[36] M. F. O’Rourke, A. Pauca, and X.-J. Jiang, “Pulse wave analysis,” *Br. J. Clin. Pharmacol.*, vol. 51, no. 6, pp. 507–522, 2001.

[37] D. Korpas, J. Hálek, and L. Doležal, “Parameters describing the pulse wave,” *Physiol. Res.*, vol. 58, no. 4, pp. 473–479, 2009.

[38] S. C. Millasseau, R. P. Kelly, J. M. Ritter, and P. J. Chowienczyk, “Determination of age-related increases in large artery stiffness by digital pulse contour analysis.,” *Clin. Sci. Lond. Engl. 1979*, vol. 103, no. 4, pp. 371–377, 2002.

[39] A. M. Dart and B. a Kingwell, “Pulse pressure—a review of mechanisms and clinical relevance,” *J. Am. Coll. Cardiol.*, vol. 37, no. 4, pp. 975–984, 2001.

[40] P. Y. Zhang and H. Y. Wang, “A framework for automatic time-domain characteristic parameters extraction of human pulse signals,” *Eurasip J. Adv. Signal Process.*, vol. 2008, 2008.

[41] W. Generation, A. Committee, I. Instrumentation, and M. Society, *IEEE Standard for Transitions , Pulses , and Related Waveforms*, vol. 2011. 2011.

[42] E. F. Treo, M. C. Herrera, and M. E. Valentinuzzi, “Algorithm for identifying and separating beats from arterial pulse records.,” *Biomed. Eng. Online*, vol. 4, p. 48, 2005.

[43] M. Aboy, J. McNames, T. Thong, D. Tsunami, M. S. Ellenby, and B. Goldstein, “An automatic beat detection algorithm for pressure signals,” *IEEE Trans. Biomed. Eng.*, vol. 52, no. 10, pp. 1662–1670, 2005.

[44] J. N. Amoore, “Extracting oscillometric pulses from the cuff pressure: does it affect the pressures determined by oscillometric blood pressure monitors?,” *Blood Press. Monit.*, vol. 11, no. 5, pp. 269–279, 2006.

[45] J. Allen, “Photoplethysmography and its application in clinical physiological measurement.,” *Physiol. Meas.*, vol. 28, no. 3, pp. R1–R39, 2007.

[46] H. Gesche, D. Grosskurth, G. Küchler, and A. Patzak, “Continuous blood pressure measurement by using the pulse transit time: Comparison to a cuff-based method,” *Eur. J. Appl. Physiol.*, vol. 112, no. 1, pp. 309–315, 2012.

[47] J. M. Padilla, E. J. Berjano, J. Saiz, L. Facila, P. Diaz, and S. Merce, “Assessment of relationships between blood pressure, pulse wave velocity and digital volume pulse,” *2006 Comput. Cardiol.*, pp. 893–896, 2006.

[48] G. U. of milano Baselli, E. U. of milano Caini, A. U. of milano Porta, N. U. of milano Montana, M. G. U. of milano Signorini, and Sergio Cerutti University of milano, “BIOMEDICAL SIGNAL PROCESSING AND Modelling in Cardiovascular Systems,” *Crit. Rev. Biomed. Eng.*, 2002.

[49] S. Lee, S. Rajan, and H. Dajani, “Determination of blood pressure using Bayesian approach,” *... I2Mtc 2011 Ieee*, 2011.

[50] M. Forouzanfar, H. R. Dajani, V. Z. Groza, M. Bolic, S. Rajan, and I. Batkin, “Ratio-Independent Blood Pressure Estimation by Modeling the Oscillometric Waveform Envelope,” vol. 63, no. 10, pp. 2501–2503, 2014.

[51] A. P. Avolio, M. Butlin, and A. Walsh, “Arterial blood pressure measurement and pulse wave analysis - their role in enhancing cardiovascular assessment,” *Physiol. Meas.*, vol. 31, no. 1, pp. R1–R47, 2010.

[52] W. V. Moer, S. Member, L. Lauwers, S. Member, D. Schoors, and K. Barbé, "Linearizing Oscillometric Blood Pressure Measurements: (Non)Sense ?," *IEEE Trans. Instrum. Meas.*, vol. 60, no. 4, pp. 1267–1275, 2011.

[53] Leslie A. Geddes, "Requirement for Reproduction of the Blood Pressure Wave," in *The Direct and Indirect Measurement of Blood Pressure*, 1st ed., Chicago: Year Book Medical Publishers, 1970, pp. 46 – 48.

[54] John G. Webster, "Harmonic Analysis of Blood Pressure Waveform," in *Medical Instrumentation Application and Design*, 4th ed., 2010, pp. 293 – 299.

[55] K. Barbé, W. Van Moer, and D. Schoors, "Analyzing the windkessel model as a potential candidate for correcting oscillometric blood-pressure measurements," *IEEE Trans. Instrum. Meas.*, vol. 61, no. 2, pp. 411–418, 2012.

[56] K. Barbe, F. Lamonaca, Y. Kurylyak, and W. Van Moer, "Using the heart harmonics in the oscillometry to extract the blood pressure," *MeMeA 2013 - IEEE Int. Symp. Med. Meas. Appl. Proc.*, pp. 21–25, 2013.

[57] J. A. De La O Serna, "Taylor-Fourier analysis of blood pressure oscillometric waveforms," *IEEE Trans. Instrum. Meas.*, vol. 62, no. 9, pp. 2511–2518, 2013.

[58] Shkti Chatterjee and Aubert Miller, *Biomedical Instrumentation*, 1st ed. New York: DelMar Cengage Learning, 2010.

[59] Wilmer W Nichols, Michael F O'Rouke, and Charalambos Vlachopoulos, *McDonald's Blood Flow in Arteries Theoretical, Experimental and Clinical Principles*, 6th ed. 2011.

[60] T. F. Coleman and Y. Li, "On the Convergence of Reflective Newton Methods for Large-Scale Nonlinear Minimization Subject to Bounds." 1994.

[61] T. F. Coleman and Y. Li, "An Interior Trust Region Approach for Nonlinear Minimization Subject to Bounds." 1996.

[62] J. Nocedal, *Numerical Optimization*. 2006.

[63] "Solve nonlinear curve-fitting (data-fitting) problems in least-squares sense - MATLAB lsqcurvefit." [Online]. Available: http://www.mathworks.com/help/optim/ug/lsqcurvefit.html. [Accessed: 12-May-2015].

[64] "Sum of Sines Models - MATLAB & Simulink." [Online]. Available: http://www.mathworks.com/help/curvefit/sum-of-sine.html?searchHighlight=sum%20of%20sine. [Accessed: 12-May-2015].

[65] J.-M. Peng and Y. Yuan, "Optimality Conditions for the Minimization of a Quadratic with Two Quadratic Constraints," *SIAM J. Optim.*, vol. 7, no. 3, pp. 579–594, 1997.

[66] D. S. Benincasa and M. I. Savic, “Co-channel speaker separation using constrained nonlinear optimization,” *1997 IEEE Int. Conf. Acoust. Speech Signal Process.*, vol. 2, pp. 1195–1198, 1997.

[67] R. Pintelon and J. Schoukens, “An improved sine-wave fitting procedure for characterizing data acquisition channels,” *IEEE Trans. Instrum. Meas.*, vol. 45, no. 2, pp. 588–593, 1996.

[68] D. Chazan, M. T. Z. Ý, R. Hoory, G. Cohen, and M. Haifa, “Efficient Periodicity Extraction Based on Sine-Wave Representation and its Application to Pitch Determination of Speech Signals,” 2001.

[69] T. F. Quatieri and R. G. Danisewicz, “An Approach to co-channel talker interference suppression using a sinusoidal model for speech,” *IEEE Trans. Acoust. Speech Signal Process.* vol. 38, no. 1, pp. 56–69, 1990.

[70] S. Ahmad, S. Chen, K. Soueidan, I. Batkin, M. Bolic, H. Dajani, and V. Groza, “Electrocardiogram-assisted blood pressure estimation,” *IEEE Trans. Biomed. Eng.*, vol. 59, no. 3, pp. 608–618, 2012.

[71] M. Razminia, A. Trivedi, J. Molnar, M. Elbzour, M. Guerrero, Y. Salem, A. Ahmed, S. Khosla, and D. L. Lubell, “Validation of a new formula for mean arterial pressure calculation: The new formula is superior to the standard formula,” *Catheter. Cardiovasc. Interv.*, vol. 63, no. 4, pp. 419–425, 2004.

[72] S. Ahmad, S. Chen, K. Soueidan, I. Batkin, M. Bolic, H. Dajani, and V. Groza, “A prototype of an integrated blood pressure and electrocardiogram device for multi-parameter physiologic monitoring,” *2010 IEEE Int. Instrum. Meas. Technol. Conf. I2MTC 2010 - Proc.*, pp. 1244–1249, 2010.